

University of Alberta

**Identification and expression patterns of Prader-Willi syndrome candidate genes:
implications for mouse models and human phenotypes.**

by

Syann Lee



A thesis submitted to the Faculty of Graduate Studies and Research in partial fulfillment
of the requirements for the degree of

Doctor of Philosophy

In

Medical Sciences – Medical Genetics

Edmonton, Alberta

Spring 2003

National Library
of Canada

Acquisitions and
Bibliographic Services

395 Wellington Street
Ottawa ON K1A 0N4
Canada

Bibliothèque nationale
du Canada

Acquisitons et
services bibliographiques

395, rue Wellington
Ottawa ON K1A 0N4
Canada

Your file *Votre référence*

ISBN: 0-612-82131-5

Our file *Notre référence*

ISBN: 0-612-82131-5

The author has granted a non-exclusive licence allowing the National Library of Canada to reproduce, loan, distribute or sell copies of this thesis in microform, paper or electronic formats.

The author retains ownership of the copyright in this thesis. Neither the thesis nor substantial extracts from it may be printed or otherwise reproduced without the author's permission.

L'auteur a accordé une licence non exclusive permettant à la Bibliothèque nationale du Canada de reproduire, prêter, distribuer ou vendre des copies de cette thèse sous la forme de microfiche/film, de reproduction sur papier ou sur format électronique.

L'auteur conserve la propriété du droit d'auteur qui protège cette thèse. Ni la thèse ni des extraits substantiels de celle-ci ne doivent être imprimés ou autrement reproduits sans son autorisation.

Canada

University of Alberta

Library Release Form

Name of Author: Syann Lee

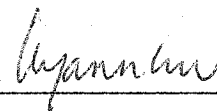
Title of Thesis: Identification and expression patterns of Prader-Willi syndrome candidate genes: implications for mouse models and human phenotypes.

Degree: Doctor of Philosophy

Year this Degree Granted: 2003

Permission is hereby granted to the University of Alberta Library to reproduce single copies of this thesis and to lend or sell such copies for private, scholarly or scientific research purposes only.

The author reserves all other publication and other rights in association with the copyright in the thesis, and except as herein before provided, neither the thesis nor any substantial portion thereof may be printed or otherwise reproduced in any material form whatever without the author's prior written permission.




3522 Hillview Crescent
Edmonton, Alberta
T6L 1C4

April 15, 2003

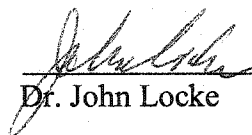
University of Alberta

Faculty of Graduate Studies and Research

The undersigned certify that they have read, and recommend to the Faculty of Graduate Studies and Research for acceptance, a thesis entitled *Identification and expression of Prader-Willi syndrome candidate genes: implications for mouse models and human phenotypes* submitted by *Syann Lee* in partial fulfillment of the requirements for the degree of *Doctor of Philosophy in Medical Sciences-Medical Genetics*.



Dr. Rachel Wevrick



Dr. John Locke



Dr. Alan Underhill



Dr. Teresa Krukoff



Dr. Sam Weiss

April 11, 2003

Date

For my parents.

寸
心
報
親
思

Abstract

Prader-Willi syndrome (PWS) is a neurobehavioral disorder that is characterized by neonatal hypotonia, global developmental delay, hyperphagia resulting in obesity, and behavioral problems. PWS is due to chromosomal aberrations that result in the loss of expression of several imprinted, paternally expressed genes along human 15q11-q13. Genes within the critical region that are paternally expressed in the brain are considered to be candidates for involvement in the neurobehavioral aspects of the syndrome. This thesis describes experiments that address the overall organization of the chromosome 15 imprinted domain, expression patterns of the candidate genes, and a preliminary functional analysis of one candidate gene, *necdin*.

Several genes were already known to be in the 15q11-q13 interval, but it was important to determine whether there were additional uncharacterized, paternally expressed genes that could contribute to PWS. To identify new genes, I mapped novel transcripts to the region and determined their imprinting status. I identified several paternally expressed transcripts that could be involved in the etiology of PWS, showed that there was a domain of paternal expression, and that the imprinting phenomena did not extend outside of 15q11-q13. In parallel, I also examined genomic sequence as it was being released by the Human Genome project. Based on gene prediction programs, I identified and cloned the gene *MAGEL2*, which is paternally imprinted and thus a candidate for involvement in PWS.

Mouse chromosome 7C is conserved with human 15q11-q13 and contains an orthologous set of imprinted genes. Determining the expression pattern of PWS genes in mouse is important for the construction and evaluation of mouse models of PWS and for

determining how each gene contributes to brain development. I surveyed the RNA expression patterns of the mouse PWS candidate in mouse brain at several developmental stages. My results suggest that PWS is a multiple-gene syndrome, with several genes responsible for various aspects of the PWS phenotype. In particular, mouse *necdin* is important for the proper development of motoneurons in the brainstem, the loss of which results in an impaired ability to generate a respiratory rhythm and neonatal respiratory distress.

Acknowledgements

I would like to thank Rachel Wevrick for taking me into her lab and allowing me to wreak havoc for 5.5 years. She has given me guidance when I have needed it, as well as the freedom to pursue my own interests. She has shown me the type of scientist I would like to become.

I would like to thank all the members of my lab for all of their scintillating discussions about science, coffee, shoes, skiing and haircuts. It is because of them that the movie industry has had record profits over the last 5 years. Most importantly, I would like to thank them for making the lab much more than just a place to work. I could not have finished without their friendship, humor and support, for which I am truly grateful.

I thank my family, especially my sister, for trying to be interested in my work, and for their patience and encouragement. I thank my dad for answering all my endless chemistry questions, his "When I was in the lab..." stories, and for introducing me to science in the first place. Finally, I thank my mom for showing me that science is both logic and humanity.

Table of Contents

<i>List of Tables</i>	
<i>List of Figures</i>	
<i>Glossary</i>	
Chapter 1. Introduction.....	1
Prader-Willi syndrome	2
Clinical features of Prader-Willi syndrome	2
Chromosomal aberrations causing PWS.....	9
Imprinting in 15q11-q13.....	11
Mouse models of PWS	16
Uniparental disomy mice	18
Deletion mice	18
Imprinting center mice.....	19
Single gene deletions	20
Parallels to other segmental aneusomy syndromes.....	22
Angelman syndrome.....	23
Williams syndrome.....	24
Smith-Magenis syndrome	26
Neurodevelopment	27
General neurodevelopment	27
Development of the hypothalamus.....	31
Paraventricular nucleus and the supraoptic nucleus.....	33
Suprachiasmatic nucleus.....	34

Hypothalamic nuclei regulating feeding behavior	34
Development of the pituitary gland.....	36
Development of the brainstem	39
Are the PWS traits reflective of a hypothalamus specific or a global dysfunction? .	43
Hypothesis and summary of studies.....	44
Chapter 2. Materials and methods.....	46
Internet resources	47
Chromosome 15 genes and ESTs.....	47
Genomic and cDNA clones	49
Cell lines and tissues	50
Patient samples.....	50
P19 cells.....	50
Mouse breeding	51
PCR reactions.....	52
DNA analysis	52
Genomic DNA extraction	52
DNA sequencing	53
Southern blot analysis.....	53
RNA analysis	54
RNA extraction	54
RT-PCR analysis	54
Northern blot analysis.....	54
cDNA library screening.....	55

Tissue Histology	56
Tissue fixation	56
Tissue sectioning	56
Thionin tissue staining	57
<i>lacZ</i> detection	57
RNA <i>in situ</i> hybridization.....	57
Probe construction	57
Labeling of probes	58
Hybridization and detection	59
 Chapter 3. Identification of novel imprinted transcripts in the Prader-Willi/Angelman syndrome deletion region	 61
Introduction.....	62
Results	68
Selection of expressed sequences: EST contig building and library screening	68
Physical mapping of unique ESTs.....	73
Imprinting status of expressed sequences	73
Expression profile of imprinted ESTs	79
Discussion.....	83
The PWS/AS region has at least eight additional imprinted transcripts.....	83
RT-PCR effectively identifies novel imprinted transcripts	84
Imprinted transcripts cluster around the PWS/AS IC.....	85
Parallel experiments	87

Chapter 4. Identification and expression analysis of the novel gene, <i>MAGEL2</i> , suggests a role in Prader-Willi syndrome	93
Introduction.....	94
Gene identification from genomic sequence.....	94
The MAGE family genes	95
Results	97
In silico identification of <i>MAGEL2</i>	97
Structure of <i>MAGEL2/Magel2</i>	101
Mapping of <i>MAGEL2/Magel2</i>	109
Expression profiles of human and mouse <i>MAGEL2</i>	112
Expression in tissues.....	112
Expression in differentiating murine P19 cells	115
Imprinting of <i>MAGEL2/Magel2</i>	116
Discussion.....	118
Chapter 5. Prader-Willi syndrome transcripts are expressed in phenotypically significant regions of the developing mouse brain.....	122
Introduction.....	123
RNA <i>in situ</i> hybridization.....	124
Using <i>Ndn</i> deficient mice to examine gene expression and function.....	124
Results	127
RNA expression of the PWS candidate genes.	127
PWS transcripts are expressed mainly in the mantle and ventricular cell layers	133
Expression in the forebrain.	135

Expression in the hypothalamic nuclei and arcuate nucleus.....	138
Expression in the hindbrain.....	141
Histological characterization of <i>Ndn</i> deficient mice.	147
Conclusion	151
RNA localization patterns.....	151
Regulation of the <i>Snurf-Snrpn</i> transcription unit	151
Implications for understanding the pathophysiology of PWS.....	152
Loss of neccdin results in motoneuron dysmorphology.....	157
PWS is a global dysfunction involving multiple genes	159
Chapter 6. Conclusion	161
The PWS region contains at least 5 candidate genes	162
Imprinting in 15q11-q13 is controlled as a domain	164
PWS is a global brain dysfunction.	165
Single gene effects.....	170
<i>Mkrn3</i> may have multiple roles throughout development.	170
A role for <i>Magel2</i> in the development and functions of the SCN and SON.	171
<i>Ndn</i> is essential for terminal differentiation and survival of specific neurons....	174
The <i>Snurf/Snrpn</i> transcript has multiple functions.....	175
Additive effects of losing multiple PWS genes.	182
<i>Mkrn3</i> and <i>MBII-85</i> may be important for auditory discrimination.....	183
<i>Magel2</i> and <i>Ndn</i> may be important for development of hypothalamic-pituitary axis.....	183
Directions for further study	188

References 192

Curriculum Vitae..... 216

List of Tables

Table 1- 1. Diagnostic criteria for PWS.....	4
Table 1- 2. Age specific criteria to prompt DNA testing for PWS.....	5
Table 2- 1. Electronic resources.....	47
Table 2- 2. <i>MAGEL2/Magel2</i> PCR primers	49
Table 3- 1. Transcription units and genes in 15q11-q13.....	66
Table 3- 2. Estimate of expression levels for imprinted transcription units.....	82
Table 4- 1. Repetitive elements along pDJ181P7.....	98
Table 4- 2. Localization of the <i>Magel2</i> gene within the mouse syntenic region on 7C..	112

List of Figures

Figure 1- 1. Organization of the human and mouse PWS/AS region.	13
Figure 1- 2. Mouse models of PWS.	17
Figure 1- 3. Time course of mouse development.	29
Figure 1- 4. Major hypothalamic nuclei implicated in PWS.	32
Figure 1- 5. Rodent pituitary development.	38
Figure 1- 6. Brainstem regions involved in respiration.	42
Figure 3- 1. Map of the PWS/AS deletion region.	71
Figure 3- 2. Flow chart illustrating the selection process for ESTs in the 15q11-q13 region.	72
Figure 3- 3. Imprinting status of genes and ESTs.	77
Figure 3- 4. Current transcript and gene organization within the PWS critical region.	90
Figure 4- 1. Gene prediction along pDJ181P7.	100
Figure 4- 2. Genomic organization of human <i>MAGEL2</i>	104
Figure 4- 3. Genomic organization of mouse <i>Magel2</i>	106
Figure 4- 4. Sequence comparisons among <i>MAGEL2</i> , <i>NDN</i> and their murine orthologs.	108
Figure 4- 5. Localization of the <i>MAGEL2</i> gene in the 15q11-13 imprinting domain.	111
Figure 4- 6. Northern blot expression analysis of <i>MAGEL2/Magel2</i>	114
Figure 4- 7. Paternal origin of <i>MAGEL2/Magel2</i> gene expression.	117
Figure 5- 1. Generation of the <i>Ndn^{tm2Snv}</i> allele.	125
Figure 5- 2. Northern analysis of RNA <i>in situ</i> probes.	129
Figure 5- 3. Embryonic expression of <i>Ndn-lacZ</i>	132

Figure 5- 4. PWS genes expressed in early development.	134
Figure 5- 5. <i>Ndn</i> , <i>Snrpn</i> and <i>Ipw</i> are highly expressed throughout the forebrain at E18.5.	136
Figure 5- 6. <i>Mkrn3</i> , <i>Magel2</i> and <i>Ndn</i> are expressed in the developing pituitary gland..	137
Figure 5- 7. <i>Ndn</i> , <i>Snrpn</i> and <i>Ipw</i> are highly expressed in regions regulating feeding at E18.5.....	139
Figure 5- 8. <i>Magel2</i> is preferentially expressed in the suprachiasmatic nucleus and the supraoptic nucleus.	140
Figure 5- 9. PWS genes are expressed in the hindbrain.....	143
Figure 5- 10. <i>Ndn</i> , <i>Snrpn</i> and <i>Ipw</i> are expressed in the raphe nucleus.	144
Figure 5- 11. <i>Ndn</i> is expressed in the fetal medulla.....	146
Figure 5- 12. <i>Ndn</i> deficient mice show motoneuron loss in the hindbrain.....	150
Figure 6- 1. Hypothetical model of the effect that PWS genes have on the development of discrete regions of the brain.....	169
Figure 6- 2. Comparison of transcripts from the <i>Snurf/Snrpn</i> and <i>Ube3a</i> promoters.....	180
Figure 6- 3. <i>Magel2</i> and <i>Ndn</i> may be members of transcription factor cascades controlling hypothalamic development	187

Glossary

Androgenetic	A diploid genome derived from paternally inherited genetic material, with no maternal contribution
aPV	Anterior periventricular nucleus
ARC	Arcuate nucleus
AS	Angelman syndrome
BAC	Bacterial artificial chromosome
cDNA	Complementary DNA
CRH	Corticotropin-releasing hormone
DIG	Digoxygenin
EST	Expressed sequence tag
GH	Growth hormone
Gynogenetic	A diploid genome derived from maternally inherited genetic material, with no paternal contribution
IC	Imprinting center
LINE	Long interspersed nuclear element
NTS	Nucleus tractus solitarius
OCD	Obsessive compulsive disorder
OT	Oxytocin hormone
PAC	P1 artificial chromosome
PCR	Polymerase chain reaction
PVN	Paraventricular nucleus of the hypothalamus
PWS	Prader-Willi syndrome
RA	Retinoic acid

RH	Radiation hybrid
RM	Raphe magnus
RT	Reverse-transcription
RT-PCR	Reverse-transcriptase polymerase chain reaction
SAS	Segmental aneusomy syndrome
SCN	Suprachiasmatic nucleus
SINE	Short interspersed nuclear elements
SMS	Smith-Magenis syndrome
snoRNA	Small nucleolar RNA
STS	Sequence tagged site
SON	Supraoptic nucleus
UPD	Uniparental disomy
UTR	Untranslated region
VMN	Ventromedial nucleus
VP	Vasopressin hormone
WS	Williams syndrome
YAC	Yeast artificial chromosome

Chapter 1. Introduction

Prader-Willi syndrome

Clinical features of Prader-Willi syndrome

Prader-Willi syndrome (PWS, Online Mendelian Inheritance in Man number 17670) was first described in 1956 (Prader et al., 1956). It is a neurobehavioral disorder that occurs at a rate of about 1/15,000 births. The major diagnostic criteria were established in 1993, and include global developmental delay and neonatal hypotonia, which occur in over 97% of patients (Gunay-Aygun et al., 2001; Holm et al., 1993). In addition, neonatal feeding difficulties with failure to thrive, hyperphagia with excessive weight gain in early childhood, characteristic facial features, and hypogonadism are also major criteria in the clinical diagnosis of PWS (Table 1-1) (Holm et al., 1993). Other common findings include behavioral problems, respiratory difficulties, sleep disturbances, short stature, as well as small hands and feet. Because some of the features of PWS vary with age, age specific criteria for molecular testing of PWS have recently been proposed (Table 1-2) (Gunay-Aygun et al., 2001).

Table 1-1. Diagnostic criteria for PWS.

The published consensus diagnostic criteria for the clinical diagnosis of PWS. To score, major weighted criteria are weighted at 1 point each, and minor criteria are 0.5 point each. Supportive findings increase the certainty of the diagnosis, but are not scored. For children under 3, 5 points are required, 4 of which should be major criteria. For children older than 3 and adults, 8 points are needed, and 5 or more should be major criteria. Table taken from Holm, V. A., Cassidy, S. B., Butler, M. G., Hanchett, J. M., Greenswag, L. R., Whitman, B. Y. and Greenberg, F. (1993). Prader-Willi syndrome: consensus diagnostic criteria. *Pediatrics* 91, 398-402.

Major Criteria

1. Neonatal and infantile central hypotonia with poor suck, improving with age.
2. Feeding problems in infancy and poor weight gain/failure to thrive.
3. Excessive or rapid weight gain between 12 months and 6 years of age; central obesity.
4. Characteristic facial features with dolichocephaly (long skull), narrow face or bifrontal diameter, almond-shaped eyes, small appearing mouth with thin upper lip, down-turned corners of the mouth (3 or more required).
5. Hypogonadism—depending on age:
 - a. Genital hypoplasia.
 - b. Delayed or incomplete gonadal maturation with delayed pubertal signs in the absence of intervention after 16 years.
6. Global developmental delay when less than 6 years of age; mild to moderate mental retardation or learning problems in older children.
7. Hyperphagia, food foraging, obsession with food.
8. Cytogenetic deletion of 15q11-q13 or other cytogenetic/molecular abnormality of the PWS region, including maternal disomy.

Minor Criteria

1. Decreased fetal movement, infantile lethargy, or weak cry, improving with age.
2. Characteristic behavior problems: temper tantrums, violent outbursts and obsessive-compulsive behavior; tendency to be argumentative, oppositional, rigid, manipulative, possessive, and stubborn, perseverating, stealing and lying (5 or more required).
3. Sleep disturbance or sleep apnea.
4. Short stature for genetic background by age 15.
5. Hypopigmentation compared to family.
6. Small hands and/or feet for height age.
7. Narrow hands with straight ulnar border.
8. Eye abnormalities (esotropia, myopia).
9. Thick, viscous saliva with crusting at corners of the mouth.
10. Speech articulation defects.
11. Skin picking.

Supportive Findings

1. High pain threshold.
2. Decreased vomiting.
3. Temperature instability in infancy or altered temperature sensitivity in older children and adults.
4. Scoliosis and/ or kyphosis.
5. Early adrenarche.
6. Osteoporosis.
7. Unusual skill with jigsaw puzzles.
8. Normal neuromuscular studies.

Table 1- 2. Age specific criteria to prompt DNA testing for PWS.

Age at Assessment	Features Sufficient to Prompt DNA Testing
Birth to 2 yrs	1. Hypotonia with poor suck.
2 yrs-6yrs	1. Hypotonia with history of poor suck. 2. Global developmental delay.
6yrs-12yrs	1. History of hypotonia with poor suck (hypotonia often persists). 2. Global developmental delay. 3. Excessive eating (hyperphagia; obsession with food) with central obesity if uncontrolled.
13yrs-adulthood	1. Cognitive impairment; usually mental retardation. 2. Excessive eating (hyperphagia; obsession with food) with central obesity if uncontrolled. 3. Hypothalamic hypogonadism and/or typical behavior problems (including temper tantrums and obsessive-compulsive features).

Table from Gunay-Aygun, M., Schwartz, S., Heeger, S., O'Riordan, M. A. and Cassidy, S. B. (2001). The changing purpose of Prader-Willi syndrome clinical diagnostic criteria and proposed revised criteria. *Pediatrics* 108, E92.

The clinical course of PWS can be divided into three phases (Descheemaeker et al., 2002; Gunay-Aygun et al., 2001). The first phase, known as the “hypotonic phase” covers the prenatal period and early infancy. During their pregnancies, mothers of PWS children often experience hydramnios and decreased fetal movements (Zellweger, 1981). There is also an increased incidence of abnormal parturition timing of PWS children, with deliveries often occurring before the 38th week and after the 42nd week of pregnancy (Wharton and Bresnan, 1989; Zellweger, 1981). PWS neonates are unresponsive, inactive and have severe hypotonia (Descheemaeker et al., 2002; Zellweger, 1981). They are also characterized by a weak cry, hypothermia, hypothalamic hypogonadism, and poor suck reflex requiring gavage feeding (Butler et al., 1986; Descheemaeker et al., 2002; Hall and

Smith, 1972). During the first year, PWS infants are described as friendly, easy going and affectionate (Descheemaeker et al., 2002).

The “hyperphagic phase” begins between the first and second year, and is characterized by hyperphagia, food foraging, and obesity (Descheemaeker et al., 2002). Other problems that arise during this period include decreased physical activity and pain sensitivity; problems with thermoregulation, speech articulation, psychomotor and cognitive skills. PWS children often develop maladaptive behavioral and emotional problems including temper tantrums, inappropriate social behavior, skin picking, stubbornness, mood lability, impulsiveness, argumentativeness, depression, anxiety, autism spectrum disorder and obsessive-compulsive symptoms.

During the “adolescence and adulthood” phase, health problems which are thought to be secondary to the obesity arise, including scoliosis, dental problems, diabetes mellitus, hypertension, hypercholesterolemia, and osteoporosis (Descheemaeker et al., 2002). Older patients with PWS also tend to show confusion, prefer to be alone, lack energy and are overtired. Many adults with PWS show psychiatric problems including acute cycloid psychosis, obsessive-compulsive disorder, and bipolar disorder. Complications due to obesity is the major cause of morbidity (Cassidy et al., 2000).

Many of the problems that characterize PWS may be due to a hypothalamic deficiency, such as abnormal parturition timing, hypogonadism, and obesity (Cassidy et al., 2000; Swaab, 1997). Abnormal hypothalamic lutenizing hormone releasing hormone neurons could result in decreased levels of sex hormones and the hypogonadism seen in PWS patients (Swaab, 1997). Hyperphagia may be due to an impaired satiety mechanism coupled with an increased drive to eat. This can be due to a hypothalamic defect, and

studies focusing on this region have found that in PWS individuals, a discrete region known as the paraventricular nucleus of the hypothalamus, is reduced in both in volume and total cell number (Swaab et al., 1995).

It is postulated that a growth hormone (GH) deficiency may be the cause of the short stature, high body-fat mass especially in the abdomen, low muscle mass, decreased bone marrow density accompanied by high incidence rates of osteoporosis and decreased insulin-like growth factor-1 levels (Costeff et al., 1990; Hoybye et al., 2002; Lee, 1995). Depending on the test conditions used, 40-100% of PWS children fulfill the criteria for a GH deficiency, defined as having peak GH levels less than 10 µg/liter in response to one or two stimulation tests (reviewed in Burman et al., 2001). Furthermore, blood sampling of PWS children shows low levels of GH secretion (Burman et al., 2001). Anatomical data supporting these findings show a 30% reduction in GH-releasing hormone neurons in the arcuate nucleus (Burman et al., 2001; Swaab, 1997).

Currently, there is no treatment for PWS, however, GH treatment has proven the most effective in alleviating the majority of the symptoms, including morbid obesity and short stature (Burman et al., 2001). Initial GH treatments leads to reduced fat mass and increased lean body mass, increased resting energy expenditure, improved physical function, and changes in carbohydrate and lipid metabolism (Burman et al., 2001; Carrel et al., 2002). However, response to GH decreases during prolonged therapy, and long-term treatment does not seem to be sufficient to normalize body composition (Carrel et al., 2002; Eiholzer et al., 2000). GH also stabilizes BMI, and improves motor performance, agility, respiratory muscle strength, ventilation and improves the sensitivity of peripheral chemoreceptors to carbon dioxide (Burman et al., 2001). There have been

several reports that suggest that GH also improves energy levels, endurance, and psychosocial functioning (Burman et al., 2001).

Recently, several groups have reported elevated levels of the enteric hormone ghrelin in PWS patients as compared to lean and obese control individuals (Cummings et al., 2002; DelParigi et al., 2002; Haqq et al., 2003). Ghrelin is produced primarily in the stomach and excreted into the blood where it is thought to be transported to the brain (Kojima et al., 1999). Ghrelin has also been detected in the hypothalamic neurons that innervate hypothalamic regions implicated in metabolism regulation (Cowley et al., 2003). Ghrelin is a ligand of the GH secretagogue receptor and regulates expression of GH from the pituitary, and may influence the release of orexigenic peptides and neurotransmitters from the hypothalamus (Cowley et al., 2003; Kojima et al., 1999). In rodents, ghrelin has also been shown to increase food intake and decrease fat metabolism resulting in increased weight (Nakazato et al., 2001; Tschop et al., 2000). In humans, levels of ghrelin in the plasma increase prior to each meal and decrease after food intake, suggesting that ghrelin is involved in the initiation of food consumption (Cummings et al., 2001; Tschop et al., 2001). Furthermore, in control subjects, ghrelin levels are inversely related to body mass index while in PWS individuals, elevated ghrelin levels were detected regardless of body weight (Cummings et al., 2002; Haqq et al., 2003). Hyperghrelinemia provides an attractive model to explain the hyperphagia and GH deficiency seen PWS individuals (Cummings et al., 2002; DelParigi et al., 2002; Haqq et al., 2003).

Chromosomal aberrations causing PWS

The first chromosomal aberration causing PWS was described in 1981 as a deletion along chromosome 15 (Ledbetter et al., 1981). Since then, four molecular causes of PWS have been discovered, all of which affect the expression of genes on the paternally inherited copy of chromosome 15.

The most common mutation resulting in PWS is a 4 Mb *de novo* deletion along the paternal copy of chromosome 15q11-q13 and is found in 70% of patients (Nicholls et al., 1998). This common deletion is related to repeated clusters at either end of the region that may predispose this region to unequal homologous recombination (Amos-Landgraf et al., 1999; Christian et al., 1999; Christian et al., 1995). Approximately 20-30% of patients have maternal uniparental disomy (UPD) of chromosome 15, where both copies of the chromosome are inherited from the mother (Mascari et al., 1992). 2-5% of patients have submicroscopic deletions that span exon 1 of the *SNRPN* gene, which abolishes expression from the paternal allele of numerous genes along 15q11-q13 (Buiting et al., 1995; Ohta et al., 1999; Shemer et al., 2000). A small fraction of PWS cases show loss of expression from the paternal allele of these genes but do not have any detectable mutations along 15q11-q13 (Buiting et al., 2003). Although deletion and UPD cases were initially thought to have identical clinical phenotypes (Robinson et al., 1991), as more patients have been identified, it has become apparent that, in general, UPD patients have milder presentations than deletion patients (Cassidy, 1997; Cassidy et al., 2000). Often, patients with UPD lack the distinctive facial features that characterize PWS. Haploinsufficiency of one or more genes within the 15q11-q13 interval may be responsible for the genotype-phenotype differences seen in UPD and deletion patients.

Although the 15q11-q13 deletions define a 4Mb genomic interval that is involved in PWS, several families with inherited microdeletions have refined the telomeric boundary for genes critical for PWS. Individuals that paternally inherit microdeletions with the centromeric breakpoint at the marker D15S174 are phenotypically normal (Burger et al., 2002; Greger et al., 1993; Hamabe et al., 1991). The microdeletion cases suggest that although the common breakpoint is defined by flanking repeats, the genes critical to PWS are centromeric to D15S174.

Less than 1% of patients have balanced translocations through the paternal copy of the 15q11-q13 region that disrupt the expression of one or more genes (Cassidy et al., 2000). Each of the reported balanced translocation cases involve different partner chromosomes. However, there are several common breakpoints in the PWS region, suggesting the presence of direct or inverted repeats or repetitive sequences that predispose the region to rearrangements (Wirth et al., 2001). Five translocation breakpoints have been mapped using DNA markers in the PWS region, and in all of these cases, the chromosome 15 breakpoint lies within the *SNRPN* gene (Conroy et al., 1997; Kuslich et al., 1999; Schulze et al., 1996; Sun et al., 1996; Wirth et al., 2001). Despite the clustering of translocation breakpoints, there is considerable phenotypic variation among the patients. Two of the translocation patients were considered to have typical presentations of PWS, presenting with the cardinal features of neonatal hypotonia, feeding problems during the neonatal period, hyperphagia, obesity, characteristic facial features and developmental delay (Kuslich et al., 1999; Sun et al., 1996). Three translocation patients were considered to have “atypical” PWS, as not all of the major features were observed (Conroy et al., 1997; Schulze et al., 1996; Wirth et al., 2001).

These translocations suggest that PWS cannot easily be explained by the loss of a single candidate gene, such as *SNRPN*. Furthermore, they suggest that the location of the breakpoint in the *SNRPN* gene may be important for the clinical course of PWS.

Imprinting in 15q11-q13

The fact that all of the molecular aberrations that cause PWS affect the paternal copy of chromosome 15 is supportive of genomic imprinting of this region. Genomic imprinting is the process by which a pair of alleles is differentially expressed between the maternal and paternal alleles (Tilghman, 1999). Parental epigenotypes, or imprints, are set during gametogenesis and transmitted to the embryos (Ferguson-Smith and Surani, 2001). Although numerous genes have been mapped to the 15q11-q13 region, only those that are imprinted and paternally expressed are candidates for PWS. As no patients have been identified with single gene mutations, PWS is thought to be a segmental aneusomy syndrome that is due to the loss of multiple, paternally expressed genes within the deletion interval (Budarf and Emanuel, 1997).

When I first began my project, 4 paternally expressed genes were already known to map to the PWS region: *MKRN3*, *NDN*, *SNRPN* and *IPW* (Figure 1-1). The first gene to be shown to be imprinted in this region was the *SNRPN* gene, which encodes the small nuclear ribonucleoprotein SmN subunit and is thought to be involved in neuron specific brain mRNA splicing (Ozcelik et al., 1992; Schmauss et al., 1989). *IPW* (imprinted in Prader-Willi) was the next gene identified, and is an untranslated RNA that is expressed exclusively from the paternal allele (Wevrick et al., 1994). *MKRN3* (*ZNF127*) is a zinc finger transcription factor that is ubiquitously expressed (Jong et al., 1999a; Jong et al., 1999b). The *MKRN3* gene is located within an overlapping antisense transcript,

MKRN3AS (ZNF127AS) and the two transcripts show mutually exclusive expression in human tissues. While *MRKN3* is paternally expressed, the imprinting status of *MKRN3AS* is unknown, although the orthologous copy in mouse is only expressed from the paternal allele. The most extensively studied paternally expressed gene in the region is neccin (*NDN*). Mouse neccin was originally identified in a screen for genes involved in the differentiation of mouse embryonic carcinoma cells into a neuronal cell fate (Aizawa et al., 1992). The human orthologue was later mapped to the PWS region and shown to be imprinted (Jay et al., 1997; MacDonald and Wevrick, 1997). The identification and cloning of the most recently identified imprinted gene, *MAGEL2* (Boccaccio et al., 1999; Lee et al., 2000), will be discussed in Chapter 4.

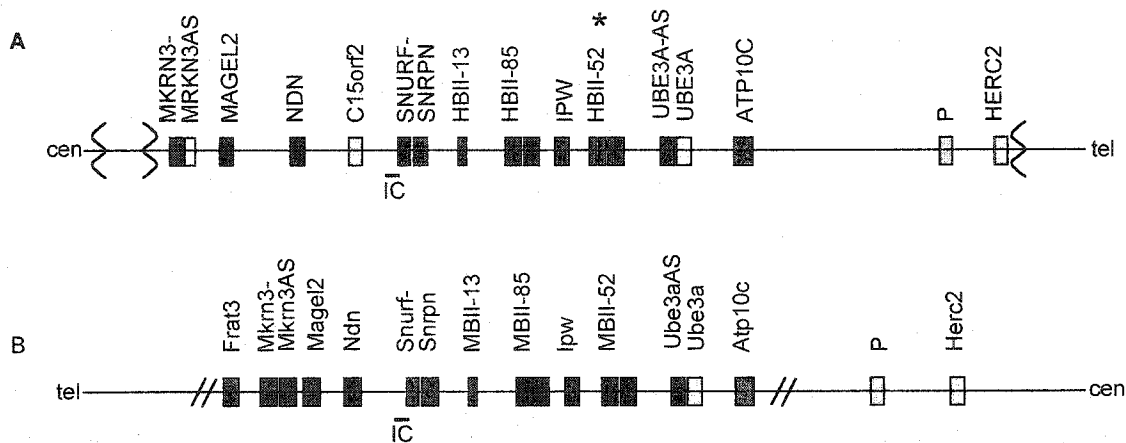


Figure 1- 1. Organization of the human and mouse PWS/AS region.

(A) The location and imprinting status of known genes along human 15q11-q13. The blue squares represent the paternally expressed genes, red squares are maternally expressed, yellow squares are biallelic, and the white square represents uncertain imprinting status. The location of the IC is represented by a short horizontal bar. The locations of the common deletion breakpoints are shown with curved lines. The location of the marker D15S174 that defines the limit of the PWS critical region is indicated by (*). The relative positions of only some of the snoRNAs are indicated. (B) The location and imprinting status of known genes in the mouse syntenic region of 7C. Diagonal lines represent a gap in the diagram. Figure adapted from Chai, J. H., Locke, D. P., Ohta, T., Grelly, J. M. and Nicholls, R. D. (2001). Retrotransposed genes such as Frat3 in the mouse Chromosome 7C Prader-Willi syndrome region acquire the imprinted status of their insertion site. *Mamm Genome* 12, 813-821.

The 15q11-q13 region also contains 2 maternally expressed genes. *UBE3A* (E6-AP ubiquitin protein ligase 3A) is involved in the transfer of ubiquitin to protein substrates in the ubiquitin-proteasome proteolytic pathway (Hochstrasser, 1996). It is expressed preferentially from the maternal allele in the brain, but shows biallelic expression in fibroblasts and lymphoblasts (Rougeulle et al., 1997; Vu and Hoffman, 1997). Loss of expression of *UBE3A* results in Angelman syndrome (discussed in “Parallels to other segmental aneusomy syndromes”). Recently, *ATP10C*, a second gene with brain-specific preferential expression from the maternal allele was identified (Herzing et al., 2001; Meguro et al., 2001a). The gene is a P-type ATPase, and mice that inherit a maternal deletion of the murine orthologue (*Atp10c/Pfatp*) develop increased levels of body fat (Dhar et al., 2000).

Recent work has shown that the *SNRPN* locus is quite complex, spanning 460 kb with at least 148 known exons (Runte et al., 2001). Exons 1-3 encode for *SNURF* (*SNRPN* upstream reading frame), a highly basic, nuclear localized protein; while exons 4-10 encode for *SNRPN* (Gray et al., 1999a). The 4.3 kb microdeletions that abolish expression of the paternally expressed genes include exon 1 and additional upstream sequence. This region has been named the imprinting center (IC), and is necessary for postzygotic maintenance of imprinting this region (Bielinska et al., 2000; El-Maarri et al., 2001). Mutations of the IC result in functional maternal UPD in PWS patients (Horsthemke, 1997). IC mutations block the resetting of the imprint in the germline, thus a failure in the switching of the imprint can result in a paternal chromosome with a maternal epigenotype. The IC has a bipartite structure, and the more centromeric portion, deleted in some AS patients, is involved in the paternal to maternal imprint switch. The

telomeric portion, deleted in some PWS patients, is responsible for the maternal to paternal epigenotype switch.

Although *IPW* has its own polyadenylation signal, it has been shown to be made up of exons 59-61 of the *SNURF/SNRPN* transcriptional unit (Figure 1-1) (Runte et al., 2001). *SNURF/SNRPN* has at least two alternative 5' start sites and several untranslated upstream exons of unknown function (Dittrich et al., 1996; Farber et al., 1999). The transcript also serves as a host for a set of imprinted, paternally expressed, small nucleolar RNAs (snoRNAs): *HBII-13*, *HBII-52*, *HBII-85*, *HBII-436*, *HBII-437*, *HBII-438A*, and *HBII-438B*. (Cavaille et al., 2000; de los Santos et al., 2000; Meguro et al., 2001b; Runte et al., 2001). The snoRNAs are located in the introns of the *SNURF/SNRPN* transcriptional unit and may be involved in rRNA processing, ribosome assembly or post-transcriptional RNA modification (Cavaille et al., 2000). *HBII-52* and *HBII-85* are unique among snoRNAs in that they are expressed from tandemly repeated genes, with 47 and 24 copies respectively, and are among the most abundant snoRNAs in the brain. *HBII-52* shows an 18 nt complementarity to the gene encoding the serotonin receptor 2C, and it has been speculated that *HBII-52* is involved in serotonin 5-HT_{2C} receptor mRNA editing, or regulation of alternative splicing (Cavaille et al., 2000).

The *SNURF/SNRPN* transcript also regulates the expression of *UBE3A*. The *UBE3A* gene has an antisense transcript that is paternally expressed, which is now shown to be part of the longer *SNURF/SNRPN* transcriptional unit (Rougeulle et al., 1998; Runte et al., 2001). In mice, the paternally expressed transcript is shown to repress the expression of mouse *Ube3a* from the paternal allele, resulting in a functionally imprinted, maternally expressed gene (Chamberlain and Brannan, 2001).

Mouse models of PWS

The human 15q11-q13 region has a syntenic region on the central region of mouse chromosome 7 (mouse 7C) (Chaillet et al., 1991), which contains an orthologous set of imprinted genes. Though the region is highly conserved between mouse and human, with the imprinted genes maintaining the same genomic organization relative to each other, there are some important differences. The imprinted region in mouse is not flanked by repeats and is thus not predisposed to recombinational events leading to deletions as seen in humans. Thus, there are no naturally occurring mouse models of PWS. The 15q11-q13 region contains a nonimprinted, testis specific gene, *C15orf2*, which is only present in humans and primates, and not in mouse (Farber et al., 2000). Furthermore, the mouse region houses two additional genes, *Frat3*, which is imprinted and expressed from the paternal allele; and *Atp5l-ps1*, a pseudogene (Chai et al., 2001). Because of the high level of conservation between human and mouse, chromosome 7C has been the focus of transgenic experiments to create a mouse model of PWS. A description of the various mouse models follows and is summarized in Figure 1-2.

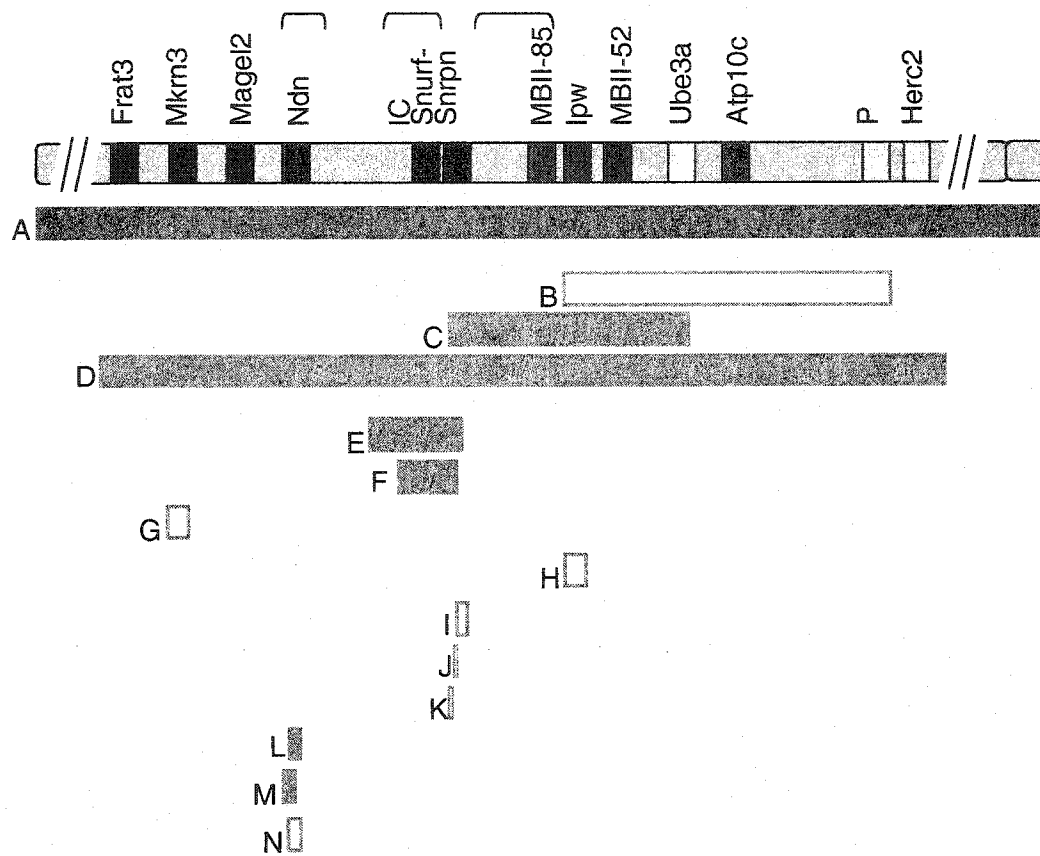


Figure 1- 2. Mouse models of PWS.

Mouse chromosome 7 is represented in gray. Paternally expressed genes are in blue, maternally expressed are red, and biallelic genes are yellow. *Ube3a* is depicted in yellow, but it is functionally maternally expressed. Pink bar represents the region involved in the maternal UPD mouse. Green bars represent sequence removed in deletion mice. Orange bars represent sequence removed in single gene deletion mice. Filled bars are mice that demonstrate a phenotype. Empty bars are mice that have no observable phenotype. Brackets define three minimal regions that are necessary for postnatal survival. See text for description of mouse models A-N.

Uniparental disomy mice

Both maternal and paternal contributions are required for complete mouse embryogenesis. Gynogenetic mouse embryos develop to the 25 somite stage; however, the extra-embryonic tissues remain rudimentary (Surani and Barton, 1983). In contrast, androgenetic mouse embryos are poorly developed reaching only the 6-8 somite stage, while the extra-embryonic tissues are well developed (Barton et al., 1984). These developmental differences are due to the differences in the expression of imprinted genes.

One method that was used to assess the effect of imprinting on the PWS syntenic region was to construct mice with a maternal uniparental disomy of 7C (Figure 1-2 A). These mice had postnatal lethality, dying within 3-8 days after birth (Cattanach et al., 1992). The mice showed reduced suckling, which is consistent with the feeding difficulties and failure to thrive seen in PWS infants.

Deletion mice

Deletions of all or part of the imprinted region on paternal mouse chromosome 7C have been constructed to determine the genes essential for survival and for the maintenance of imprinting. In one set of experiments a series of radiation induced deletions were generated along mouse 7C (Johnson et al., 1995). One line of mice had a deletion beginning around *Ipw* and continuing distally to include the non-imprinted *P* and *Rjs/Herc2* genes (Figure 1-2 B). This deletion was lethal when inherited in a homozygous state, but did not produce a phenotype when paternally inherited. However, mice carrying a paternally inherited targeted deletion of exon 2 of *Snrpn* to exon 2 of *Ube3a* showed decreased movement, hypotonia, and decreased ability to right themselves when placed on their backs (Figure 1-2 C) (Tsai et al., 1999b). The newborn mice were able to suckle,

but had less milk in their stomachs than wildtype littermates. 50% of the mice that inherited the paternal deletion died by postnatal day 12, and 78% died before weaning. The mice also showed severe growth retardation, and were underweight when compared to littermates. This deletion did not affect the IC, as the paternal expression of *Ndn* was maintained. The data from these two deletion lines suggests the presence of a transcript between *Snrpn* and *Ipw*, such as *MBII-85*, which may be important for survival and growth in the postnatal period.

A third mouse deletion model was generated by a transgene insertion into 7C, which unexpectedly deleted the complete PWS/AS-homologous region (Figure 1-2 D) (Gabriel et al., 1999). Pups inheriting the paternal deletion showed a decreased growth rate, appeared dehydrated, although milk was observed in their stomachs, decreased movement, irregular respiratory rates and died within 1 week. The intact homologous chromosome 7C maintained imprinting in somatic cells, and no expression was detected from the imprinted genes *Snurf*, *Snrpn*, *Ipw*, *Mkrn3* and *Ndn*, confirming that these genes are expressed exclusively from the paternal allele.

Imprinting center mice

Mice with targeted deletions of the homologous murine IC have also been created. A 42 kb deletion removing exons 1-6 of *Snrpn*, as well as 16 kb of upstream sequence including the IC, was created (Figure 1-2 E) (Yang et al., 1998). At birth, mice with paternally inherited deletions of the IC were smaller than wildtype littermates. The heterozygous mice also appeared hypotonic, and were unable to support themselves on their hind paws. Most mice died within 72 hours, and all within 7 days. Mice that survived past the initial perinatal period appeared dehydrated and weak, did not maintain

normal growth rates, had less milk in their stomachs, and lower blood glucose levels. No expression of *Ndn*, *Ipw* and *Mkrn3* could be detected in the heterozygotes. A second IC deficient mouse was created by deleting 4.8 kb of sequence around *Snrpn* exon 1 (Figure 1-2 F) (Bressler et al., 2001). When the deletion was inherited on the paternal chromosome, it resulted in a 40% postnatal lethality. Though surviving mice were fertile, they showed severe growth retardation. The expression of paternal, imprinted genes were assayed in the heterozygous mice, and was decreased compared to wild type mice suggesting a partial defect in imprinting. These experiments show that the function and location of the IC is conserved between humans and mice.

Single gene deletions

Individual gene knockouts have been constructed for most of the PWS orthologous mouse genes. Deletions of *Mkrn3* and *Ipw* do not produce a phenotypic effect (Figure 1-2 G, H) (Gerard et al., 1999). The *SNURF/SNRPN* locus has been proposed to be the sole candidate gene for PWS syndrome based on patients with disruptions around the locus. Microdeletions that center around exon 1 and the IC silence expression from the paternal allele of the imprinted genes (Buiting et al., 1995; Horsthemke, 1997; Ohta et al., 1999; Sutcliffe et al., 1994). As well, PWS patients have been described with translocations disrupting *SNRPN* (Kuslich et al., 1999; Sun et al., 1996). However, mice that were engineered with a deletion of exon 6, and portions of exons 5 and 7, were viable and had no phenotypic or histological defects (Figure 1-2 I) (Yang et al., 1998). Mice with deletions of exon 2 were also fertile and viable (Figure 1-2 J) (Tsai et al., 1999b). Finally, a 0.9 kb deletion spanning exon 1 and some upstream sequence also produced normal mice (Figure 1-2 K) (Bressler et al., 2001). These results

show that the coding regions of *Snrpn* are not essential for proper growth, nor are they important for the maintenance of imprinting.

Three separate mouse *ndn* knockouts have been constructed, two of which have a neonatal lethal phenotype. The first knockout was created by a targeted insertion of the reporter gene *lacZ*, replacing the *Ndn* open reading frame (Figure 1-2 L) (Gerard et al., 1999). Mice with a paternal inherited deletion died within 30 hours after birth, and 10% of them had milk in their stomachs. Pups were cyanotic and dyspneic. The frequency of respiratory contractions dropped just prior to death and was accompanied by hypotonia. Histological analysis of the mutant mice showed that the lungs were either uninflated or only partially inflated. A second line of *Ndn* deficient mice was created in which the promoter and the first two-thirds of the open reading frame were deleted (Figure 1-2 M) (Muscatelli et al., 2000). These mice showed a partial, early postnatal lethality due to cyanosis and respiratory distress, however the survival rate was higher. A 29% decrease in the number of oxytocin expressing neurons was found in the paraventricular nucleus. These *Ndn* deficient mice also showed behavioral changes including increased skin scraping and increased spatial memory when assayed with the Morris water maze test (Muscatelli et al., 2000). A third *Ndn* deficient mouse was created, also by substituting the open reading frame with a *lacZ* reporter gene, however, this construct did not produce a noticeable phenotype when paternally inherited (Figure 1-2 N) (Tsai et al., 1999a). Differences in the resulting phenotype of the three *Ndn* deficient lines may be due to differences in the targeting constructs used to remove the paternal allele and/or differences in genetic background between the mice.

The various mouse models have shown that imprinting control and organization is conserved between the human 15q11-q13 region and the syntenic mouse region on 7C. Mice exhibit very similar phenotypes when the imprinted, paternal alleles are silenced, whether by uniparental disomy, deletions of the imprinted region, or mutations of the imprinting center. Although useful for investigating the molecular mechanisms of imprinting in this region, the mouse models do not fully recapitulate the PWS phenotype. In particular, none of the mice develop the hallmark hyperphagia and obesity seen in PWS.

Parallels to other segmental aneusomy syndromes

PWS is considered to be a contiguous deletion syndrome, or more accurately, a segmental aneusomy syndrome, in that the disorder results from an inappropriate dosage of one or more critical genes within the genomic segment 15q11-q13 (Budarf and Emanuel, 1997). There have yet to be any patients identified with a mutation disrupting a single gene, suggesting that PWS is most likely due to the combined loss of several paternally expressed genes in the imprinted domain (Nicholls et al., 1998).

The identification of the genes affected in segmental aneusomies with neurological phenotypes will give insights into the molecular basis of specific features of human cognition and behavior. Segmental aneusomies can affect the expression of multiple genes. One of the challenges of understanding the pathophysiology of these syndromes is to determine whether the phenotype is the result of a single causative gene, or whether the cumulative loss of several genes contributes to the final phenotype (Budarf and Emanuel, 1997). The first step in dissecting segmental aneusomies is to identify all of the genes that are affected. However, for most non-imprinted genes, a 50%

alteration in gene dosage does not have a phenotypic effect (Tassabehji et al., 1999). The functional role of a gene is often tested by constructing transgenic mice that either lack or over-express the gene in question; however, it is often difficult to detect cognitive or behavioral defects in mice. Furthermore, it is difficult to predict how a human neurological defect will manifest in mice, making human-mouse cross-species comparisons difficult. Thus, the power of transgenic mice is limited for studying neurological disorders. Finally, cognitive and behavioral problems are often strongly influenced by genetic background in both mice and humans.

There are numerous segmental aneusomies that have a neurological phenotype, including Angelman syndrome, a single gene disorder; Williams syndrome, a multiple gene disorder; and Smith-Magenis syndrome, in which the number of critical genes is unclear. Candidate genes for segmental aneusomies should be dosage sensitive with haploinsufficiency effects. Genes involved in PWS and Angelman syndrome are the exception. As both of these disorders are imprinted, a candidate gene would produce a phenotype only when completely absent.

Angelman syndrome

Angelman syndrome (AS, OMIM 105830) is a single gene disorder of the ubiquitin-dependent proteosomal pathway for protein degradation. AS occurs at a rate of 1/10,000 to 1/15,000 and is a severe neurological disorder that is clinically distinct from PWS, but which involves the same region of 15q11-q13 (Williams et al., 1995). AS is characterized by severe developmental delay, ataxia, absence of speech or minimal use of words, and a behavioral profile of frequent laughter, happy demeanor, and excitable personality. Less common features include microcephaly, seizures and abnormal

electroencephalograms. Approximately 70% of AS cases are due to a deletion of 15q11-q13 on the maternal chromosome, 10-15% are due to mutations of the gene E6-AP ubiquitin-protein ligase (*UBE3A*), 3-5% are due to paternal UPD of chromosome 15, 2-5% are due to mutations in the imprinting center, and less than 1% are a result of translocations through the PWS/AS critical region (Cassidy et al., 2000). In 10% of cases, the molecular cause of AS is not known. Because structural mutations affect the maternal copy of 15q11-q13 or disrupt the maternally expressed *UBE3A*, AS is recognized to be an imprinted disorder. Although the 15q11-q13 region houses many genes, including another maternally expressed gene, *ATP10C* (Herzing et al., 2001; Meguro et al., 2001a), the loss of *UBE3A* alone is sufficient to cause AS, and the syndrome can be classified as a single gene disorder (Kishino et al., 1997; Matsuura et al., 1997). Further evidence for the involvement of *UBE3A* in AS comes from mouse knockout experiments. Mice with a maternally inherited, targeted disruption of exon 2 of *UBE3A* have phenotypic abnormalities that resemble AS including inducible seizures, abnormal electroencephalograms, defective context dependent learning and increased cytoplasmic p53 in neurons that is suggestive of a defect in the ubiquitin pathway (Jiang et al., 1998).

Williams syndrome

When several genes contribute to the phenotype of a segmental aneusomy, it is often possible to determine the contribution of each gene to the final phenotype through the identification of single gene mutations or smaller deletions that result in a partial or milder phenotype. This approach was taken to elucidate the role of some of the genes involved in the neurodevelopmental disorder, Williams syndrome (WS, OMIM 194050).

WS occurs at a frequency of 1/20,000 and is the result of unequal meiotic recombination at human chromosome 7q11.23 (Donnai and Karmiloff-Smith, 2000; Francke, 1999; Osborne and Pober, 2001). Similar to PWS, this region on chromosome 7 is flanked by repeats that are thought to predispose it to deletions. Haploinsufficiency of several genes along the 1.5 Mb deletion leads to the development of WS. Patients present with a characteristic facial appearance, dental problems, growth delay, and cardiovascular lesions which are the major cause of morbidity. WS patients also have a unique cognitive and behavioral profile. In addition to impaired cognition, they have hypersensitivity to sound, visuospatial constructive cognition dysfunction, delayed expressive and receptive language skills, and motor problems affecting balance, strength and coordination. Most patients have attention-deficit hyperactivity disorder, and commonly experience anxiety and phobias.

At least 17 genes map to the WS deletion (Osborne and Pober, 2001). Attempts to correlate individual genes with specific phenotypic traits have focused on the analysis of individual gene mutations and patients with atypical deletions. Mutations in the gene elastin, *ELN*, result in a distinct cardiovascular disorder (Ewart et al., 1993). *ELN* was shown to be deleted in WS, and is the cause of the supravalvular aortic stenosis seen in WS individuals, but does not contribute to the other cognitive or behavioral defects. Several patients with supravalvular aortic stenosis and visuospatial cognition defects due to a small deletion spanning the *ELN* and the adjacent LIM kinase 1 (*LIMK1*) gene suggested that *LIMK1* was responsible for the visuospatial cognition deficits of WS (Frangiskakis et al., 1996). This link has not been conclusively demonstrated as several individuals have also been identified with mutations of *LIMK1*, but who do not have

visuospatial impairment (Osborne and Pober, 2001; Tassabehji et al., 1999). Recent work in mice suggests that *CYLN2* may be responsible for many of the neurological problems (Hoogenraad et al., 2002). Mice with a heterozygous deletion of the *Cyln2* gene have mild growth deficiencies, larger brain ventricular volume, smaller corpus callosum, defects in hippocampal function and impaired motor coordination that are reminiscent of WS. Thus, WS is considered to be due to the heterozygous loss of at least two genes, *ELN* and *CYLN2*.

Smith-Magenis syndrome

Smith-Magenis syndrome (SMS, OMIM 182290) is a rare multiple congenital anomaly and mental retardation syndrome, occurring at a rate of 1/25,000 (Smith et al., 1998). The molecular mechanisms behind SMS are not well understood. Most cases are due to a heterozygous 4 Mb deletion on chromosome 17p11.12. However, rare patients with atypical deletions have been used to define a 1.1 Mb critical region (Bi et al., 2002). The most common traits associated with SMS are characteristic facies, mental retardation, speech delay, ocular findings, peripheral neuropathy, and sleep disturbances due to an inverted circadian rhythm in melatonin levels (De Leersnyder et al., 2001; Potocki et al., 2000; Smith et al., 1998). Behavioral problems, including self-injurious behavior are the major management issues associated with SMS. The critical region contains 30 known genes and putative genes, but like PWS, it is not known how many of these genes contribute to the phenotype (Bi et al., 2002). Targeted deletions of several of the mouse orthologues in the mouse syntenic region have not produced a phenotype when inherited in the heterozygous state.

Neurodevelopment

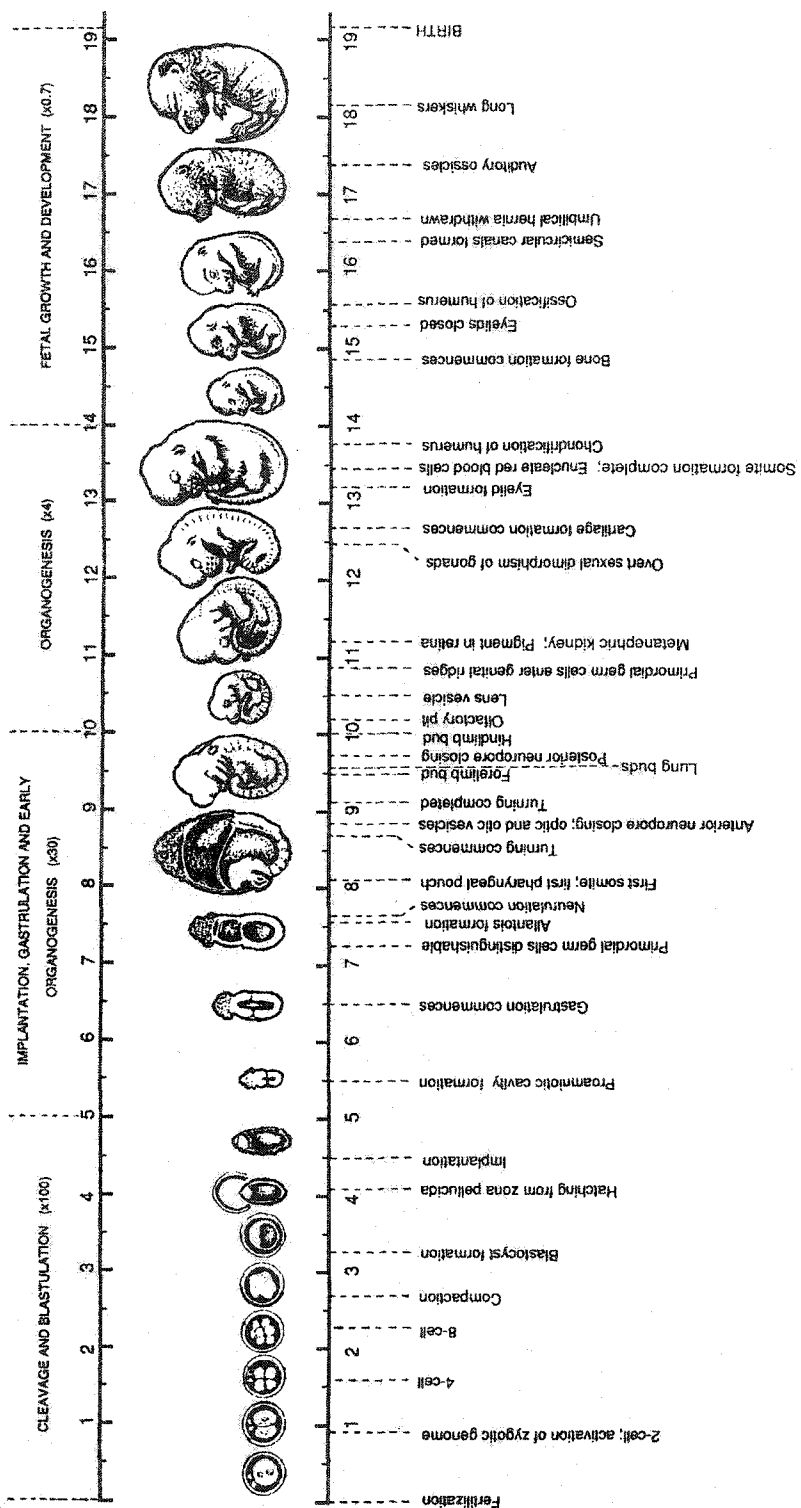
It is proposed that PWS is a disorder of disturbed neuronal development. (Cassidy et al., 2000; Swaab, 1997). The higher incidence rates of fetal inactivity, incorrect fetal position at birth, breathing difficulties at birth, and abnormal parturition timing suggest that a neuronal defect is present before birth (Swaab, 1997). Thus, an investigation into the pathophysiology of PWS must include the fetal brain.

General neurodevelopment

The development of the nervous system is similar in vertebrates, and many of the findings made in mouse have been applied to human development. The mouse central nervous system is the first system to develop and differentiate, and continues to do so until after birth. Embryonic development begins with fertilization, and the typical gestation period is 19-20 days depending on the mouse strain (Figure 1-3) (Hogan et al., 1994). By convention, the morning after fertilization is considered embryonic day 0.5 (E0.5). Neurodevelopment begins at E7.5 in mouse, and the typical mammalian brain structure is identifiable by E14.

Figure 1- 3. Time course of mouse development.

Mouse development from conception (E0) to birth (E19). The major stages of development are cleavage and blastulation, implantation, gastrulation, organogenesis, and fetal growth and development. Embryonic stages are presented along the horizontal axis. Characteristic features of each of the major stages are listed below the embryos. Figure taken from Hogan, B., Beddington, R., Costantini, F. and Lacy, E. (1994). *Manipulating the Mouse Embryo*. Plainview: Cold Spring Harbor Laboratory Press.



Neurodevelopment begins with neural induction, in which signals sent by underlying mesoderm cells signal the neural plate, a specialized region of the ectoderm containing neuronal precursors, to become committed to neural differentiation (Diez del Corral and Storey, 2001; Martin and Jessell, 1991). Neurulation begins around E7.5 with the folding of the neural plate into the neural tube (Martin and Jessell, 1991; Rugh, 1968). The cavity of the neural tube gives rise to the ventricular system of the CNS, and the neural epithelial cells lining the neural tube walls develop into neurons and glial cells.

Early in neurodevelopment, the developing brain undergoes regional specialization (Martin and Jessell, 1991). At E8.5, the caudal portion of the neural tube becomes the spinal cord, the rostral portion forms three primary vesicles: the forebrain, midbrain and hindbrain (Martin and Jessell, 1991; Rugh, 1968). At E10, the forebrain subdivides to give the telencephalon and diencephalon. The midbrain (mesencephalon) does not divide further during development. The hindbrain becomes the metencephalon and the myelencephalon. Cells are organized into three zones in the early embryonic brain (Kent, 1992). The ventricular layer contains actively dividing neuronal precursors (Diez del Corral and Storey, 2001). Cells then migrate into the intermediate/mantle layer, where cells are postmitotic and begin to differentiate. The marginal layer is mostly a thin, non-nuclear, fibrous network surrounding the inner two layers (Kent, 1992).

At E11, the brain bends and begins to take on its characteristic shape (Rugh, 1968). The cerebellum begins to develop, and by E14-E15, most of the brain structures are formed, and the brain continues to increase in size until birth. The cerebellum is the only structure that requires further development, transverse folds begin to develop at E17, and further differentiation continues after birth.

The major structures thought to be involved in the neurobehavioral aspects of PWS include the hypothalamus, the hindbrain and the pituitary. Their role in PWS and their development will be discussed below.

Development of the hypothalamus

The hypothalamus is important for the neural control of homeostasis.

Hypothalamic nuclei regulate the autonomic nervous system, pituitary, gonads, blood osmolarity, blood pressure, body temperature, energy balance, sexual behavior as well as water and food intake (Kupfermann, 1991; Michaud, 2001). The adult hypothalamus can be divided into three regions: (1) the chiasmatic region containing the suprachiasmatic, sexually dimorphic, supraoptic, and paraventricular nuclei; (2) the tuberal region, containing the ventromedial, dorsomedial, arcuate nucleus, lateral tuberal, and tuberomammillary nuclei; and (3) the mammillary complex (Swaab et al., 1993).

At E11, the hypothalamus is not well developed, but begins to increase in volume (Rugh, 1968). Each cell layer differentiates into a set of discrete nuclei beginning at about days E15-16. The internal ventricular layer differentiates into the hypothalamus, preoptic, ventromedial hypothalamic, suprachiasmatic and supraoptic nuclei. The mantle layer differentiates into the medial preoptic nuclei, the anterior, ventromedial, dorsomedial, dorsal and posterior hypothalamic nuclei, most of the paraventricular nucleus, as well as nuclei for the mammillary body. Cells also migrate away from the ventricles to become the lateral preoptic, mamilloinfundibulum, lateral hypothalamic, subthalamic and entopeduncular nuclei. These nuclei, as well as less well defined areas, all have defined physiological functions. The nuclei that are relevant to the PWS phenotype are discussed below in greater detail (Figure 1-4).

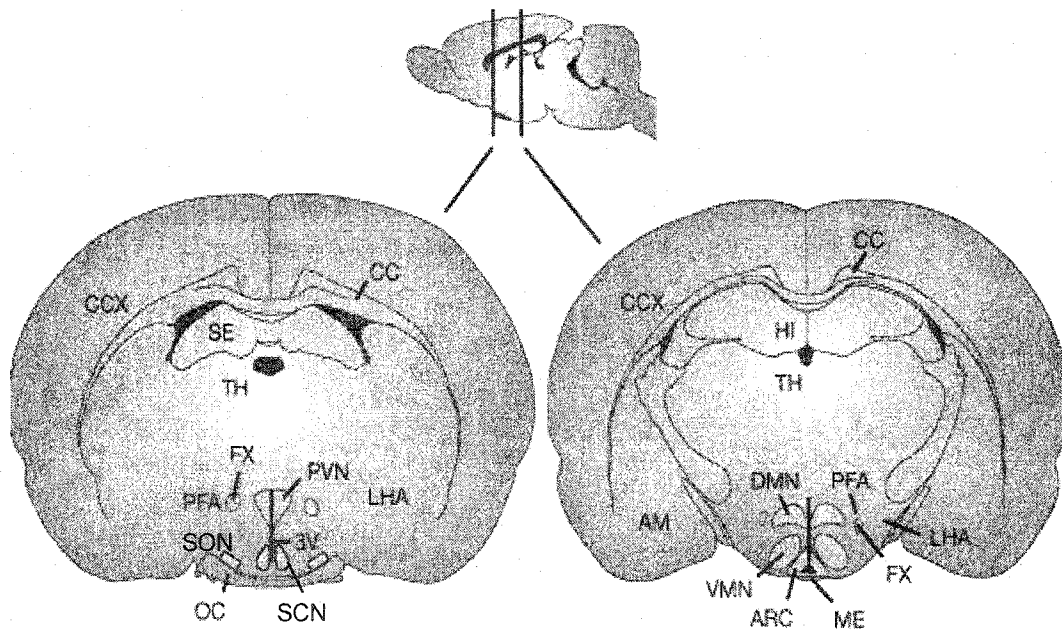


Figure 1- 4. Major hypothalamic nuclei implicated in PWS.

Diagrams of the rodent brain, showing the nuclei that may be involved in the pathophysiology of PWS and neuronal landmarks. The top figure is a sagittal view of the rodent brain, with the olfactory bulb at the anterior end on the left, and the hindbrain on the right. The vertical lines indicate the level of the cross-sections shown below. Nuclei that may be involved are the ARC, arcuate nucleus; LHA, lateral hypothalamic area; PFA, perifornical area; PVN, paraventricular nucleus; SCN, suprachiasmatic nucleus; SON, supraoptic nucleus; and VMN, ventral medial nucleus. Major landmarks are the 3V, third ventricle; AM, amygdala; CC, corpus callosum; CCX, cerebral cortex; DMN, dorsal medial nucleus; FX, fornix; HI, hippocampus; ME, median eminence; OC, optic chiasm; SE, septum; and TH, thalamus. Figure adapted from Schwartz, M. W., Woods, S. C., Porte, D., Jr., Seeley, R. J. and Baskin, D. G. (2000). Central nervous system control of food intake. *Nature* 404, 661-671.

Paraventricular nucleus and the supraoptic nucleus

The paraventricular nucleus (PVN) and the supraoptic nucleus (SON) are secretory nuclei best known for the production of oxytocin (OT) and vasopressin (VP). The PVN consists mainly of magnocellular and parvocellular neurons (Michaud, 2001). Magnocellular neurons project to the posterior pituitary and secrete OT and VP into the general circulation. OT is important for the timing of parturition and lactation, and also affects food intake, maternal and reproductive behavior (Swaab et al., 1993). VP acts an anti-diuretic in kidneys to regulate salt and water balance, and is involved in fetal adaptation to the stress of labor by redistributing fetal blood flow during birth towards the brain, pituitary, heart and adrenals (Swaab, 1995; Swaab et al., 1993; Young, 1992). VP and OT may also be important for fetal development as increased levels are detected in the pituitary and brain at this stage (Swaab, 1995). Interestingly, mice that inherit paternal deficiencies of *Ndn* have decreased numbers of OT neurons in the PVN (Muscatelli et al., 2000). Studies in PWS patients have found that the PVN is reduced in size, and contains 42% fewer OT neurons (Swaab et al., 1995). Because OT regulates numerous physiological processes, a deficiency may be the cause of the abnormal parturition timing and obesity in patients (Swaab et al., 1995; Wharton and Bresnan, 1989).

Parvocellular neurons indirectly control pituitary secretion by projecting to the medial eminence where they secrete the hormones thyrotropin-releasing hormone, corticotropin-releasing hormone (CRH) and somatostatin, which are then transported to the pituitary (Michaud, 2001). CRH is involved in stress response such as hypertonic saline stress, exposure to cold, chronic ethanol exposure and electrical shock (Young, 1992). In the fetus, CRH may be involved in the initiation of labor. CRH is also thought

to be the key regulator of the hypothalamo-pituitary-adrenal axis (Young, 1992), and PWS can be thought of as a disruption along this axis (Muller, 1997). The parvocellular neurons send axons to nuclei in the brainstem, such as the nucleus of the solitary tract and the dorsal motor nucleus of the vagus nerve, to control energy balance and blood pressure (Swaab et al., 1995).

Suprachiasmatic nucleus

Circadian rhythms are biological processes that have roughly 24 hour cycles and that are maintained independent of external stimuli such as light and temperature (Harmer et al., 2001; Panda et al., 2002). The suprachiasmatic nucleus (SCN) is the circadian pacemaker in the mammalian brain, coordinating digestion, body temperature regulation, hormone secretion and behaviors such as the onset of sleep (Swaab et al., 1993).

Circadian rhythms are present before birth, but are generally driven by the mother.

Neuronal populations in the SCN are segregated and are defined by the hormone that is produced, and they project throughout the brain enforcing circadian rhythms on a wide range of brain functions (Moore, 1992; Swaab et al., 1993).

There are several reports of PWS patients with sleep disturbances, such as excessive daytime sleepiness as well as rapid-eye movement that occurs at the onset of sleep (Vela-Bueno et al., 1984). These may be due to a disturbance in the circadian rhythm (Nixon and Brouillette, 2002). This is supported by the finding of one PWS patient has been found with increased numbers of neurons in the SCN (Kremer, 1992).

Hypothalamic nuclei regulating feeding behavior

The hyperphagia and the resulting morbid obesity seen in PWS patients is thought to be due to a hypothalamic defect. Classical experiments involving brain lesioning and

stimulation in rodents have established the hypothalamus as the major center controlling food intake and body weight. The control of energy homeostasis by the hypothalamus is most likely made up of integrated and redundant pathways controlled by several nuclei.

The arcuate nucleus (ARC) contains neurons producing catecholamine, somatostatin, neuropeptide Y and neurotensin (Swaab et al., 1993). Disruption of the ARC results in increased food intake and obesity (Choi and Dallman, 1999). It has been proposed that the ARC contains neurons that detect circulating satiety signals, such as the hormones leptin and insulin, and transmits the information to other brain regions (Schwartz et al., 2000). Brain regions that are innervated by the ARC would therefore contain neurons indirectly involved in the energy homeostasis circuit. Axons from the ARC are known to project to the PVN, zona incerta, perifornical area, and lateral hypothalamic area.

Most research has focused on the role of the PVN in feeding. Lesions to the PVN increase appetite and result in obesity (Choi and Dallman, 1999; Michaud, 2001). Signals affecting food intake are synthesized in the PVN, include the hormone CRH, which can cause anorexia and thyrotropin releasing hormone and OT, which reduce food intake (Schwartz et al., 2000). A reduction in the number of OT neurons in the PVN of PWS has lead to the suggestion that those neurons make up a satiety center (Swaab et al., 1995).

The onset of satiety is a biological state induced by neurohormonal stimuli that is generated when food is consumed, leading to the termination of a meal (Schwartz et al., 2000). Satiety signals are produced in the gastrointestinal tract and are conveyed by the vagus nerve and the spinal cord to the nucleus of the solitary tract (nucleus tractus

solitarius, NTS), in the brainstem, where the signals are integrated. The NTS is interconnected with the PVN, suggesting that the integration of satiety and energy homeostasis involves multiple brain centers.

Additional regions that are speculated to be involved in obesity are the ventromedial nucleus (VMN) and the subparaventricular zone. The VMN is involved in feeding, aggression, sexual behavior, metabolism and gonadotrophic secretion (Swaab et al., 1993) (Elmqvist et al., 1998). The VMN influences higher cortical functions and behavior through connections to the nuclei of the basal forebrain, which in turn project throughout the cerebral cortex. Lesions of the VMN result in metabolic obesity that is independent of increased food intake (Choi and Dallman, 1999). The subparaventricular zone is innervated by the VMN and the SCN, and is thought to integrate circadian and metabolic information into a neuroendocrine response (Elmqvist et al., 1998).

Development of the pituitary gland

The GH deficiencies seen in PWS are suggestive of a defect in the pituitary gland, as it is the site of GH secretion (Miller et al., 1996). Furthermore, patients with a complete absence or size reduction of the posterior pituitary bright spot have been reported (Miller et al., 1996). The integrity of this structure is reflective of hypothalamic/pituitary function. GH synthesis and secretion is under the control of two hypothalamic hormones, GH-releasing hormone and somatostatin, as well as ghrelin, which is produced by the gastrointestinal system (Kojima et al., 1999; Miller et al., 1996).

The pituitary gland regulates growth and development after birth, and is also important in maintaining homeostasis (Dattani and Robinson, 2000). It receives signals

from the hypothalamus regarding metabolism, growth and reproduction, and relays the information to peripheral endocrine organs. The pituitary is divided into the anterior and intermediate lobes, which are derived from the oral ectoderm; and the posterior lobe, which develops from the neural ectoderm. The anterior pituitary has five hormone producing cell types: corticotropes, thyrotropes, gonadotropes (including lutenizing hormone), somatotropes (including growth hormone), and lactotropes. The posterior pituitary secretes oxytocin and vasopressin.

The development of the pituitary begins at E8.5 with the thickening of roof of the primitive mouth, which subsequently invaginates to form the rudimentary Rathke's pouch at E9.5 (Figure 1-6) (Sheng and Westphal, 1999). The formation of the definitive pouch is complete by E12.5 and involves the further development of the Rathke's pouch upwards; while a second invagination, the infundibulum, forms from the floor of the forebrain. As the pituitary develops, Rathke's pouch and the infundibulum remain in close proximity. At E12.5, individual hormone secreting cells develop in a precise spatial and temporal pattern, and development is complete by E17.

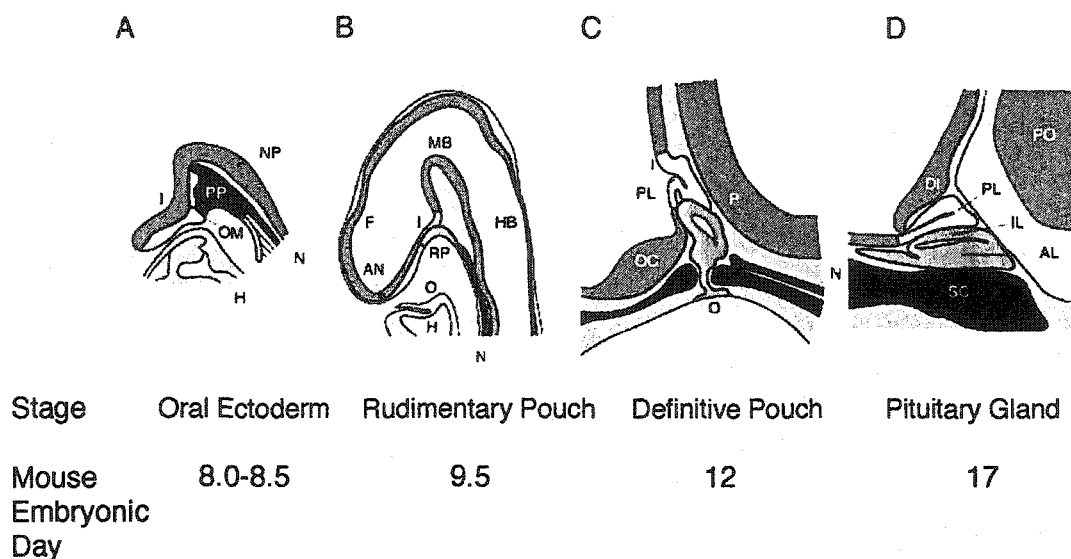


Figure 1- 5. Rodent pituitary development.

Midsagittal or parasagittal drawings of rodent embryos showing pituitary development. (A) Growth of oral ectoderm (orange). (B) Invagination of oral ectoderm upwards and formation of a primitive Rathke's pouch (red). The infundibulum (yellow) begins to develop as an extension of the neural ectoderm downwards (C) The formation of the definitive Rathke's pouch (orange) and posterior lobe (yellow). (D) Nascent pituitary gland. AL, anterior lobe; AN, anterior neural pore; DI, diencephalon; F, forebrain; HB, hindbrain; I, infundibulum; IL, intermediate lobe; MB, midbrain; N, notochord; NP, neural plate; O, oral cavity; OC, optic chiasma; OM, oral membrane; P, pontine flexure; PL, posterior lobe; PO, pons; PP, prechordal plate; RP, Rathke's pouch; SC, sphenoid cartilage. Figure adapted from Sheng, H. Z. and Westphal, H. (1999). Early steps in pituitary organogenesis. *Trends Genet* 15, 236-240.

Development of the brainstem

A defect in the brainstem may result in the elevated hypercapnic arousal thresholds during sleep seen in PWS patients, as well as lower resting diastolic blood pressures, abnormal pupil constriction, abnormal temperature regulation, increased pain tolerance, and thick, concentrated saliva (Brandt and Rosen, 1998; DiMario et al., 1994; Hart, 1998; Livingston et al., 1995). Abnormalities in the brainstem may also be responsible for the neonatal respiratory depression, abnormal ventilatory response and depressed central respiratory drive seen in patients (Lindgren et al., 1999; Menendez, 1999; Wharton and Bresnan, 1989). The brainstem is made up of the medulla, pons and midbrain (Figure 1-5) (Role and Kelly, 1991). The midbrain contains both sensory and motor neurons, as well as the nuclei of the cranial nerves. The reticular formation consists of neurons that are not part of the major nuclear groups of the brain stem, and are arranged in functional groups based on their connections and the neurotransmitter produced. The neurons of the reticular formation relay information along the neural tube, and are important for integrating and coordinating rhythmic breathing, cardiac function, muscle stretch reflexes and tone, behavioral arousal and awareness, and the modulation of pain sensation (Cordes, 2001; Role and Kelly, 1991).

The raphe nuclei are a collection of nuclei that are aligned along the midline seam (or raphe) of the brainstem (Role and Kelly, 1991). Most serotonergic neurons are located within the raphe nuclei and their surrounding nuclei. Axons descending from the raphe modulate spinal sensory and motor neurons. Raphe nuclei in the midbrain and the pons project to the cortex, striatum, limbic system, olfactory tubercle, hippocampus and

diencephalon. Low levels of serotonin have been associated with impulsive, aggressive and self-injurious behavior (Hellings and Warnock, 1994). PWS children often demonstrate severe, compulsive skin picking, which can result in persistent sores and infections. Treatment with selective serotonin reuptake inhibitors has been beneficial in cases of self-injurious skin picking. Skin picking can also be considered to be a variant of the broader obsessive compulsive disorder (OCD). 80% of patients in one study showed adaptive impairment due to obsessive compulsive related behaviors such as hoarding, concern for symmetry or exactness, and a need to tell or ask (Dykens et al., 1996). Selective serotonin reuptake inhibitors have also been effective in these cases (Dimitropoulos et al., 2000; Dykens et al., 1996)

From E8 to E12 in mice, the hindbrain is transiently divided into seven rhombomeres, each which can be defined by an unique set of molecular and cellular markers (Trainor and Krumlauf, 2000). Rhombomeres develop into specific regions of the adult hindbrain, and are important in the anatomical and functional organization of cranial ganglia, branchiomotor nerves and neural crest cell migration. The rhombomeres provide anteroposterior positional information, cell to cell interactions, and dorsoventral signals essential for proper development (Cordes, 2001).

At the end of rhombomere formation (E12 in mice and the first month of gestation in humans) the hindbrain displays consistent and organized discharges from the central respiratory center (Champagnat and Fortin, 1997; Cordes, 2001). Fetal breathing begins in the third month of pregnancy in humans, and at E15.5 in mice as coordinated, rhythmic movements of the rib cage, opening of the mouth and flexing of the neck and body. (Champagnat and Fortin, 1997). In adults, the respiratory rhythm consists of bilaterally

synchronized coordinated activities of the cranial motor neurons, spinal motor axons that innervate the diaphragm, and the intercostal and abdominal muscles. Breathing is regulated by sensory inputs from peripheral mechanoreceptors such as lungs, and chemoreceptors. A network of rhythmic respiratory reticular neurons sequentially controls motoneurons during inspiration, post-inspiration and expiration. The network is organized rostral-caudally into the pontine, dorsal and ventral respiratory groups (Figure 1-5). Only the ventral respiratory group is essential for rhythm generation, and it contains the pre-Bötzinger complex with pacemaker neurons that generate the respiratory rhythm in mammals (Richter and Spyer, 2001; Smith et al., 1991)

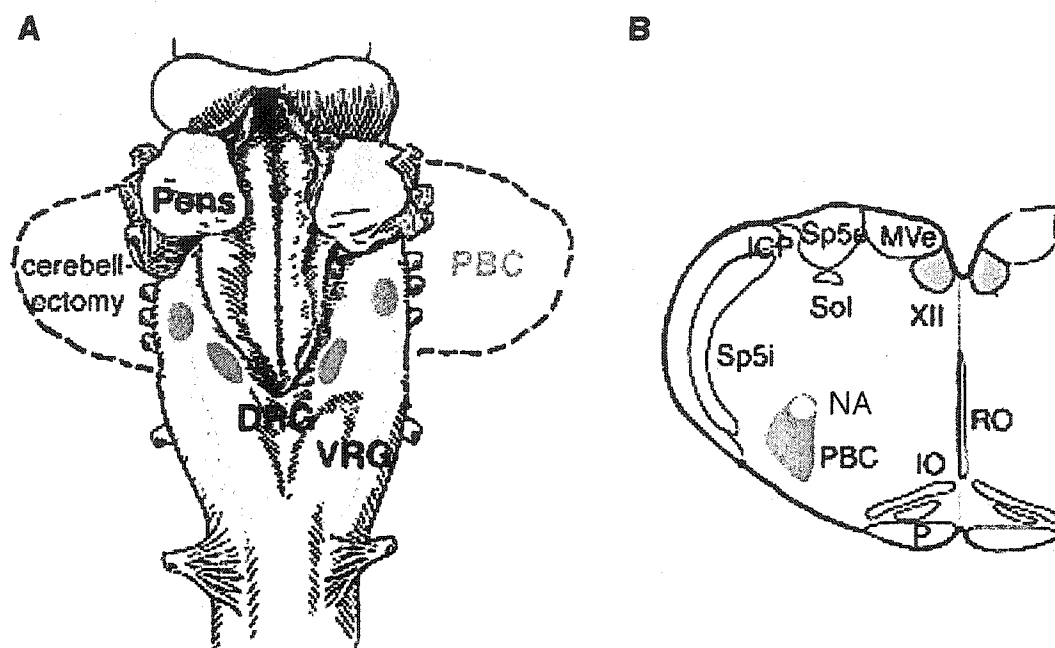


Figure 1- 6. Brainstem regions involved in respiration.

(A) Dorsal view of the brainstem after the cerebellum has been removed. The three groups of respiratory neurons are labeled. The dorsal respiratory group (DRG) is localized around the nucleus of the tractus solitarius (lower blue area). The pontine group (Pons) is represented by the upper pink circles. The ventral respiratory group runs bilaterally and is shown in orange. The pre-Bötzinger complex (PBC) is shown in red. (B) A coronal section through the medulla at the level of the PBC. Characteristic structures of this rhythm generating brain slice are: NA, nucleus ambiguus; ICP, inferior cerebellar peduncle; IO, inferior olive; MVe, medial vestibular nucleus; P, pyramidal tract; RO, raphe obscurus; Sol, nucleus of the solitary tract containing DRG neurons; Sp5i, spinal trigeminal nucleus; XII, nucleus of the twelfth nerve (hypoglossal). Figure adapted from Richter, D. W. and Spyer, K. M. (2001). Studying rhythmogenesis of breathing: comparison of in vivo and in vitro models. *Trends Neurosci* 24, 464-472.

The raphe magnus (RM) consists of medullary raphe and ventromedial reticular nuclei located in the brainstem that may be involved in homeostatic function such as thermoregulation, vasomotor control, sleep/wake cycles, motor control, pain modulation and sexual function (Mason, 2001). Recent work also suggests that they may have a more general function in the modulation of stimulus evoked arousal or alerting by controlling the flow of information from the spinal cord. This region is mainly innervated by axons originating from the hypothalamus, while the main efferent target of neurons in the medullary raphe and reticular region is the spinal cord, while a few project to the facial nuclei. In addition, some RM cells project to the medial preoptic area, the hypothalamic center for temperature regulation.

Are the PWS traits reflective of a hypothalamus-specific or a global dysfunction?

Based on the current clinical evidence, it is difficult to speculate as to the pathophysiology of PWS. Many authors believe that the majority of the phenotypic traits seen in PWS can be explained by a hypothalamic deficiency. The hypothalamic nuclei control many aspects of biological functioning such as circadian rhythms and feeding. Furthermore, the hypothalamus exerts control over many parts of the brain either through axonal connections (i.e. to the brainstem) or through hormone secretion (i.e. to the pituitary). PWS may be due to the loss of one or more paternally expressed genes that are important to the development of the hypothalamus.

On the other hand, it is possible that the range of problems associated with PWS are due to dysfunctions in multiple neuronal systems that would include the hypothalamus, brainstem and the pituitary. This could be the result of the loss of a

paternally expressed gene that is important for the proper neuronal development in general, such as a neuronal growth factor or a transcription factor. Alternatively, multiple genes, each required for the proper development of different regions of the brain could be affected in PWS, resulting in the complex phenotype seen in patients.

Hypothesis and summary of studies

As there has yet to be a PWS patient with a mutation in a single gene, I hypothesize that PWS is due to the loss of expression from several of the paternally expressed genes along 15q11-q13. To understand PWS, it is essential to determine how many genes are absent, and how each of these genes contributes to the overall phenotype.

To be a candidate for involvement in PWS, a gene must be expressed in the brain and be imprinted. Although 4 paternally expressed genes were known to be in the PWS deletion region at the time, a region of that size could be expected to have up to 100 genes. Under this premise, I used two methods to search for novel genes. Firstly, as described in Chapter 3, I constructed a transcript map of the deletion interval by mapping novel transcripts to the region and by determining their imprinting status. The map not only identified novel candidate genes for PWS, but also revealed how imprinted genes were organized along 15q11-13. The experiments in Chapter 4 describe an *in silico* approach, in which genomic sequence produced by the Human Genome Project was analyzed to identify *MAGEL2*. Conventional molecular techniques were then used to clone the gene and investigate its expression pattern.

Because PWS is a neurobehavioral disorder, the genes involved must be expressed in the developing brain. In Chapter 5, I used RNA *in situ* hybridization

methodologies to broadly examine the role of all of the known PWS candidate genes in mouse brain development.

These experiments form the foundation for dissecting the pathophysiology of PWS. They are not only important for understanding the neuronal basis of the disorder, but are critical for interpreting future studies of PWS mouse models.

Chapter 2. Materials and methods

Internet resources

Internet based programs and databases were used to analyze genomic sequences and expressed transcripts (Table 2-1). Sequence from human chromosome 15 PAC pDJ181P7 (GenBank accession number AC006596) was analyzed for novel genes using the programs listed in Table 2-1. From this analysis, the gene *MAGEL2* was identified, its complete sequence in human (Accession number 200625), and mouse (Accession number 212306) were submitted to GenBank.

Table 2- 1. Electronic resources.

Program	URL	Feature
GeneMap'98	www.ncbi.nlm.nih.gov/genemap98/	EST database
GeneMap'99	www.ncbi.nlm.nih.gov/genemap99/	EST database
UniGene	www.ncbi.nlm.nih.gov/entrez/query.fcgi?db=unigene	EST database
MapView	www.ncbi.nlm.nih.gov/mapview/map_search.cgi	Human chromosome maps
GenScan	bioweb.pasteur.fr/seqanal/interfaces/genescan.html	Gene prediction
MetaGene	rgd.mcw.edu/METAGENE/	Gene prediction
Grail	compbio.ornl.gov/Grail-1.3/	Gene prediction
OMIM	www.ncbi.nlm.nih.gov/omim/	Disease database
RepeatMasker	ftp.genome.washington.edu/cgi-bin/RepeatMasker	Repetitive DNA database
BLASTN	www.ncbi.nlm.nih.gov/BLAST/	Nucleotide database search
BLASTX	www.ncbi.nlm.nih.gov/blast/	Protein database search
GenBank	www.ncbi.nlm.nih.gov/Genbank/GenbankSearch.html	Gene sequence database
ClustalW	clustalw.genome.ad.jp/	Protein alignment

Chromosome 15 genes and ESTs

For imprinting analysis, 40 novel ESTs were selected from GeneMap'98 GB4, GeneMap'99 GB4 and an integrated YAC contig map (Christian et al., 1998). The 40 chosen ESTs are listed below according to their mapping source, and their analysis is summarized in Figure 3-2. The 27 unique ESTs used for mapping and imprinting analysis

are printed in bold typeface (see also Figure 3-1 and Table 3-1). Primers for these 27 ESTs were obtained either from Research Genetics (Huntsville, AL), Invitrogen (Burlington, ON), or the University of Alberta oligonucleotide synthesis facility. New primers were designed for BCD1279 (BCD1279-3F 5'-GTT GAT CCC TTT TTG CTC CA and BCD1279-4R, 5'GAA GCT GGC AAT ATG TCA ACC). Sequence was unavailable for *BCL8* (R. Chaganti, Memorial Sloan-Kettering Cancer Center, personal communication). ESTs derived from the GeneMap'98 GB4 map were: **NIB1540**, **A002B45**, **SGC32610**, **WI-15987**, **BCD1279**, **stSG9006**, **stSG10131**, **stSG26368**, **sts-H58001**, **WI-15028**, **WI-13791**, **WI-15655**, **WI-14946**, **A009W43**, **stSG3346**, **A005C48**, **sts-N21972**, **SGC44643**, **stSG12920**, **stSG15842**, **WI-16777**, **stSG2525**, **sts-T16604**, **WI-6654**, **stSG9627**, **Cda0jb12**, and **WI-15959**. **stGDB:451595** mapped to 2 different chromosomes and was not analyzed further. ESTs derived from the GeneMap'99 GB4 map were: **stSG45529**, **stSG52513**, **WIAF-831**, **stSG53014**, **WIAF-778**, and **stSG47701**. ESTs derived from an integrated YAC contig (Christian et al., 1998) were: **SHGC13938**, **SHGC15126**, **SHGC17218**, **A008B26**, **WI-14097**, **SGC32570**, and **WI-4477**. **SHGC17218** mapped to 2 different chromosomes and was not analyzed further.

Unique ESTs for known genes were: **A006B10** (*MN7*), **SGC35648** (*ZNF127*), **NDN-5F** and **NDN-6R** (*NDN*) (MacDonald and Wevrick, 1997), **SGC31492**, **R99003** (*SNRPN*), **IPW-60A** and **IPW-60B** (*IPW*) (Wevrick et al., 1996), **WI-6519**, (*UBE3A*), and **SGNE1-1F**, 5'TAG GCC TCA GCA TGG CTT AT, and **SGNE1-2R**, 5'CCA AGG GCT GGG TGA ACT AC (*SGNE1*). Primers designed for the analysis of *MAGEL2/Magel2* are listed in Table 2-2.

Table 2- 2. *MAGEL2/Magel2* PCR primers

Primer	Sequence (5'-3')
NLG 1F	AGA AGG CCG CCA CTC ACA TC
Nlg 2F	CAG TCC CCA TCC TCA CTA ATA GA
Nlg 3F	CAA GAT GGC GTA CCC TCA GT
NLG 3R	TCT TGG AGG CCT CTT GAG TG
Nlg 4R	GGC TGG TTC TCG TAG AGT GC
NLG 5F	CCA CCT TCC TGA TGG CTA CAG
NLG 6F	GAG GTC GCA AGT GTC TCT CC
NLG 7R	GCC ACC AAA TTC CCT GTA TGG
NLG 8F	CCA CGC CTA TAT TAT CAT CAA C
NLG 9R	TCT CCA GAC AGT ATT TTA CCG ATG
NLG 10F	AAA AGA CCG CAT GAT CTT TGC T
NLG 11R	GAC CTC CCA GTC ACT CAG ATT TAG
NLG 12R	GTA CAA AGC TTT GGC AGA TAC G

Genomic and cDNA clones

YAC clones 931C4, 925C12, 959G3, 776A9, 957E9, 922F3, 897B10, and 962D11 were obtained from Research Genetics or from the MRC CGAT Genome Resource Facility (Hospital for Sick Children, Toronto, ON). YAC DNA was isolated by lysis of cells with 0.5 mm diameter acid washed glass beads (Sigma-Aldrich Canada, Oakville, ON), followed by treatment with 2% Triton X-100, 1% SDS, 100 mM NaCl, 10 mM Tris-HCl, pH 8.0, 1 mM EDTA and 200 μ l of phenol/chloroform/isoamyl alcohol (25:24: 1) and precipitation with ammonium acetate and ethanol (Scherer and Tsui, 1991). Fifty ng of YAC DNA was then used directly for PCR.

Human PAC clones pDJ50I2, pDJ121M14, pDJ121D5, pDJ134I14, pDJ181P7; and mouse PAC clones 480A23, 509A13, and 665K16 were obtained from the Genome

Resource Facility, and DNA was prepared by alkaline lysis (Sambrook and Russell, 2001).

Human and mouse cDNAs were obtained from Research Genetics and were sequenced using the Thermo Sequenase fluorescent labeled primer cycle sequencing kit with 7-deaza dGTP (Amersham Biosciences, Buckinghamshire, England) and Li-Cor technology (Li-Cor 4200 Automatic Sequencer, Lincoln, Nebraska). Human cDNAs selected from the UniGene cluster Hs.141496 representing *MAGEL2* were IMAGE clones, 760047, 27053, and 281910. Mouse *Magel2* cDNAs have clone names mj49f12, mr52b10, mv40f06. IMAGE clone 360433 was also obtained from Research Genetics.

Cell lines and tissues

Patient samples

Chromosome 15 deletion lymphoblast cell lines from a PWS patient (GM09024B), AS patient (GM11515), and control fibroblasts (GM00909) were obtained from the NIGMS Human Genetic Mutant Cell Repository (Camden, NJ). A PWS deletion fibroblast cell line, PWS deletion brain sample (1889) and control cerebellum sample (2144) were obtained from the University of Miami Brain and Tissue Bank for Developmental Disorders. The AS frontal cortex sample (CBTB #293) was generously provided by Dr. Marc Lalande, University of Connecticut. Control lymphoblast cell lines were obtained from Dr. Ian MacDonald, University of Alberta. AS fibroblasts were generously provided by Dr. Arthur Beaudet, Baylor College of Medicine.

P19 cells

P19 cells were obtained from the American Type Culture Collection (ATCC, Manassas, VA) and cultured in Minimum Essential Medium (MEM) α (Invitrogen,

Carlsbad, CA) supplemented with 10% FBS (Invitrogen). Undifferentiated cells were propagated in adherent tissue culture flasks. To induce differentiation, 3×10^6 cells were placed in 100 mm x 15 mm bacteria grade petri dishes and treated with 0.5 μ M all-trans retinoic acid (Sigma-Aldrich Canada). Cell aggregates were allowed to form during the retinoic acid treatment. After four days aggregates were transferred to T75 adherent tissue culture flasks. Cells were cultured in MEM α medium for one day, and subsequently, in media supplemented with 5 μ g/ml of cytosine beta-D-arabinofuranoside hydrochloride (Sigma-Aldrich Canada). Cells were collected at 24 hour time points and processed for RNA extraction.

Mouse breeding

Procedures for animal care were approved by the Health Sciences Animal Policy and Welfare Committee (HSAPWC) at the University of Alberta. For embryo staging, the appearance of sperm plugs in the breeding females was considered to be E0.5. Crl:CD-1 $\text{\textcircled{R}}$ (ICR)BR (CD-1) embryos (Charles River Canada, Saint-Constant, QC) were used for the collection of E12.5 embryos. *Mus musculus* C57Bl/6 embryos (Jackson Labs, Bar Harbor, ME) were used for RNA *in situ* hybridization on tissue sections from E15.5 to E18.5. *Mus spretus* SPRET/Ei (Jackson labs) and *Mus musculus* C57Bl/6 were mated to obtain F1 hybrid crosses. Tissues were collected from embryonic and postnatal mice up to one year of age, frozen in liquid nitrogen and stored at -80 $^{\circ}$ C until DNA or RNA was extracted.

Ndn deficient mice carrying the *Ndn*^{tm2S^{tw}} allele (Gerard et al., 1999) were maintained on a C57Bl/6 background by breeding through the female line with wildtype males. To generate mutant mice, heterozygous males carrying the *Ndn*^{tm2S^{tw}} construct on

the maternal allele, which were phenotypically normal, were bred to wildtype females to produce experimental offspring and embryos. In these litters, on average, one half of the offspring were wildtype, and half carried a paternally inherited *Ndn* deletion and were functionally null.

PCR reactions

All PCR reactions were performed in 20 μ l reactions containing 0.5 units of recombinant Taq DNA polymerase, 1.0-3.0 mM MgCl₂, 0.2 mM dNTP (Invitrogen), 0.5 μ M primers, and 100 ng of cDNA or 50ng of control genomic DNA. The reactions were performed in a MJ Research PTC 100 or PTC 200 with an initial denaturation at 95° C for 5 minutes, followed by 30-35 cycles of denaturation at 95° C for 30 seconds, annealing at 50-62° C for 30 seconds, extension at 72° C for 30 seconds, followed by a final extension at 72° C for 10 minutes. The reaction products were resolved on 2% agarose gels, stained with ethidium bromide and visualized using an ImageMaster VDS gel documentation system (Amersham Biosciences).

DNA analysis

Genomic DNA extraction

Human and mouse tissues were crushed under liquid nitrogen. DNA was extracted by proteinase K/SDS digestion, phenol/chloroform extraction and ethanol precipitation (Sambrook and Russell, 2001). DNA for genotyping of *Ndn* deficient mice was obtained from ear notch samples or embryonic tail biopsies using the DNeasy Tissue Kit (Qiagen, Mississauga, ON) according to manufacturer's directions.

DNA sequencing

DNA sequencing of PCR products was used to identify single nucleotide polymorphisms in *MAGEL2* and *Magel2*. Primers Nlg2F/9R and 8F/12R were used to amplify PCR products from mouse and human DNA respectively. Before sequencing, 5-10 μ l of each PCR reaction was treated with 10 U of Exonuclease I (United States Biochemical, Cleveland, OH) and 1 U of Shrimp Alkaline Phosphatase (Amersham Biosciences), incubated for 37°C for 20 minutes and then heat inactivated for 10 minutes at 70°C. The PCR products were then labeled with 33 P-dideoxynucleotides (Amersham Biosciences) using the Thermo Sequenase Radiolabeled Terminator Sequencing Kit (USB) according to the manufacturer's directions. Sequencing reactions were performed with the same forward and reverse primers used for the initial PCR reaction. Labeled products were run on a 5% denaturing acrylamide gel made with Long Ranger™ acrylamide (BioProducts, Rockland, ME). Gels were exposed to Biomax Film (Kodak, Rochester, NY) at -80°C until the appropriate signal intensity was obtained.

DNA sequencing from a plasmid template was used to sequence clones obtained from the cDNA library screen. Plasmid DNA from a pBluescript SK(-) phagemid was obtained by an alkaline lysis miniprep. Two μ l of the miniprep, and vector primers SK and KS were used to label the DNA as described above.

Southern blot analysis

Five to ten μ g of YAC DNA was digested with EcoR I and Hind III restriction enzymes and electrophoresed on a 1% agarose gel and blotted to a Hybond-N nylon membrane (Amersham Biosciences) using standard Southern blotting procedures (Southern, 1975).

RNA analysis

RNA extraction

Dissected tissues were frozen in liquid nitrogen and stored at -80°C until RNA was extracted. Tissue culture cells were resuspended in Trizol Reagent (Invitrogen) and stored at -80°C . RNA was extracted with Trizol Reagent according to the manufacturer's directions. RNA was resuspended in diethyl pyrocarbonate (DEPC) (Sigma-Aldrich Canada) treated water at 55°C and stored at -80°C . Poly(A) RNA was isolated from 100 μg of total RNA using the PolyAtract® mRNA Isolation System (Promega, Madison, WI) following the manufacturer's protocol.

RT-PCR analysis

RNA was treated with one unit of RQ1 RNase-Free DNase (Promega). Reverse transcription (RT) was performed with 100 ng of random primer p(dN)₆, 200 units of Superscript II reverse transcriptase, 4 μl 5x first strand buffer, 10 mM DTT, and 0.5 mM dNTP (Invitrogen). RT reactions were carried out in a MJ Research PTC 100 or PTC 200 thermal cycler, with a 45 minute incubation at 42°C followed by a 95°C incubation for 5 minutes. PCR reactions were performed as described above. All RT-PCR experiments for imprinting analysis were repeated at least twice.

Northern blot analysis

RNA samples were mixed with 25% formalin, 67% formamide and 1.6xMOPS buffer (3-(N-Morpholino)propanesulfonic acid) and denatured at 55°C before loading on a gel. Denaturing gels (1% agarose) were made with 1xMOPS buffer and 1.8% formalin. Electrophoresis was conducted in a running buffer of 1xMOPS and 1.6% formalin. RNA was transferred to Hybond-N nylon membranes (Amersham Biosciences) in 10XSSC

(1.5 M NaCl, 0.15 M sodium acetate). For the P19 northern blot, approximately 2.5 µg of poly(A) RNA was loaded in each lane. Fifteen µg of total RNA per lane was used to make the embryonic mouse blot to test the specificity of the *MBII-85* probe. The Human Brain Multiple Tissue Northern Blot II (Catalogue number 7755-1), and Human Fetal Multiple Tissue Northern Blot II (Catalogue number 7756-1) were purchased from Clontech Laboratories (Palo Alto, CA)

Gene specific DNA fragments were random primed and ³²P-dCTP labeled with the Random Primers DNA Labeling System (Invitrogen). Labeled probes were hybridized to northern blots in ExpressHyb solution (Clontech Laboratories) according to manufacturer's directions. The final wash was performed at 50°C in 0.2XSSC, 0.1%SDS twice for 20 minutes each time. Northern blots were exposed to Biomax Film (Kodak) at -80° C until the appropriate signal intensity was obtained. Control probes using human ubiquitin, or mouse *Gapdh* and ethidium bromide staining of the RNA in the agarose gel demonstrated approximately equal loading in all lanes. The PCR product generated from NLG10F/11R was used to hybridize to the human northern blots described above. PCR products from primer pairs Nlg 2F/9R; Ndn3F (5' CCC ATA CTA GGG CTG TGT AA), Ndn4R (5' TCA GTC CCA TAC AAA GGA AC) were used to hybridize to the P19 northern. Probes to test the specificity of *Mkrn3*, *Snrpn* and *MBII-85* were generated as described below.

cDNA library screening

An adult human, left ventricular heart cDNA library (Stratagene, La Jolla, CA) with a titer of 1.5×10^6 plaque forming units/µl (pfu/µl) and average insert size of 0.5 kb was used for library screening. After library amplification the titer was of 1×10^{11} pfu/ml.

cDNA library screening was carried out according to the manufacturer's protocol. A fragment of the cDNA clone IMAGE 360433 (Research Genetics), containing the EST WI-15655, was used for a primary screen of 500,000 pfu. Positive clones were carried through to a tertiary screen and sequenced.

Tissue Histology

Tissue fixation

Mouse embryos for general tissue staining and RNA *in situ* hybridization were fixed as follows. E12.5 mouse embryos were incubated in 4% paraformaldehyde in 1 x phosphate buffered saline (PBS) at 4° C overnight. E15.5 and E18.5 embryos were fixed through a cardiac perfusion of the pregnant female with a 0.9% sodium chloride (Baxter, Toronto, ON) flush, followed by ice cold 4% paraformaldehyde. Embryos were dissected out and incubated in 4% paraformaldehyde at 4° C for several hours. Tissues for β -galactosidase staining were fixed in a similar manner with ice cold Webster's fix (2.5% glutaraldehyde and 0.5% paraformaldehyde in 0.1 M phosphate buffer, pH 7.3 to 8.5).

Tissue sectioning

Mouse tissues were fixed as described above. Tissues were rinsed in 1 x PBS and then cryoprotected by equilibrating tissues in a 30% sucrose solution made in 1 x PBS at 4° C. Tissues were then frozen in Cryomatrix Frozen Specimen Embedding Medium (Shandon, Pittsburgh, PA) over dry ice and stored at -80°C. Cryosections between 20 μ m-60 μ m were made on a Leica CM1900 cryostat (Leica Microsystems, Heidelberg Strasse, Germany) at a cutting temperature of -10°C to -25°C.

Thionin tissue staining

Twenty μm cryostat sections of mouse E18.5 brain were mounted on SuperFrost Plus slides (Fisher, Nepean, ON) and baked at 42°C overnight. Slides were dehydrated in 50% ethanol, rinsed in water and stained in thionin for 30 seconds. Slides were rinsed in water and then destained in 95% and 100% ethanol followed by xylenes and mounted in Entellan mounting media (EM Industries, Gibbstown, NJ).

***lacZ* detection**

Identification of mutant offspring was carried out by PCR genotyping with *lacZ* oligonucleotide primers (LACZ1942F, 5'GTG TCG TTG CTG CAT AAA CC and LACZ2406R, 5'TCG TCT GCT CAT CCA TGA CC) and/or by histochemical detection in tissues. For detection of β -galactosidase activity, cryostat sections of mouse tissue were mounted on SuperFrost Plus slides (Fisher) and incubated at 37° C for 5 minutes. Slides were fixed in a 10% formalin, 7.5% sucrose solution made in "M/15 Phosphate buffer", pH 7.4 (8:2 ratio of Na_2HPO_4 : KH_2PO_4). Tissues were incubated in X-gal (5-bromo-4-cholor-3-indolyl- β -D-galactopyranoside) (Invitrogen) staining solution at 37°C until the appropriate staining intensity was achieved (Hogan et al., 1994). Fixed whole mount embryos were rinsed in 0.1 M phosphate and incubated with the X-gal staining solution as described above.

RNA *in situ* hybridization

Probe construction

Probes for *Snrpn* and *Mkrn3* were derived from PCR fragments amplified from genomic DNA with recombinant Taq DNA polymerase (Invitrogen) and cloned into a pBluescript vector (Stratagene). The *Snrpn* probe includes the 5' untranslated region and

the first two-thirds of the open reading frame (positions 1-604 of GenBank accession number NM_013670). The *Mkrn3* probe spans part of the 3' untranslated region (positions 2319-1699 of GenBank accession number NM_011746). The *Magel2* probe corresponds to the second half of the open reading frame (positions 984-1754 of GenBank accession number NM_013779). The *Ndn* probe contains the open reading frame and extends into the 3' untranslated region (positions 162-1235 of GenBank accession number M80840). The *Ipw* probe was previously described as *mbr0* and includes 2 copies of exon A, exon B, exon C and part of exon F cloned into pBluescript vector (Wevrick et al., 1996). A probe for the snoRNA transcripts was designed based on the consensus sequence of the *MBII-85 C/D* box snoRNA (Cavaille et al., 2000). Complementary oligonucleotides that lack the inverted repeats and contain Pst I compatible overhangs were synthesized (Invitrogen). (MBII-85LF 5' AAT GAT GAT TCC CAG TCA AAC ATT CCT TGG AAA AGC TGA ACA AAA TGA GTG AAA ACT CTG TAC TGC CAC TCT CAT CGG AAC TGA TGC A and MBII-85LR 5' TCA GTT CCG ATG AGA GTG GCA GTA CAG AGT TTT CAC TCA TTT TGT TCA GCT TTT CCA AGG AAT GTT TGA CTG GGA ATC ATC ATT TGC A). The complementary oligonucleotides were annealed, ligated to form concatamers and then ligated into the Pst I site of pBluescript. The final probe contains 4 partial *MBII-85* copies in the same orientation. This probe was constructed by Christine Walker, in the laboratory of Dr. Rachel Wevrick.

Labeling of probes

Template DNA for probe labeling was PCR amplified using Recombinant Taq DNA Polymerase (Invitrogen) using the primers M13F-20 5' GTA AAA CGA CGG CCA

GT) and M13R 5'GGA AAC AGC TAT GAC CAT G. Antisense riboprobes were generated using T7 RNA polymerase (Invitrogen) and a digoxigenin (DIG) RNA Labeling Mix (Roche Diagnostics, Laval, QC).

Hybridization and detection

Timed pregnant females were sacrificed and the embryos were fixed as described above. Sixty μm cryostat sections of mouse embryos were mounted on slides, and baked at 50°C for 5 minutes. Slides were dehydrated in an ethanol: 1xPBS gradient and then rehydrated. Tissues were treated with $1\ \mu\text{g}/\text{ml}$ of proteinase K in 1xPBS with 0.1% Tween-20 (PBT) for 5 minutes at 37°C . Tissues were post-fixed in 10% formalin, and then incubated in a hybridization solution of 50% formamide, 5xSSC, pH 4.5 adjusted with citric acid, 1% SDS, $50\ \mu\text{g}/\text{ml}$ yeast RNA (Roche Diagnostics) and $50\ \mu\text{g}/\text{ml}$ heparin (Fisher) for 2 hours at 68°C in a humidified chamber. Fresh hybridization solution with 0.5-1 $\mu\text{g}/\text{ml}$ of DIG labeled probe was added to the slides, and incubated overnight at 68°C . Slides were washed in 50% formamide, 5xSSC, pH 4.5, and 1% SDS at 68°C . A second post-hybridization wash was done in 50% formamide and 2xSSC, pH 4.5 at 68°C . Sections were pre-blocked in 5% Blocking Reagent (Roche Diagnostics) in 25 mM Tris-HCl, pH 7.5 with 1% Tween-20 and 0.15 M NaCl (TBST) at room temperature for 90 minutes. Anti-DIG-alkaline phosphatase conjugated antibodies (Roche Diagnostics) were preabsorbed with E11.5 embryonic mouse acetone powder made by incubating cold acetone with homogenized embryos several times, then drying and storing the embryo powder at -20°C . Preabsorbed antibodies were added to tissues along with 1% heat inactivated sheep serum (Sigma-Aldrich Canada) and 2 mM levamisole for 6 hours at room temperature. Antibodies were detected with nitroblue

tetrazolium chloride and 5-bromo-4-chloro-3-indolyl phosphate (NBT/BCIP) stock solution (Roche Diagnostics) in a solution of 100 mM NaCl, 100 mM Tris-HCl, pH9.5, 50 mM MgCl₂, 0.1% Tween-20 and 2 mM levamisole. Images were obtained using Leica DMRBE and DMRE microscopes (Leica Microsystems), SensiCam camera (Cooke Corporation, Auburn Hills, MI), Northern Eclipse software (Empix, Mississauga, ON), and ImagePro Plus software (MediaCybernetics, Carlsbad, CA). Structures were labeled according to a reference mouse atlas (Jacobowitz and Abbott, 1998; Stoykova et al., 1996).

Chapter 3. Identification of novel imprinted transcripts in the Prader-Willi/Angelman syndrome deletion region

Parts of this chapter have been previously published.

Lee, S. and Wevrick, R. (2000). Identification of novel imprinted transcripts in the Prader-Willi syndrome and Angelman syndrome deletion region: further evidence for regional imprinting control. *Am J Hum Genet* 66, 848-858. (Permission has been given to republish this material).

All of the results presented in this chapter were done by Syann Lee.

Introduction

Prior to the completion of the Human Genome Project, it was commonly accepted that the human genome contained between 50,000 to 100,000 genes (Fields et al., 1994). These estimates were based on several assumptions about the genome, including: gene density estimates in gene rich and gene poor regions, analyzing CpG islands which are associated with about half of reported genes, and assuming that the average gene size is between 10 to 30 kb. Based on these predictions, the 4 Mb region along human 15q11-q13 that is commonly deleted in both PWS and AS was thought to potentially contain up to 100 genes (Christian et al., 1998).

One aspect of the genome sequencing initiative was the construction of expressed sequence tag (EST) libraries. Complementary DNA (cDNA) libraries were constructed from specific tissues, and individual cDNA clones were isolated and sequenced from both ends. The expressed sequences are ESTs, while Sequence Tagged Sites (STSs) include expressed and non-expressed sequences that are physically mapped on a chromosome map or relative to a DNA marker (Gerhold and Caskey, 1996). High throughput mapping of ESTs is performed by using EST-specific PCR primers to screen radiation hybrid (RH) panels. Human cells are treated with radiation to induce chromosome breakage. Random chromosome fragments are fused with cultured hamster cells, which are then characterized to determine the identity of the human fragment in each cell. The approximate map location of a pair of EST primers can be determined by screening the RH panel. Thus, ESTs are sequence based unique identifiers of transcribed genes, and are useful for identifying new genes at a specified genetic locus as well as in *in silico* comparisons of expression levels of genes across tissues.

Several databases have been developed to organize the wealth of information obtained from the construction of ESTs and STSs. UniGene is a database that sorts ESTs and STSs into non-redundant clusters, each of which potentially represents a separate transcriptional unit (Boguski and Schuler, 1995). UniGene also provides a short summary of the available bioinformatic data for each gene, including sequence similarities to known proteins, homologies to genes in other organisms, and a list of tissues from which the ESTs associated with the gene are derived. Sequences from Unigene can be analyzed using gene prediction algorithms such as BLASTX, which compares a nucleotide sequence against a protein database. GeneMap'98 and GeneMap'99 contain the mapping locations of over 30,000 unique ESTs that have been assembled and integrated with RH mapping information (Deloukas et al., 1998). The GeneMaps have been used for positional cloning of genes involved in disease, construction of physical maps of chromosomes, and comparative analysis of chromosome structure across species. RH mapping, however, provides only a rough estimate of a marker's location. A more refined map can be achieved by localizing the ESTs and STSs to cloned genomic fragments such as P1 artificial chromosomes (PACs), that contain 30-40 kb inserts, and yeast artificial chromosomes (YACs), that contain several hundred kb inserts.

When the effort to sequence the human genome began, only 10 well characterized genes had been localized to the PWS/AS region. The paternally expressed genes, *NDN* and *SNURF/SNRPN* were first cloned based on their roles in neuronal development and function, and later mapped to the PWS region (Figure 3-1) (Gray et al., 1999a; Jay et al., 1997; MacDonald and Wevrick, 1997; Ozcelik et al., 1992; Sutcliffe et al., 1997). *ZNF127 (MKRN3)* and *IPW* were identified through positional cloning strategies to

identify genes specifically in the PWS region (Jong et al., 1999b; Wevrick et al., 1994). *UBE3A* was localized to a region telomeric to the paternally expressed cluster of genes, and its expression was known to be strongly biased towards expression of the maternal allele in specific regions of the brain, with overall reduced levels in AS brain (Nakao et al., 1994; Rougeulle et al., 1997; Vu and Hoffman, 1997). Two non-imprinted genes, *P* (Lee et al., 1994; Rinchik et al., 1993) and *HERC2*, which is homologous to the MN7 family of repeats (Ji et al., 1999), are located at the telomeric end of the deleted region. The imprinting status of the three gamma-butyric acid receptor genes, *GABRB3*, *GABRA5*, and *GABRG3*, was unclear (Gabriel et al., 1998; Meguro et al., 1997). These genes are located towards the telomeric part of the deletion interval. Early experiments also identified several transcripts of unknown function in the 15q11-q13 region: the paternally expressed transcripts PAR-1 and PAR-5 (Sutcliffe et al., 1994), the non-imprinted transcript PAR-2 (Nakao et al., 1994) and two low-level transcripts of unknown imprinting status, PAR-4 and PAR-7 (Sutcliffe et al., 1994). Repeated sequences with high sequence similarity to each other were identified at either end of the common deletion region and predispose the PWS/AS region to deletions (Amos-Landgraf et al., 1999; Christian et al., 1999). The gene *BCL8*, which was shown to be disrupted in rearrangements leading to diffuse large cell lymphomas (Dyomin et al., 1997), and the gene *MYLE /DEXI*, had both been localized to the common breakpoints flanking the PWS/AS critical region (Christian et al., 1998; Kelly et al., 2001).

Table 3- 1. Transcription units and genes in 15q11-q13.

ESTs were selected from GeneMap'98, GeneMap'99, and an integrated YAC contig [Christian, 1998 #431]. ESTs were placed into the correct physical mapping interval with respect to the STS markers D15S1035, D15S128, D15S122, D15S156 and D15S165 by YAC mapping (Y) from Christian, S. L., Bhatt, N. K., Martin, S. A., Sutcliffe, J. S., Kubota, T., Huang, B., Mutirangura, A., Chinault, A. C., Beaudet, A. L. and Ledbetter, D. H. (1998). Integrated YAC contig map of the Prader-Willi/Angelman region on chromosome 15q11-q13 with average STS spacing of 35 kb. *Genome Res* **8**, 146-157.. Otherwise ESTs were placed in the appropriate interval according to the radiation hybrid (RH) mapping data but are not ordered with respect to each other in this Table. Some ESTs (plain type) were found to be part of the same transcriptional unit on the basis of database searches, but were not previously included in the UniGene cluster. Previously known genes (underlined) and transcripts are also included in this Table. ESTs or primers used for RT-PCR analysis are indicated in bold. The UniGene cluster information was obtained through a search of the UniGene database. ESTs marked “-“ in the column labeled UniGene cluster have not yet been assigned to a UniGene cluster.

EST or gene	Unigene cluster	Map source
NIB1540 , stSG45529, stSG52513	Hs.83724	YAC
SHGC13938	-	YAC
A002B45	Hs.8177	YAC
D15S1035		YAC
MYLE , SHGC15126	Hs.11902	YAC
SGC32610	Hs.126738	YAC
MN7 , A006B10	Hs.174087	YAC
A008B26	Hs.15543	YAC
ZNF127	Hs.72964	YAC
WI15987 , WIAF831	Hs.138750	YAC
NDN , NDN5F/6R	Hs.50130	YAC
stSG53014	Hs.180992	RH
BCD1279-3F/4R	-	RH
stSG9006	Hs.931125	RH
stSG10131 , stSG26368	Hs.15548	RH
sts-H58001	Hs.37456	RH
D15S128		YAC
SNRPN , SGC31492, R99003	Hs.48375, Hs.131891	YAC
PAR-5	Hs.179987	YAC
WI-15028	Hs.31797	YAC
WI-13791 , WI-15655	Hs.22543, Hs.23231	YAC
IPW , IPW-60A/60B ,	Hs.5022	YAC
WI-14946 , A009W43, WIAF-778	-	YAC
PAR-1	-	YAC
stSG3346	-	YAC
A005C48	-	YAC
UBE3A , WI-6519 , stSG3525, WI-13724	Hs.180686	YAC
PAR-2	-	YAC
sts-N21972	Hs.43052	RH
SGC44643	-	RH
stSG12920	-	RH
stSG47701	Hs.163845	RH
stSG15842	-	RH
D15S122		YAC
WI-16777	-	YAC
WI-15959	Hs.143997	YAC
GABRB3	Hs.1440	YAC
GABRA5	Hs.24969	YAC
GABRG3	-	YAC
D15S156		YAC
APBA2 , WI-14097	Hs.26468	YAC
SGC32570	Hs.167626	YAC
P	Hs.82027	YAC
WI-4477	-	YAC
D15S165		YAC
SGNE1 , SGNE1-1F/2R	Hs.2265	RH

Although four paternally expressed genes, *MKRN3*, *NDN*, *SNRPN* and *IPW*, had been identified within the PWS deletion region, there was no correlation between the loss of expression of a specific PWS region gene and the PWS phenotype. Furthermore, no affected individuals had been identified with a mutation affecting the expression of a single PWS region gene, suggesting that the loss of expression of several genes was required for the full manifestation of the disorder. Although the PWS/AS common deletion spans the 4 Mb interval between the flanking repeated sequences, a telomeric boundary for genes critical to PWS was limited by a deletion breakpoint marker (D15S174) identified in a family segregating an unusual submicroscopic deletion of proximal human chromosome 15 (Greger et al., 1993; Hamabe et al., 1991).

As comparisons with the syntenic mouse region showed that the homologous genes were in the same order in both species (Chaillet et al., 1991), PWS mouse models were used to define a critical imprinting region. A comparison of mouse deletion models suggested the presence of an unidentified, paternally expressed gene in the critical PWS region, whose loss of expression could contribute to the PWS phenotype. A mouse with a radiation-induced deletion generated between *P* and *Ipw* did not produce a phenotype when paternally inherited (Johnson et al., 1995). However, a genetically engineered paternal deletion from *Snrpn* to *Ube3a* causes hypotonia, growth retardation and partial lethality. This suggested the presence of a gene contributing to these aspects of PWS located between *Snrpn* and *Ipw* (Tsai et al., 1999b), and potentially, a similar situation exists in humans. Additionally, the phenotype could also be affected by paternally expressed genes located in the centromeric part of the common deletion region.

The experiments in this chapter were designed to define the boundaries of the imprinted region through the analysis of ESTs (Boguski and Schuler, 1995). The framework for these experiments was a physical map of the human 15q11-q13 region that was constructed containing 118 YACs and 118 STSs (Christian et al., 1998). The map included 49 genes and ESTs, with an average density of 1 STS for every 35 kb of sequence. To address the possibility that additional imprinted genes reside within 15q11-q13, I analyzed a set of 40 ESTs that had either been physically or radiation hybrid mapped to chromosome 15q11-q13. Using an RT-PCR assay and physical mapping on a YAC contig, I identified seven uncharacterized ESTs that were exclusively expressed from the paternal allele, and one EST that was primarily maternally expressed in a tissue-specific manner. My results suggested that at least 13 paternally expressed transcriptional units resided in the PWS critical region, of which ten are centromeric to D15S174 and therefore might play a role in the PWS phenotype. The clustering of paternally expressed transcripts further suggested a strong regional control of imprinting.

Results

Selection of expressed sequences: EST contig building and library screening

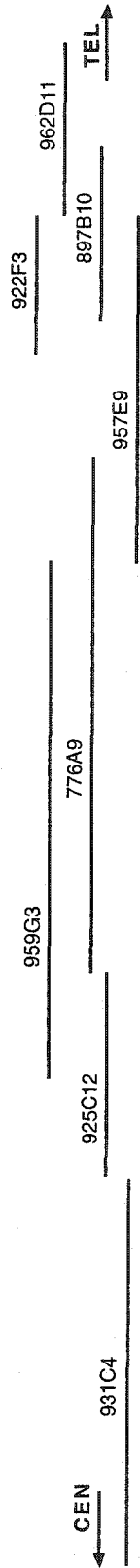
The predicted critical region for PWS genes is centromeric to D15S174 (Greger et al., 1993). To focus on this region, while taking into account the imprecision of radiation hybrid mapping, ESTs were initially chosen from the region between the markers D15S1035 and D15S156, that flank the smaller PWS-critical region (See Figure 3-1, Table 3-1). All ESTs localized to this RH mapping interval in GeneMap'98 were analyzed and those that corresponded to known genes were excluded (Figure 3-2). Two ESTs were present on more than one chromosome by radiation hybrid analysis and were

also not analyzed. Of the remaining EST set, 27 ESTs were selected for analysis. Six ESTs identified by similar analysis of GeneMap'99 were added. During the course of this analysis, a YAC map of the PWS/AS deletion region was published (Christian et al., 1998) from which I selected seven additional ESTs, for a total of 40 ESTs. The centromeric part of the PWS/AS deletion region was emphasized in the EST selection, so that not all ESTs from the more telomeric region were included in this study. I then analyzed the information in UniGene to eliminate ESTs that were members of the same transcribed cluster. A set of 28 ESTs remained after this step.

A 3.2 kb cDNA clone was identified from an adult heart cDNA library by screening with a fragment of the cDNA I360433, which contains the EST WI-15655. Sequence from the 3.2 kb overlapped with another cDNA clone, I31299, which contained the EST WI-13791. These results indicated that the ESTs WI-15655 and WI-13791, and their respective UniGene clusters, were part of the same transcriptional unit and separated by 4.4 kb of cDNA sequence. After database analysis and grouping into EST clusters, a final set of 27 unique ESTs that did not correspond to known genes remained and was further analyzed (Figure 3-2).

Figure 3- 1. Map of the PWS/AS deletion region.

The PWS/AS common deletion region is marked by the large double headed arrow, with the portion in gray denoting the PWS critical region. A minimal set of overlapping YAC clones (top) was used to localize ESTs (middle) within the deletion region. Genes are indicated in bold. STS (D15S) markers are noted below the YACs on the map. The imprinted expression profile for the ESTs and genes is indicated at the bottom. Previously reported results are in brackets, whereas results from this study are not. Tissues studied were lymphoblast cell lines (LCL), fibroblast cell lines (FB) and brain (BR). Other symbols used are: -, not expressed; blank, not done; ?, not certain since contradictory results have been obtained using different methods. Expression was detected in the RT-PCR assay as indicated: B, biparental; P, paternal; M/B, biased maternal. The relative order of markers in brackets was not determined. BP2, BP3A and BP3B represent the repeated units that flank the common PWS/AS deletion region. The order of ESTs and markers within BP2 is according to Christian et al. (Christian et al. 1999). These markers are repeated in BP3A and BP3B but are not shown on this map. The cluster of paternally-expressed transcripts is boxed. ESTs stSG9006 and stSG10131 (&) were present on YAC 931C4, placing them in the interval between and including markers BCL8 and A008B26, but have not been more finely localized so are drawn next to A008B26.



Item	Category	Value
BCL8	LCL	B
NIB1540	FB	B
SHGC13938	BR	B
A002B45		B
SHGC15126 (MYLE)		B
SGC32610		B
A006B10 (MNT)		B
A008B26		B
& S1SG9006		B
& S1SG10131		B
ZNF127		(P)
WI-15987		P
MDN		P
S1S-H58001		P
S1SG53014		P
SGC44643		P
SNRPN		P
PAR-5		(P)
WI-15028		P
WI-13791		P
IPW		P
WI-14946		B
PAR-1		(P)
S1SG12920		P
S1SG3946		P
S1S-N21972		P
BCD1279		B
A005C48		P
UB33A		B
PAR-2		(B)
WI-16777		B
S1SG47701		P
S1SG15842		P
WI-15959		B
GABRB3		(P)
GABRA5		(P)
GABRG3		(P)
WI-14097 (APBA2)		B
SGC32570		B
P		(B)
WI-4477		(B)
HERC2		B
SGNE1		B

D15S165 BP3A/BS
D15S156
D15S122
D15S174
D15S128
D15S1035 BP2

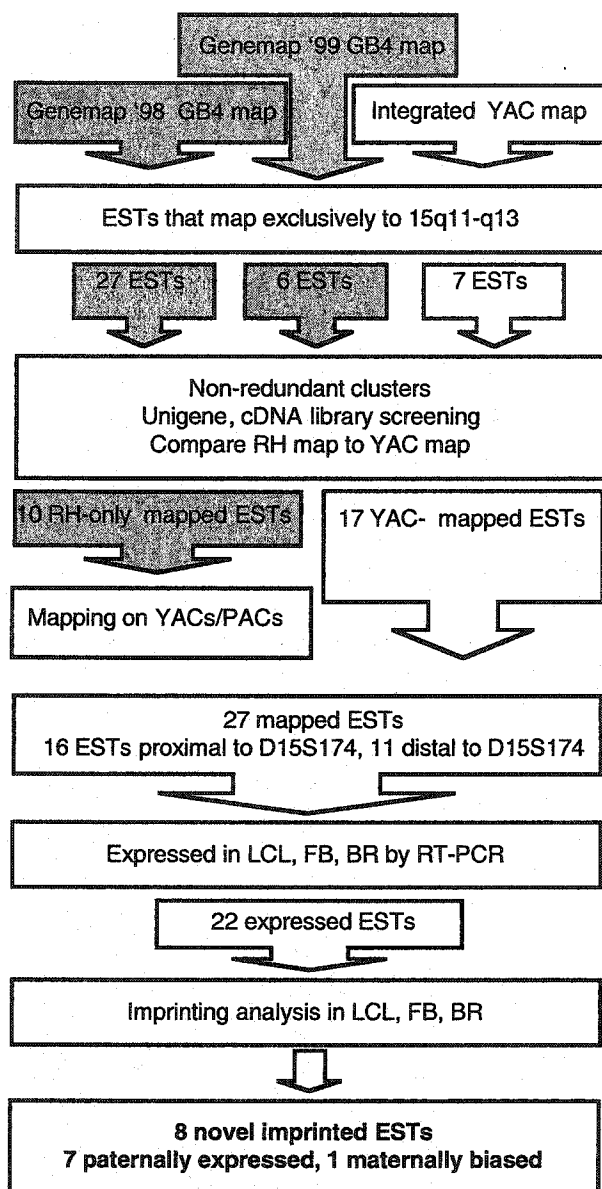


Figure 3- 2. Flow chart illustrating the selection process for ESTs in the 15q11-q13 region.

The source of the ESTs is indicated at the top. The process by which ESTs were sorted for redundancy, placed on the physical map, and tested for expression and imprinted is represented, with the resulting identification of eight novel imprinted transcripts indicated at the bottom of the flowchart. Large arrows in gray represent ESTs that are not yet physically mapped.

Physical mapping of unique ESTs

Physical maps of the PWS deletion region and its flanking repeats have been generated based on large-insert DNA clones (Amos-Landgraf et al., 1999; Christian et al., 1998; Christian et al., 1999). One group of ESTs, represented by the ESTs SGC32610, SHGC-15126 (*MYLE*), SHGC17218, A008B26, and A006B10 (MN7), had previously been shown to be present in at least three copies, located at the centromeric and telomeric breakpoints of the common deletion region (Christian et al., 1999). Of the 27 unique ESTs selected, 10 had not been physically mapped but were predicted to be in or near the PWS deletion interval on the basis of their location between D15S1035 and D15S122 on the radiation hybrid map (Table 3-1). To place these ESTs on the physical map, DNA was isolated from a series of overlapping YACs spanning the PWS common deletion region and tested for content of known markers to confirm their identity (Figure 3-1). YAC DNA was then tested by PCR with EST primers placing the 10 ESTs on the physical map (Figure 3-1). Three ESTs, SGC44643, sts-H58001 and stSG53014 were located in the interval between *NDN* and *SNRPN*, a region important for PWS but not previously known to contain any genes. Two ESTs (stSG9006 and stG10131) were located proximally on YAC931C4 but could not be more finely mapped. Three ESTs (stSG12920, sts-N21972 and BCD1279) were located on the overlapping YACs 959G3 and 776A9. These ESTs were more finely mapped using PAC clones from this region containing reference STS markers.

Imprinting status of expressed sequences

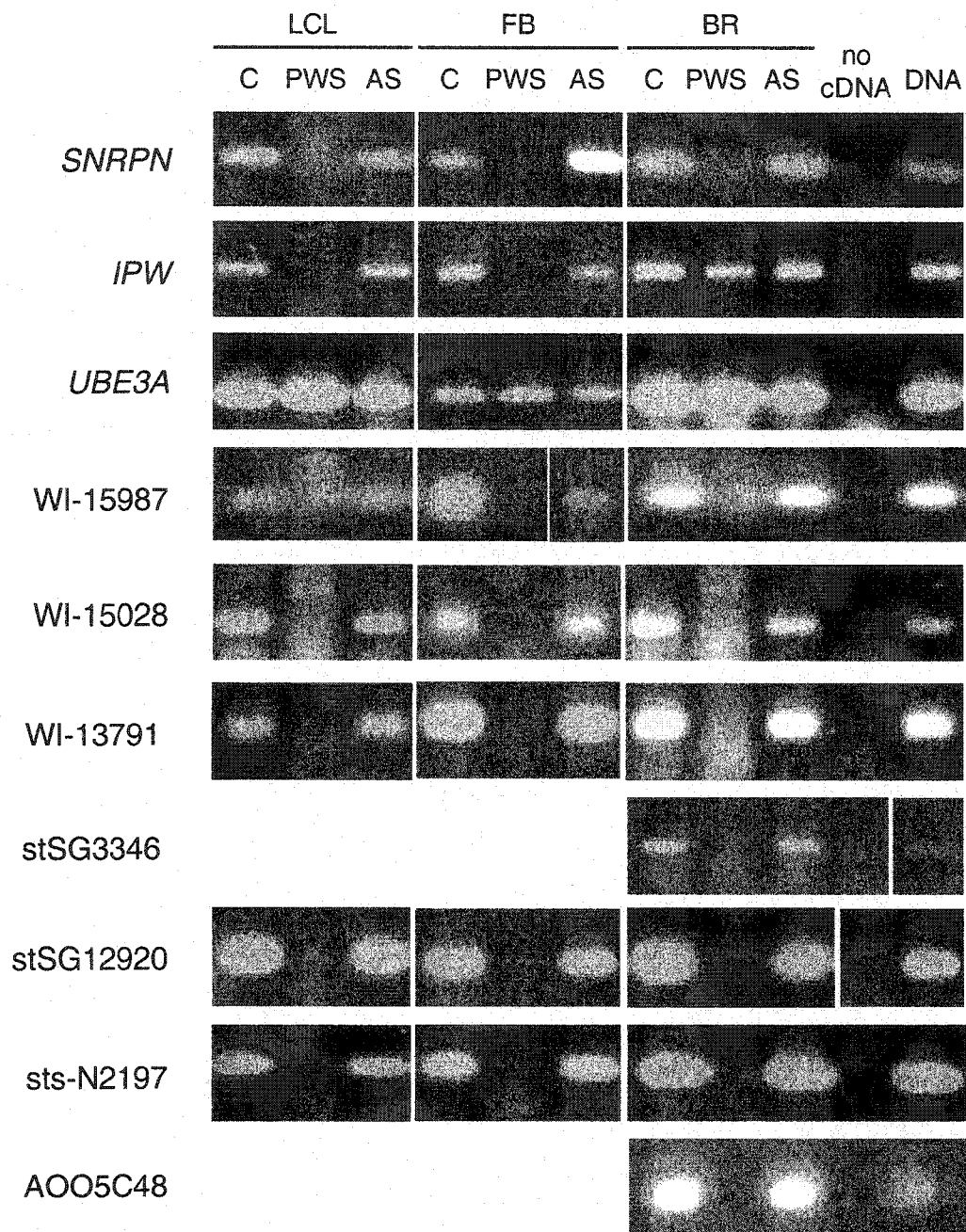
The PWS/AS common deletion region contains biallelically expressed genes, paternally expressed genes, and one gene expressed predominantly from the maternal

allele in a tissue-specific fashion. In addition to the known imprinted genes, several cDNA fragments located within the common deletion region, PAR-5, and PAR-1 (Ning et al., 1996; Sutcliffe et al., 1994) were reported to be paternally expressed, while PAR-2 (Nakao et al., 1994), was biallelically expressed. However, the allelic expression pattern of other ESTs mapped to the PWS/AS common deletion region had not been assessed. To address this, an RT-PCR assay that detected parent-of-origin specific expression was designed. RNA was isolated from brains, lymphoblast and fibroblast cell lines of control individuals, PWS patients with a paternal 15q11-q13 deletion, and AS patients with a maternal 15q11-q13 deletion. Because of the deletions in the patient samples, I predicted that genes in 15q11-q13 that were exclusively paternally expressed would show no expression in the PWS samples, as previously demonstrated for *SNRPN* (Wevrick and Francke, 1996). Similarly, genes that were exclusively maternally expressed would show no expression in the AS-derived samples. To test this hypothesis, RNA samples from lymphoblasts, fibroblasts, and brain from control, PWS and AS individuals were tested by RT-PCR with gene primers from the 15q11-q13 region. As expected, the known imprinted, paternally expressed *NDN* and *SNRPN* genes were expressed only in AS and control samples, with no product visible in the PWS samples (Figure 3-3). *NDN* is not expressed in lymphoblasts, so this cell type could not be assessed for imprinting. Surprisingly, *IPW* RNA was detected in control, PWS and AS brain but restricted to control and AS samples in fibroblasts and lymphoblasts, suggesting that its imprinting is tissue-specific (Figure 3-3). The *MN7* transcripts were equally active regardless of the parental origin of the allele(s) present. *UBE3A* was previously shown to have biallelic expression in fibroblasts and lymphoblasts by RT-PCR (Nakao et al., 1994), and a bias

towards maternal expression in brain (Rougeulle et al., 1997; Vu and Hoffman, 1997). In this non-quantitative assay, expression appeared biallelic in all tissues including brain (Figure 3- 3). These results validated the RT-PCR assay, although no maternally expressed gene was available as a control for maternal-only expression.

Figure 3- 3. Imprinting status of genes and ESTs.

RT-PCR was performed on RNA derived from lymphoblasts (LCL), fibroblasts (FB) and brain (BR) from control (C), deletion Prader-Willi syndrome (PWS), and deletion Angelman syndrome (AS) individuals. The second last lane shows a PCR amplification with no cDNA added, and the last lane shows amplification with human genomic DNA. Negative control PCR reactions with no reverse transcriptase were performed but are not shown. The ESTs stSG3346 and A005C48 are not expressed in lymphoblasts or fibroblasts.



I then tested all 27 ESTs for expression in control RNA samples from lymphoblasts, fibroblasts and brain. Five ESTs (SGC44643, WI-4477, stSG53014, stSG47701 and sts-H58001) were eliminated from further analysis because their transcripts could not be detected by RT-PCR. The remaining 22 unique ESTs showed expression in at least one tissue source, so RT-PCR was performed on control, PWS and AS RNAs (Figs. 3-1, 3-3). From these results, the ESTs could be classified as having biparental expression (14 ESTs), paternal-only expression (7 ESTs) or maternal-biased expression (1 EST) in at least one tissue source. Of the seven new paternally expressed transcriptional units identified, four localized to the PWS critical region between D15S1035 and D15S174, and three were located just telomeric to D15S174 but centromeric to *UBE3A* (Figure 3-1). Two apparently biallelically expressed transcripts, represented by EST WI-14946 and BCD1279, were located among the set of paternally expressed transcripts. With one exception, all ESTs located centromeric to the deletion, or to within the flanking repeated regions were biparentally expressed. As there were at least three copies of most of the ESTs in the breakpoint repeats (Christian et al., 1999), the assay could not distinguish among the ESTs in the breakpoint repeated clusters. It is possible that the apparently biallelic RT-PCR products for ESTs within the breakpoint region (SGC32610, SHGC-15126, A006B10 (MN7), and A008B26) represent amplification from transcripts derived from multiple loci. This could mask a monoallelic expression profile from one of these loci, as previously noted for MN7 (Ji et al., 1999). Surprisingly, the EST SGC32610, located within the breakpoint repeat, displayed maternal-biased expression in lymphoblasts, with reproducibly reduced expression evident in lymphoblasts from two different AS individuals. However, given the non-

quantitative nature of this assay, further experiments are necessary to conclude definitively that SGC32610 is imprinted. One final gene, *SGNEI*, is located on chromosome 15 distal to the PWS deletion (Mattei et al., 1990), and was chosen for study because previous studies had indicated possible changes in protein level in PWS brain (Gabreels et al., 1998; Gabreels et al., 1994; Graham et al., 1992). However, the *SGNEI* transcript was expressed from both alleles in this assay.

Expression profile of imprinted ESTs

The RT-PCR and mapping analysis indicated that seven newly identified paternally expressed ESTs are located within the 4 Mb PWS/AS common deletion region (see box in Figure 3-1). As well, one EST that appeared to show maternally biased expression was located within the breakpoint repeats. These ESTs are represented among cDNAs identified as part of the dbEST portion of the Human Genome project (Boguski and Schuler, 1995), and have been grouped into UniGene clusters. To estimate the expression level and range of tissue expression of the cDNAs represented by each EST, the UniGene clusters to which each imprinted gene or EST belongs were examined (Table 3-2). In two cases (stSG12920 and A005C48), cDNA clones linked to the EST markers in GeneMap'98 were used because no UniGene cluster had been assigned to this EST. No cDNA clones were available in dbEST for PAR-1. The number of cDNA clones in each UniGene cluster gives a relative estimate of the gene's expression level. Each cDNA was counted only once in the analysis, even if both the 5' and the 3' ends were present in the UniGene cluster. Analysis of the UniGene clusters for *SNRPN*, *NDN*, *ZNF127*, *IPW* and *UBE3A* (Table 3-2) revealed a range of tissue expression for each gene. In comparison, a more limited range of tissue expression was seen for the newly

described imprinted ESTs and PAR-5, a previously identified paternally expressed cDNA fragment. Using the moderately expressed *SNRPN* gene as a comparison, the eight new imprinted transcription units showed low expression levels in the tissues commonly used for generation of ESTs. The UniGene clusters for ESTs not corresponding to known genes were also examined for coding potential through sequence analysis using the BLASTX algorithm, but no protein coding regions nor significant potential open reading frames were found.

Table 3- 2. Estimate of expression levels for imprinted transcription units.

Representation in UniGene and dbEST was used to estimate the expression levels and tissue distribution of paternally expressed (PAT) and biased maternal expressed (MAT) transcripts and genes. In adult tissues, brain includes cDNA libraries constructed from infant brain, CNS, brain, MS lesion, cerebellum, NT-2 cells, and Schwannoma tumor. Checkmarks indicate that a cDNA(s) from this tissue is in the UniGene cluster.

	PAT											MAT		
	ZNF127	WI-15987	NDN	SNRPN	PAR-5	WI-15028	WI-13791	IPW	stSG3346	stSG12920	sits-N21972	A005C48	SGC32610	UBESA
Fetal tissues														
brain, fetal		✓	✓	✓		✓	✓							✓
cochlea, fetal		✓									✓			
heart, fetal				✓		✓	✓							
liver spleen, fetal				✓			✓		✓			✓	✓	
embryo		✓	✓											✓
Adult tissues														
adrenal gland			✓	✓				✓						
brain	✓	✓	✓	✓	✓	✓	✓	✓	✓			✓		✓
bone														✓
breast				✓										
colon				✓										✓
eye, retina, fovea			✓	✓	✓		✓							✓
gall bladder				✓										
germ cell, testis			✓	✓	✓			✓						✓
heart/aorta			✓	✓	✓		✓							✓
kidney			✓	✓			✓	✓						✓
liver				✓										
lung		✓	✓	✓	✓		✓	✓						✓
muscle			✓	✓			✓							✓
ovary				✓										✓
pancreas			✓	✓										✓
parathyroid								✓						✓
placenta														✓
prostate			✓	✓										✓
skin														✓
stomach				✓			✓	✓						✓
synovial membrane				✓										
T-cells, blood cells	✓			✓				✓						
thyroid				✓										✓
tonsil							✓							✓
uterus		✓	✓	✓				✓						✓
number of cDNA clones	3	4	41	126	7	2	15	36	1	1	1	1	3	142

Discussion

The PWS/AS region has at least eight additional imprinted transcripts

From this set of experiments, I identified a set of transcripts in the PWS/AS deletion region and determined the genomic imprinting status for each. I identified eight novel imprinted transcription units within the PWS/AS deletion region. Among these, four new paternally expressed ESTs were located within the PWS critical region as defined by the markers D15S1035 and D15S174 (Greger et al., 1993). Assuming that the gene order is conserved in mouse, and that the novel ESTs are conserved between human and mouse, then only the three genes represented by WI-15987, WI-15028 and WI-13791 are inside the critical region as defined by radiation induced deletions in mouse (Johnson et al., 1995). The eight new imprinted transcription units generated lower level transcripts than the previously identified PWS region genes based on analysis of cDNAs in UniGene. Other developmentally important genes are expressed at low levels in fetal and adult tissues, but are nonetheless essential at critical developmental stages and may cause abnormal development when absent (Odent et al., 1999). By RT-PCR, transcripts associated with all seven paternally expressed ESTs could be detected in brain, the major organ of involvement in PWS (Figure 3-1). Furthermore, five of the imprinted ESTs were represented in cDNA libraries derived from brain (Table 3-2). These results suggested that the genes represented by these ESTs should be included with previously identified paternally expressed genes as potentially responsible for the manifestations of PWS.

The phenotype of AS is thought to be primarily due to the absence of *UBE3A* expression, since a subset of AS patients carries mutations only in the *UBE3A* gene. However, there is evidence to suggest that deletion cases are more severely affected than

non-deletion ones (Rougeulle and Lalande, 1998). The EST SGC32610, located in the repeats that flank the PWS/AS deletion, appeared to be preferentially maternally expressed in lymphoblasts. This is similar to previous results for *UBE3A* that showed incomplete imprinting in brain. The transcript represented by SGC32610 is the first example of a gene that could modify the Angelman syndrome phenotype, through loss of expression in deletion and imprinting center AS cases. Over-expression of the gene represented by the EST SGC32610 may also be implicated in the phenotype of patients with additional maternally derived copies of chromosome 15q11-q13 (Huang et al., 1997; Rougeulle and Lalande, 1998). A complete transcript map will aid in the identification of genes for other disorders associated with 15q11-q13, including spastic paraplegia, obsessive-compulsive disorder, bipolar illness and autism (Christian et al., 1998). Further investigation of the genes associated with the imprinted ESTs and their imprinting status in other tissues and developmental stages is clearly needed to understand their possible roles in the etiology of disorders involving 15q11-q13.

RT-PCR effectively identifies novel imprinted transcripts

The EST RT-PCR assay described here is an extension of a *SNRPN* RT-PCR assay previously proposed as a rapid diagnostic test for PWS in small blood samples (Wevrick and Francke, 1996). A similar assay has also been used to analyze the X-inactivation status of a number of transcribed sequences across the Xp11 region of the human X-chromosome (Miller and Willard, 1998). While RT-PCR is very sensitive for the detection of low-level transcripts, I have used it in a non-quantitative fashion. Thus, imprinted transcripts that might have unequal allelic expression would appear to have biallelic expression in this assay. Furthermore, transcripts that are imprinted in a tissue-

specific manner may not reveal monoallelic expression in the limited tissue types tested. For example, in the Beckwith-Wiedemann syndrome region, transcripts have shown monoallelic expression during embryogenesis, with gradual loss of imprinting in adult tissues (Dao et al., 1998). Finally, some imprinted genes are associated with antisense transcripts, which may or may not have the same imprinting profile (Jong et al., 1999b; Lee et al., 1999a; Lee et al., 1999b; Mitsuya et al., 1999; Rougeulle et al., 1998). Imprinted genes associated with antisense transcripts could appear biallelic in the RT-PCR assay if the EST primers also amplify the antisense transcript. This can be resolved by performing a strand-specific reverse transcription followed by PCR. In summary, this set of experiments has demonstrated that the EST RT-PCR assay is an effective tool to identify imprinted transcripts, although it may falsely identify some imprinted transcripts as having biallelic expression.

Imprinted transcripts cluster around the PWS/AS IC

The data strongly suggests that the imprinted and paternally expressed regions are bound on the centromeric side by the centromeric repeat region near D15S1035, since all transcripts centromeric to this marker appeared to be expressed biallelically. On the telomeric side, the paternally expressed domain is bound by *UBE3A*, with all tested transcripts distal to this gene expressed from both alleles. EST SGC32610, located within the breakpoint repeats, appears to show a bias towards maternal expression, although the apparent reduction in expression from the maternal allele must be confirmed by a quantitative assay on additional AS samples. These data are consistent with prior observations that imprinted genes tend to occur in clusters in both the human and mouse genomes (Reik and Walter, 1998). Two transcripts (WI-14946 and BCD1279), located

among the cluster of paternally expressed transcripts were biallelically expressed. Studies from the imprinted chromosome 11p15 region have shown that biallelically expressed genes can be found within a group of imprinted genes (Lee et al., 1999b). Alternatively, these transcripts may show tissue-specific imprinting undetected in the limited number of tissues tested in our assay, or may have undetected unequal allelic expression.

Both gene-specific and regional cues have been implicated to explain the clustering of imprinted genes and the common occurrence of oppositely imprinted genes in the same genomic vicinity (Barlow, 1997; Constancia et al., 1998). The clustering of imprinted genes, and a need for oppositely imprinted genes in the same chromosomal vicinity may indicate a mechanism for imprinting control at the gamete stage. In the PWS region, deletion of the IC results in failure of imprinted genes to adopt the proper epigenetic imprint during gametogenesis (Horsthemke, 1997). When paternally inherited, these deletions result in PWS because of the loss of expression of genes that are normally expressed from the paternal allele. The range over which genes are controlled by the IC is unknown, but is not necessarily confined to the common deletion interval, as defined by breakpoint repeats that predispose to deletion. The identification of an imprinted gene outside these boundaries would implicate either a second imprinting control element, or would point to a model whereby the *SNRPN*-associated imprinting center could skip over a cluster of non-imprinted genes and act on a gene beyond this cluster. More complete understanding of the range of action of the Imprinting Center awaits further analysis of imprinting of genes on proximal chromosome 15q.

Parallel experiments

Since the completion of the transcript map discussed in this chapter, several groups have also published similar imprinting assays along 15q11-q13 using complementary techniques. Human monochromosomal hybrids are mouse cell lines that carry a single paternal or maternal human chromosome 15. RT-PCR reactions from the paternal and maternal cell lines of ESTs previously known to map in the 15q11-q13 region were analyzed for preferential expression from either the paternal or maternal alleles (Meguro et al., 2001b). Of the 118 ESTs analyzed by this group, nine were identified as having a strong bias towards paternal expression. These results confirmed my initial findings for ESTs WI-15028, WI-13791, SGC44643, and sts-N21972. The human monochromosomal hybrid assay also identified the paternally expressed snoRNA *HBII-85*, as well as two novel ESTs, H75355 and H73492. Neither of these two novel transcripts could be amplified from genomic clones specific to the region. Interestingly, this assay found that the EST WI-14946 was paternally expressed, whereas, my results suggested that it was biallelic. The conflicting results may be due to the RT-PCR process as previously discussed, differences in imprinting between monochromosomal hybrid panels and deletion samples, or it due to endogenous variabilites in imprinting at that locus.

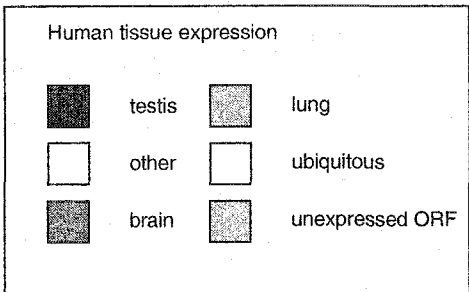
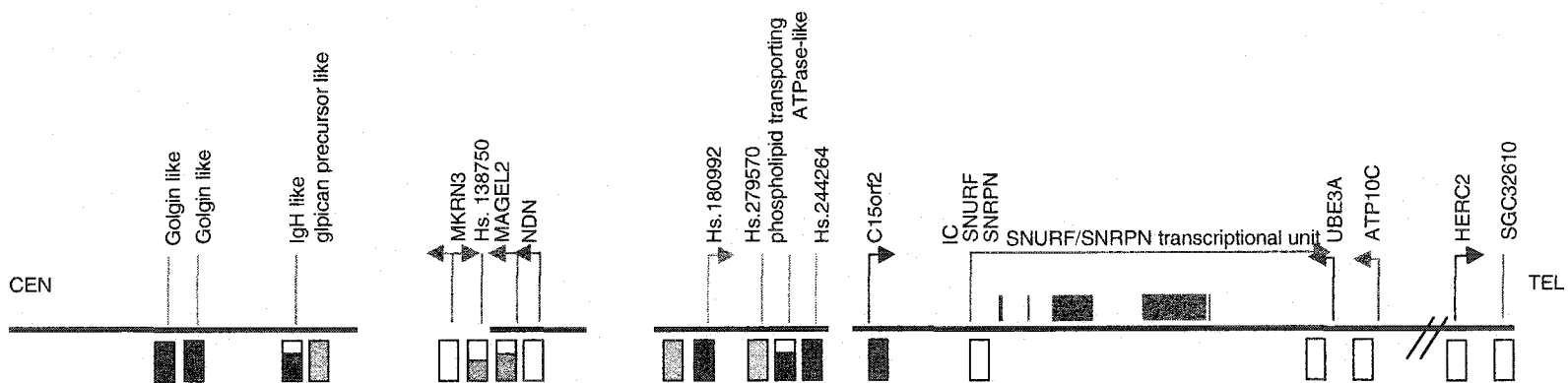
Another group compared the expression levels of control samples with PWS patient samples using a custom designed microarray chip containing transcripts from the 15q11-q13 region (Bittel et al., 2002). Hybridization signals were compared between lymphoblast RNA of PWS patients and obese comparison subjects. The custom microarray identified one new paternally expressed EST WI-6654, which maps to a

genomic fragment containing *HBII-85* and *HBII-52*, and thus is most likely, a part of the untranslated portion of the *SNURF/SNRPN* transcript. This approach also showed paternal expression for STSG12920, sts-N21972, and biased maternal expression for SGC32610, corroborating my findings.

Through the sequencing efforts of the Human Genome Project, a majority of the 15q11-q13 region has been sequenced and can be viewed electronically using the MapViewer program from the National Center for Biotechnology Information. In May 2002, three gaps remained in the final sequence (Figure 3-4). A re-evaluation of the region using gene prediction programs and the UniGene EST database does not reveal additional PWS candidate genes. Criteria for candidate genes included transcripts that are localized between *SNRPN* and the centromeric breakpoint, expression in the brain, and preferential expression from the paternal allele.

Figure 3- 4. Current transcript and gene organization within the PWS critical region.

The location of genes, UniGene clusters, and pseudogenes in the PWS critical region. The horizontal black line represents the known sequence in May 2002 obtained through the Human Genome Project, breaks in the line represent gaps in the sequence. Vertical colored lines represent active transcription with arrow heads indicating gene orientation, black represents biallelic expression, blue are paternally expressed, red are maternally expressed and green are unknown. Blue boxes above the horizontal line represent the snoRNAs. Colored boxes below the horizontal line represent the tissue distribution of each transcript. Diagonal lines represent sequence that is omitted from this figure, *HERC2* and EST SGC32610 are repeated in the breakpoint clusters, but are only shown once.



Many of the ESTs originally thought to represent unique genes are now shown to be part of the extended *SNURF/SNRPN* transcript. *PAR7* is now known as *HBII-85* and *PAR-5* as *HBII-13* (Cavaille et al., 2000). *sts-N21972*, which I first identified in my transcript assay, is now known to be part of the untranslated exons of the *SNURF/SNRPN* transcript, in the portion previously known as *IPW* (Runte et al., 2001). Analysis of the published sequence for the 15q11-q13 region shows that EST WI-13791 is also part of this untranslated transcript. Based on the results presented in this chapter, I had identified the ESTs WI-15987, WI-15028 and WI-13791 as strong candidate genes for involvement in PWS based on their paternal expression in brain as well as their location within the PWS critical region. Both WI-15028 and WI-13791 are now known to be part of the *SNURF/SNRPN* transcript. UniGene cluster Hs. 138750 contains the EST WI-15987 and consists of four transcripts from brain, uterus and cancer cells. Though it has a potential open reading frame, it does not have sequence similarities to known proteins.

In summary, the PWS/AS critical region currently contains the paternally imprinted genes *MKRN3*, *MAGEL2*, *NDN* and the *SNURF/SNRPN* transcriptional unit (Figure 3-4). The maternally expressed gene, *UBE3A*, is now understood to be regulated by a silencing of the paternal alleles by the *SNURF/SNRPN* transcript (Rougeulle et al., 1998; Runte et al., 2001). *ATP10C* is a recently identified maternally expressed gene that may also be regulated by *SNURF/SNRPN* promoter (Runte et al., 2001). The recently cloned *C15orf2* is biallelic but expressed in testis only. Seven uncharacterized UniGene clusters between the proximal breakpoint and the start of the *SNURF/SNRPN* transcript can be identified based on sequence analysis. An additional UniGene cluster, Hs. 138750 is located in one of the unsequenced regions. Six of these UniGene clusters are expressed

exclusively or predominantly in testis, while UniGene cluster Hs.279570 contains lung specific transcripts. Several of the UniGene clusters have sequence homologies. Two adjacent clusters, Hs.351473 and Hs.169639, are both expressed in the testis and show strong homologies to a Golgi protein. Hs.304741 is also expressed in the testis and shows high sequence identity to immunoglobulin heavy chain variable region. Most of the transcripts associated with Hs.120397 are expressed in the testis and may encode for a putative phospholipid-transporting ATPase. Sequence analysis reveals two putative open reading frames that are not associated with any transcribed sequence, and may represent pseudogenes.

Although the 15q11-q13 region was originally thought to house over 100 genes, sequence analysis now suggests that this number is considerably lower. Total gene estimates for the entire genome have also been lowered from 100,000 genes to 30,000 (Ewing and Green, 2000; Venter et al., 2001). Analysis of genomic sequence and mapped ESTs suggest that there is a scarcity of genes between the *NDN* and *SNRPN* loci. Within the PWS critical region, there appears to only be 5 strong candidate genes responsible for the PWS phenotype: *MRKN3*, *MAGEL2*, *NDN*, *SNURF/SNRPN*, and the snoRNA *HBII-85*. Functional analysis into the role of each of these in the etiology of PWS still needs to be carried out.

Chapter 4. Identification and expression analysis of the novel gene, *MAGEL2*, suggests a role in Prader-Willi syndrome

Parts of this chapter have been previously published.

Lee, S., Kozlov, S., Hernandez, L., Chamberlain, S. J., Brannan, C. I., Stewart, C. L. and Wevrick, R. (2000). Expression and imprinting of *MAGEL2* suggest a role in Prader-Willi syndrome and the homologous murine imprinting phenotype. *Hum Mol Genet* 9, 1813-1819. (Permission has been given to republish this material).

All of the results presented in this chapter were done by Syann Lee

Introduction

Gene identification from genomic sequence

One of the goals of the Human Genome Project was that long uninterrupted stretches of genomic sequence would allow investigators to identify novel genes based solely on nucleotide sequence information. Many automated programs have been designed to facilitate the analysis of large amounts of genomic sequence. The BLASTN algorithm compares a nucleotide sequence against an EST database. BLASTN is useful for identifying clusters of transcripts that may be indicative of an active gene. GenScan is a program that identifies genes based on transcriptional, translational and splicing signals (Burge and Karlin, 1997). Grail is another gene prediction program that not only uses similar criteria to identify potential genes, but also evaluates the predictions and eliminates unlikely candidates (Xu et al., 1994). In addition, Grail also identifies regions where the cytosine and guanosine content is greater than 50%. As CpG islands are often associated with gene regulation, this can be used to predict the location of unknown genes.

Analysis of genomic sequence has also shown that 36% of the genome is made up of interspersed repetitive elements, which are degenerate copies of transposable elements (Smit, 1996). The two major classes of repetitive elements are short interspersed nuclear elements (SINEs) and long interspersed nuclear elements (LINEs), while retrovirus-like elements and DNA transposon fossils make up the remainder of repeats. The RepeatMasker Web Server screens DNA sequences against a database of repetitive sequences to identify repeats. Masking repetitive elements and searching for gene coding

sequences in repeat-free regions of the genome reduces the amount of redundant sequence that needs to be analyzed.

The MAGE family genes

By using gene prediction programs to analyze non-repetitive genomic DNA, I identified a new gene within the PWS critical region that is a member of the MAGE (melanoma associated antigen) gene family. The MAGE genes were initially characterized by their expression in tumor cells (Barker and Salehi, 2002; Chomez et al., 2001). Nonapeptides from MAGE products are bound by major histocompatibility complexes and presented to the cell surface. The genes share a central MAGE homology domain of 165-171 amino acids in length while the amino- and carboxy-termini are poorly conserved. The MAGE domain does not have homology to any known proteins. Most MAGE proteins have a small, potential transmembrane domain, which may function in protein-protein interactions (De Plaen et al., 1994). Despite their protein similarities, MAGE promoters are highly variable, suggesting a transcriptional specificity resulting in regional and temporal specificity. Type I MAGE genes were the first to be identified, and are located in clusters along the X-chromosome (Barker and Salehi, 2002). Their expression is restricted to testis, cancer cells and occasionally placenta. Type I genes are thought to have arisen from retrotransposition and duplication events from a founder gene (Chomez et al., 2001). Type II genes are phylogenetically distinct genes that are not necessarily X-linked, and mainly identified based on sequence similarity to Type I genes. Putative MAGE genes have been identified in zebrafish, *Drosophila*, *Aspergillus*, and *Arabidopsis* and have the highest sequence identity to type II genes. Type II genes are widely expressed throughout development and some are also highly

expressed in some forms of cancer. It has been suggested that they may be important in cell survival, cell cycle regulation and apoptosis.

Necdin was the first member of the Type II MAGE genes to be identified (Chomez et al., 2001; Maruyama et al., 1991). Murine *Ndn* was first identified in a screen for genes that were upregulated in retinoic acid (RA)-treated, differentiated P19 cells (Maruyama et al., 1991). P19 mouse embryonal carcinoma cell cultures are commonly used to investigate early developmental events (McBurney, 1993). The cells are derived from tumors created by transplanting an E7.5 embryo into the testis. As the pluripotent P19 cells can be induced to differentiate into muscles or neuronal cells, the system is most often used in studies of cell fate determination.

Induction of P19 cells with dimethyl sulfoxide produces mesodermal and endodermal cells, including cardiocytes, skeletal muscle, epithelium, endothelium and chondrocytes. Treatment of P19 cells with RA induces differentiation into post-mitotic neurons, astroglia and microglia (McBurney, 1993). RA induces a developmental cascade by acting on a group of nuclear retinoic acid receptors that are ligand-dependent transcription factors. Cell cultures can be enriched for the non-mitotic neurons with the addition of the mitotic inhibitor cytosine arabioside (Rudnicki and McBurney, 1987). Neurons produced from P19 cells have many of the same physiological and molecular properties as *in vivo* neurons (McBurney, 1993). In addition to studying the developmental cascade that is initiated during neuroectodermal differentiation, P19 cells are also extensively used to study the expression of cell cycle regulatory factors during the terminal differentiation of neurons.

In vitro cell culture experiments have implicated necdin in cell cycle control. Overexpression of *Ndn* in the mouse NIH3T3 myeloma and SAOS-2 osteosarcoma cell lines causes arrested cell growth but does not affect cell viability (Hayashi et al., 1995). Furthermore, necdin has been shown to interact with several cell cycle proteins, p53, a tumor suppressor, E2F1, a Rb-binding transcription factor involved in the cell cycle progression of dividing cells, and E1A, a viral oncogene that complexes with Rb (Taniura et al., 1999; Taniura et al., 1998). Necdin has also been shown to be a transcriptional repressor that binds to guanosine clusters (Matsumoto et al., 2001). This body of data suggests that necdin may act upon the cell cycle as a transcriptional repressor or co-repressor (Barker and Salehi, 2002).

This chapter describes the identification of the novel gene, *MAGEL2*, from the genomic sequence PAC pDJ181P7. The sequence of *MAGEL2* is similar to that of *NDN*, and suggests that they may also have similar functions. I also present expression analysis of the gene in humans and mice. Its expression profile and its location within the PWS critical region suggest that *MAGEL2* is a strong candidate for involvement in the pathophysiology of PWS.

Results

In silico* identification of *MAGEL2

The genomic PAC clone, pDJ181P7 (GenBank Accession #AC006596), consisting of 103 kb, was the first completely sequenced stretch of genomic DNA in the PWS critical region. The location of the PAC within the 15q11-q13 deletion interval was confirmed by the identification of *NDN* in the finished sequence. In order to simplify the sequence analysis, I first identified regions that contained homologous sequence to

known repetitive elements. Preliminary annotation of repetitive elements was performed by the sequencing group at the University of Texas Southwestern Medical Center, and was released with the completed sequence. I also used the RepeatMasker Web Server to identify additional repeats. Repeats fragmented by small insertions or deletions were considered as one repetitive element. From this analysis, 103 repetitive elements were identified, comprising 55% of the sequence (Table 4-1).

Table 4- 1. Repetitive elements along pDJ181P7.

The genomic clone PAC pDJ181P7 was analyzed using RepeatMasker for the following repetitive elements: short interspersed nuclear elements (SINEs), long interspersed nuclear elements (LINEs), retroviral elements, DNA transposons and small, repetitive RNAs.

Repetitive Element	Number	% of pDJ181P7
SINEs	44	12
LINEs	43	33
retroviral elements	13	10
DNA transposons	3	<1
Small RNA	1	<1
TOTAL	104	55

After masking the repetitive sequences, pDJ181P7 was analyzed using the BLASTN algorithm. ESTs were distributed between four loci along the PAC (Table 4-1). Single ESTs were found at either end of the genomic sequence, but these were not investigated further. Two large EST clusters were identified by BLASTN analysis, one corresponding to *NDN*, and one comprising a cluster of 9 ESTs 41 kb from *NDN*. This novel cluster matched members of the UniGene cluster Hs.141496. Furthermore, the

human ESTs had high sequence homology to several mouse ESTs, suggesting that the gene associated with the cluster was evolutionarily conserved.

As different gene prediction programs emphasize different gene characteristics, several algorithms were used to analyze the pDJ181P7 genomic sequence, and the results were compared to determine which predictions were most likely to represent novel genes (Figure 4-1). MetaGene is a program that simultaneously analyzes genomic sequences using several gene prediction algorithms including GenScan and Grail. GenScan identified three potential genes. The first predicted gene corresponded to the previously cloned *NDN*, while the second gene was predicted to be 37 kb downstream of *NDN*, corresponding to the novel EST cluster identified using the BLASTN algorithm. A third gene was also predicted on the opposite strand. The Grail program identified four open reading frames in the genomic sequence. In addition to *NDN*, two short, upstream open reading frames were also identified. Grail also identified the same protein-coding sequence downstream of *NDN* as GenScan. Three CpG islands were identified in the PAC clone: two CpG islands were associated with the *NDN* gene, with 70% and 60% GC contents, and a third CpG island with 76% GC content was located approximately 40kb downstream of *NDN*.

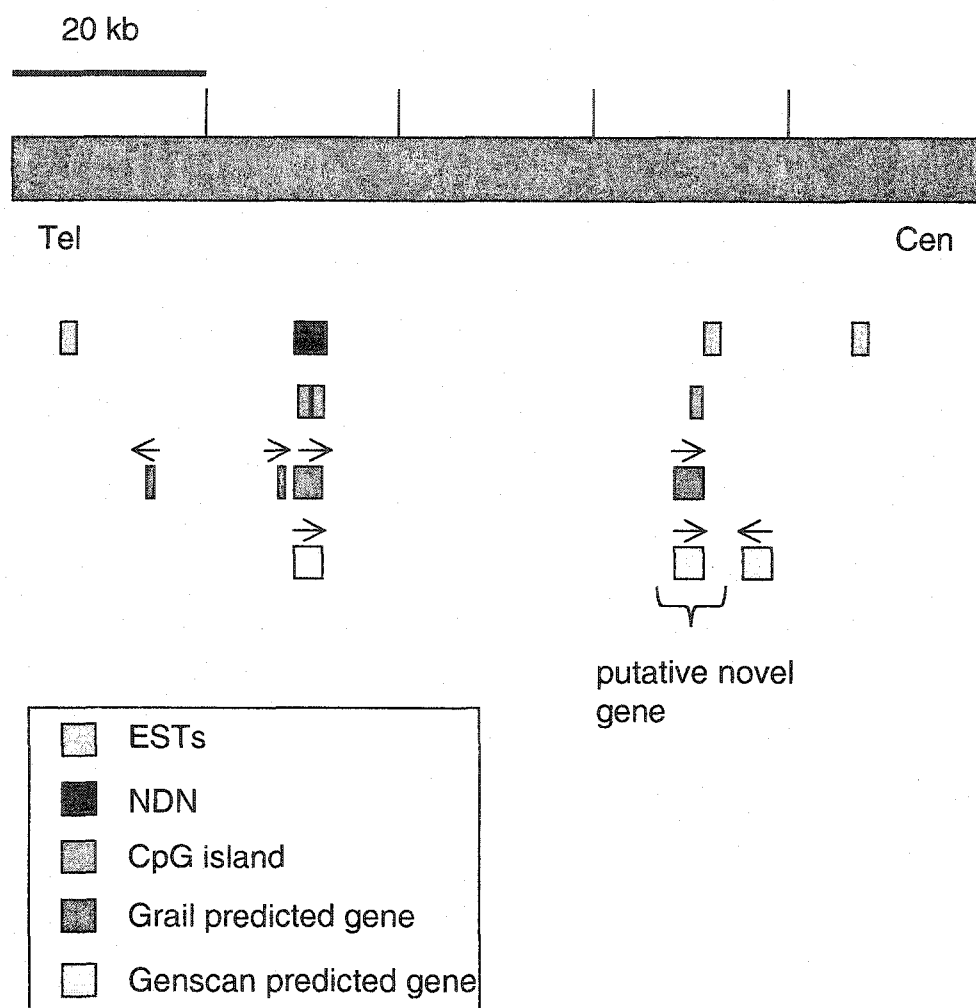


Figure 4- 1. Gene prediction along pDJ181P7.

A summary of the results from several gene prediction programs. The green rectangle represents the genomic sequence from PAC clone pDJ181P7. A scale bar is shown above. EST clusters, the *NDN* gene, CpG islands, and predicted genes are shown below. Arrows represent predicted gene orientations. The bracket marks the location of the putative novel gene (*MAGEL2*) that was further characterized.

I chose to further characterize the potential gene located downstream of *NDN* because of the presence of a strong CpG island, a long open reading frame, clusters of human and mouse ESTs, its location within a region of non-repetitive DNA, and because it was identified by multiple gene prediction algorithms. These features suggested that the region 37-41 kb downstream of *NDN* contained a transcriptionally active gene that was conserved between humans and mice. Furthermore, because of its location adjacent to *NDN*, it was a candidate for involvement in PWS. Preliminary comparisons of the 10 kb of genomic sequence around the predicted gene using BLASTN showed strong nucleotide homology to *NDN*. I originally named this gene, necdin-like 1 (*NDNLI*), but during the course of these experiments, the gene was independently cloned and named *MAGEL2*, and will be referred to as such in the remainder of this chapter.

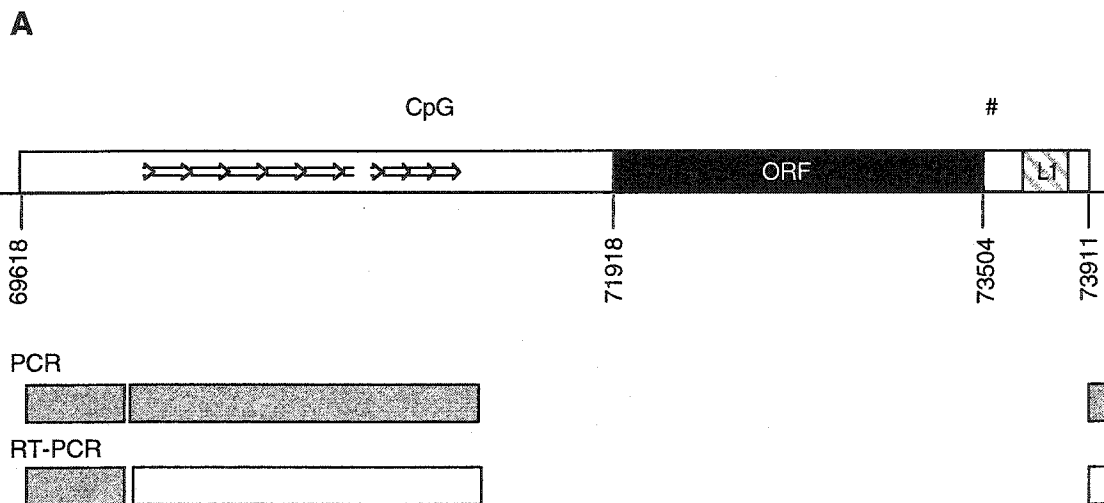
Structure of *MAGEL2/Magel2*

Sequence analysis of cDNAs from the Hs.141496 defined the limits of the cDNA cluster as nucleotide 71651 at the 5' end to nucleotide 73911 at the 3' end (numbering as in the PAC pDJ181P7 sequence) (Figure 4-2). The 5' untranslated region (UTR) of *MAGEL2* contains a series of head-to-tail tandem repeats. Depending on the stringency of the similarity of comparison, there are between 23-27 tandem copies of a 30 bp repeat that lies 5' to a predicted CpG island. This is followed by a spacer region, and then between 9-18 tandem copies of a 21 bp repeat within the CpG island. The 3' UTR contains a short L1 LINE fragment starting at nucleotide 73660. I performed RT-PCR on human brain RNA to demonstrate that no RT-PCR product could be amplified from the region 3' to position 73911, but RT-PCR products were obtained in the upstream region from position 69618 to 69919 which I predicted to be in the 5' end of the transcript. I was

unable to amplify fragments that included the repeats (i.e. from position 69919-71651) using either reverse transcribed RNA or genomic DNA templates, suggesting that this region may be transcribed but is refractory to RT-PCR and cDNA cloning. In support of this hypothesis, the 5' repeats are not represented among the cDNA clones I had identified to date. It is unlikely that there is additional 3' untranslated sequence, since the human cDNAs derived from UniGene cluster Hs.141496 share a common region for their 3' ends, and several have poly-A tails suggesting that position 73911 is the 3' end of the transcript. From the UniGene cluster, I selected four cDNA clones for sequencing. The cDNA sequence directly aligned with the genomic sequence and suggested that *MAGEL2* is a single exon gene. The complete sequence was submitted to GenBank (Accession #200625).

Figure 4- 2. Genomic organization of human *MAGEL2*.

(A) The predicted open reading frame (ORF, black box), upstream repeats (open arrows), L1 repeat (hatched box), and the location of the single nucleotide polymorphism used for imprinting analysis (#) are indicated. The extent of the transcribed region predicted from overlapping cDNAs, RT and Northern blot results are indicated by the white box. Numbering is as in the pDJ181P7 sequence. Rectangles below *MAGEL2* represent portions of *MAGEL2* covered by PCR and RT-PCR primers. Filled rectangles could be amplified, empty rectangles could not. (B) The sequence of the 30 bp repeat present in 23 copies 5' of the CpG island in the 5' untranslated region. (C) The sequence of the 21 bp repeat present in 9 copies.



B

```

GATGACCCAG CCTCGCTGCC CCTAGGGGGCCC
GATAGTCCCG GGCTCCCCCG CTGGGGGGCCC
GATGGGTAAG CCTCCGACTC CCGGGGTCTT
GATGGTGTCAT CCTCCACCTC CGGGAGCCCC
GATGGCCCAG CCTCCGACCC CGGGAGTCTT
GATGGTGTCAT CCTTCAGCTC CCGGAGCTCC
CATGGCCCAT CCTCCTCCTC CGGGGACCCC
AATGTCCCAC CCTCCCCCTC CGGGGACCCC
AATGGCCCAT CCTCCTCCTC CGGGGACCCC
GATGGCCCAT CCTCCTCCTC CGGGGACCCC
GATGGTGTCAT CCTCCTCCTC CGGGGACCCC
GATGGCTCAT CCTCCCCCTC CGGGGACACC
GATGGCTCAT CCTCCCCCTC CGGGGACACC
GATGGCTCAT CCTCCACCTC CGGGGACACC
GATGGCTCAT CCTCCCCCTC CGGGTACACC
GATGGCCCAG CCTCCAGCTC CGGGAGTCTT
GATGGCCCAG CCTCTGACTC CGGGAGTCTT
GATGGTCCAG CCTGCTGCTC CGGGAGCACC
GATGGTCCAG CCGCCTCCAG CNNNAGCCAT
GATGACCCAG CCTCAGCCTT CAGGAGCACC
GATGGCCAAG CCTCCAGGTC CAGGAGTCTT
GATGATTCAT CCTCCAGGTG CGAGAGCTCC
GATGACCCAG CCTCCAGCTT CAGGAGCACC

```

C

```

CTGATCCGCC AGGCCCCACC G
GTGATCCGCC AGGCCCCACC C
GTGATCCGCC AGGCCCCACC C
GTGATCCGCC AGGCCCCCGC T
GTGATCCGCC AGGCCCCACC T
GTGATCCGCC AGGCCCCACC T
GTGATCCGCC AGGCTCCACC T
GTGATCCGCC AGGCCCCGCC G
CTGATCCGCC AGGCGCCGCC G

```

Dr. Serguei Kozlov, in the laboratory of our collaborator, Dr. Colin Stewart, at the National Cancer Institute in Frederick, Maryland obtained and sequenced mouse genomic clones that contained mouse *Magel2*. I also sequenced 2 overlapping mouse cDNA clones whose ESTs had high sequence similarity to *MAGEL2*. From the genomic and cDNA sequence, I identified a predicted open reading frame with significant similarity to *MAGEL2* (Accession #AF212306). A series of repeats was located upstream of the mouse open reading frame and consists of an 18 bp repeat reiterated 14.5 times (Figure 4-3). The mouse cDNAs have a 3' UTR of 427 bp, approximately the same size as the human 3'UTR. These results suggested that the *MAGEL2* cDNA was at least 4.3 kb in length, and included the repeats at the 5' end.

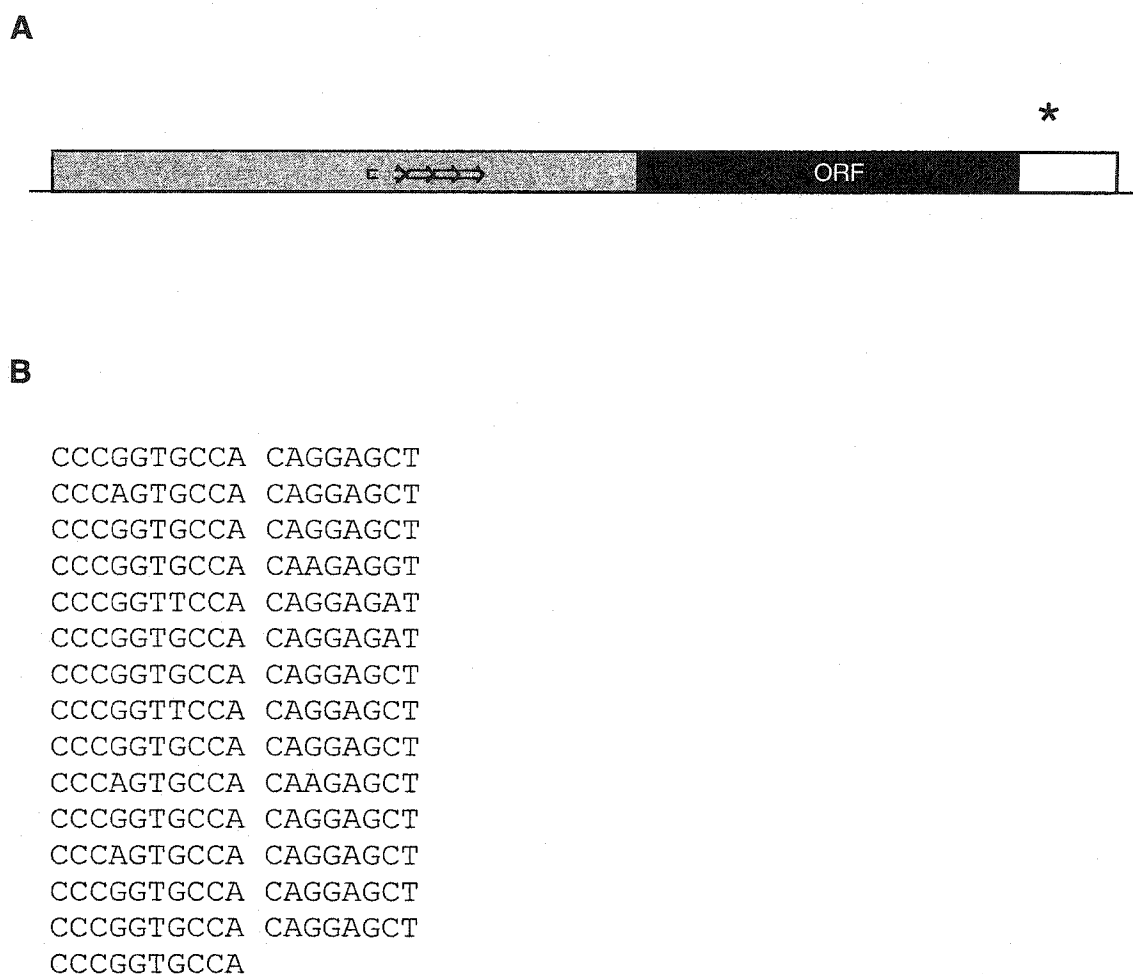


Figure 4- 3. Genomic organization of mouse *Magel2*.

(A) The predicted open reading frame (ORF, black box), upstream and the interspecific polymorphism used for imprinting analysis (*) are indicated. The 5'-untranslated region (gray box) is predicted from the 4.5 kb transcript size determined by Northern blot analysis and by comparison with the human predicted cDNA. (B) The sequence of the 18 bp tandem repeats present in 14.5 copies located in the 5' region.

The predicted proteins derived from *MAGEL2* and its murine counterpart encode putative proteins of 529 and 525 amino acids respectively (Figure 4-4). I predicted the first methionine to be the initiating methionine based on a superior Kozak consensus sequence (Kozak, 1989) and significant amino acid similarity in the region between the first methionine and the second methionine. The amino acid sequences of the putative proteins derived from *NDN*, *Ndn*, *MAGEL2* and *Magel2* were compared using the ClustalW algorithm to annotate fully, strongly, and weakly conserved residues between the proteins (Figure 4-4B). *MAGEL2* and *NDN* have the greatest sequence divergence at the amino termini. *MAGEL2* contains an additional 188 amino acids at the amino-terminus as compared to *NDN*. Furthermore, *MAGEL2* does not have the proline rich, acidic amino-terminus that is found in *NDN* (Maruyama et al., 1991). The region of highest similarity among *MAGEL2*, *NDN*, the MAGE and MAGE-related proteins is in necdin "region 2", a region of strong human-mouse conservation within necdin (Nakada et al., 1998). *MAGEL2* has high similarity to the MAGE family of proteins in the region containing an antigenic nonapeptide implicated in tumor rejection (Itoh et al., 1996). Necdin, however, does not share this region of homology with the other MAGE proteins.

A

Magel2	M APSGEGPSSLE P R P PRERAPARDKK G P K ERMFIGAT F CA P RGAS S SHAYVETAM K	60
MAGEL2	M QGLFYR Q GSSKER T SSKERRA T SKDRMIFAAT F CA P KAVEA R AHL G AAW K	54
Magel2	N PA S ET P ATERV T ST H FP A SS N A F RGPSA A SE S PK S LP F AL O DP Y AG V EAL P A V	120
MAGEL2	N PA P ET F APSS S V T A L SO F Q A SL N A F RGPSA A SE T PK S LP Y AL O DF A C V ELL P A V	114
Magel2	F W V F Y ED G A S S A CK S T E A IL A V A A A PO A S A T A A F AK S - S S E P R P G K A TR K K H L E P	179
MAGEL2	F W V EP Q PN M A S K A SO A V P T F L N A T A A PO A T A T T O E AK S T S V E P PR S SK A TR K K H L E A	174
Magel2	K E N C G R L SS R A R GP R T G NP S H D W E L O R A M O L L G R E S L Y T P Q L N D G C P N I S R M	239
MAGEL2	Q E S R G H T L A F H D Q Q R P H E L N L S D W E V O S P I O V S D W E H P N T F R G L S G E G S T S R I	234
Magel2	P R S L E G P ----- S T S R D Q E F C G D S G S Q T W M A S E V P S V R G S S A G E D P D R S	287
MAGEL2	L S G W E G S A S W A L S A W E G P S T S R A L G L S E S P O S S L F V V S E V A S V P G S S A T O D N S K V E A	294
	region 1 ←→ region 2	
Magel2	D R I S P L D E R A N A L V O F L L V K D O A K V P V O L S E M N V V I R E Y K D D S L D I N R A N T K L E C T F G	347
MAGEL2	D P S P L D E R A N A L V O L L V K D O A K V P V O R S E M V K V I L R E Y K D E C L D I N R A N K L E C A F G	354
Magel2	C O L K E V D T K T P T L V R G M A P Q C N L A S T L E R P K S L M V V L S L V R K G Y C I R E N L L S	407
MAGEL2	Y O K E L D V K N E A T L I N K L G T H T G M E V A S V L D R R K G L A N V L S L I P K K N C V E D L I F N	414
Magel2	F L F Q L G L D V Q E T S G L F R I P K L I T S V F V H R Y L E F R Q I P T E R A F Y E L L I N G P R A F L R T N R	467
MAGEL2	F L F K L G L D V R E I N G L G N T K K L E T E V F V Q K Y L E Y R L E Y T E P A E V E F L A G P R A L E T S K	474
Magel2	V H I L R F L A L Y E N O P O I N S C O Y L D S L A L E Y K D A N A A A E S H D S D D D A D P T S S E H P H	525
MAGEL2	M L V L R F L A K H K K D E S W P F H Y E A L A S C W E D T D --- E D E P D T G D S A G P T S R P P E R	529

B

% similarity	MAGEL2	NDN	Ndn	NDN region 1	NDN region 2
MAGEL2	100	51	48	45	54
Magel2	72	44	46	34	48

Figure 4- 4. Sequence comparisons among *MAGEL2*, *NDN* and their murine orthologs.

(A) Alignment of mouse and human *MAGEL2* protein sequences. Identical amino acids are shaded dark gray, conserved amino acids are shaded light gray. The MAGE-like nonapeptide is indicated by a thick line above the sequence. Regions 1 and 2 of necdin represent two domains in the necdin protein as previously defined in Nakada, Y., Taniura, H., Uetsuki, T., Inazawa, J. and Yoshikawa, K. (1998). The human chromosomal gene for necdin, a neuronal growth suppressor, in the Prader-Willi syndrome deletion region. *Gene* 213, 65-72. (B) Amino acid similarity of the necdin and *MAGEL2* genes.

Mapping of *MAGEL2/Magel2*

To physically map the gene, YAC clones that were previously mapped to the PWS region were analyzed. A Southern blot containing DNA from YACs spanning the PWS region showed hybridization of a *MAGEL2* fragment to YACs 925C12 and 959G3 (Figure 4-5). PCR primers specific for *MAGEL2* also amplified DNA from the same YACs. However, *NDN* primers have previously been shown to only amplify DNA from YAC 925C12, but not 959G3 (MacDonald and Wevrick, 1997). This suggested that *MAGEL2* was located within the domain of paternally expressed genes and was telomeric to *NDN*. A mouse *Magel2* specific probe was hybridized to a Southern blot containing genomic DNA from 28 PAC clones from the syntenic region of 7C. *Magel2* hybridized to PACs pDJ665K18, pDJ575A9, pDJ480A23 and pDJ388B18. As the presence of *Magel2* in pDJ575A9 could not be confirmed by PCR using gene specific primers, the data from pDJ5759 was excluded. *Magel2* primers produced a strong PCR amplification product from pDJ509A13 DNA, but failed to hybridize to the PAC on a genomic southern. By PCR, the PAC clones pDJ509A13, pDJ388B18, pDJ612H12, pDJ480A23 and pDJ665K16 were previously shown to contain *Mkx3* and/or *Ndn* (Table 4-2). Because the mouse PACs were unordered, it was not possible to determine the location of *Magel2* relative to *Mkx3* or *Ndn*. However, co-amplification from the pDJ509A13 suggested that the three genes are closely linked, and further suggested that the conserved synteny between the human and murine gene clusters extended to *MAGEL2/Magel2*.

Figure 4- 5. Localization of the *MAGEL2* gene in the 15q11-13 imprinting domain.

(A) The PWS/AS deletion interval is indicated by the open double-headed arrow. The transcriptional orientations of *NDN* and *MAGEL2* are both 5' → 3' centromeric; *MAGEL2* lies within PAC clone pDJ181P7 (closed box) and the two YAC clones (open boxes). *MAGEL2* is within the PWS critical deletion region (gray box), centromeric to the imprinting center (IC) and within a domain of genes (large box) of which many are imprinted in a least one tissue. Two ESTs, stSG3346 and sts-N21972, have not been ordered with respect to each other (square bracket). (B) A probe specific to *MAGEL2* hybridizes to genomic DNA from YACs 925C12 and 959G3 by Southern analysis. Arrows indicate hybridization signal.

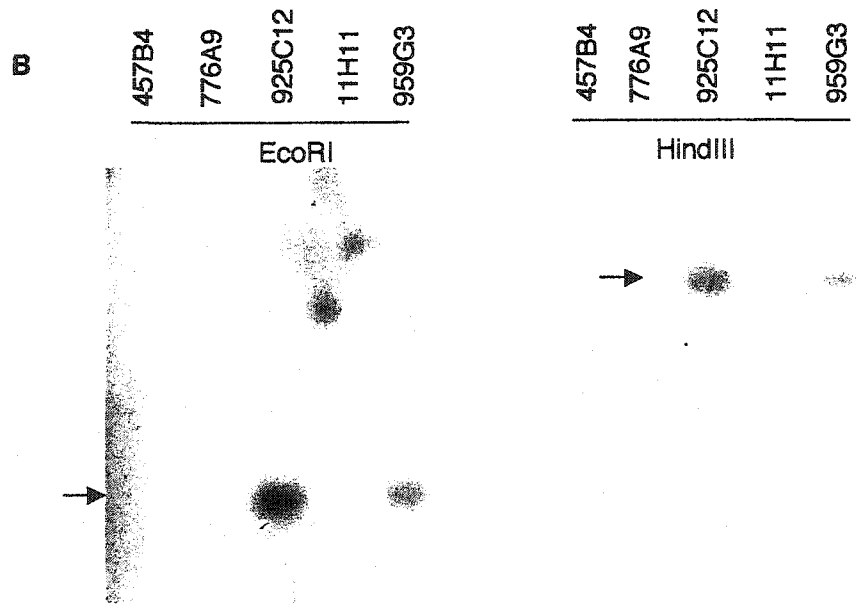
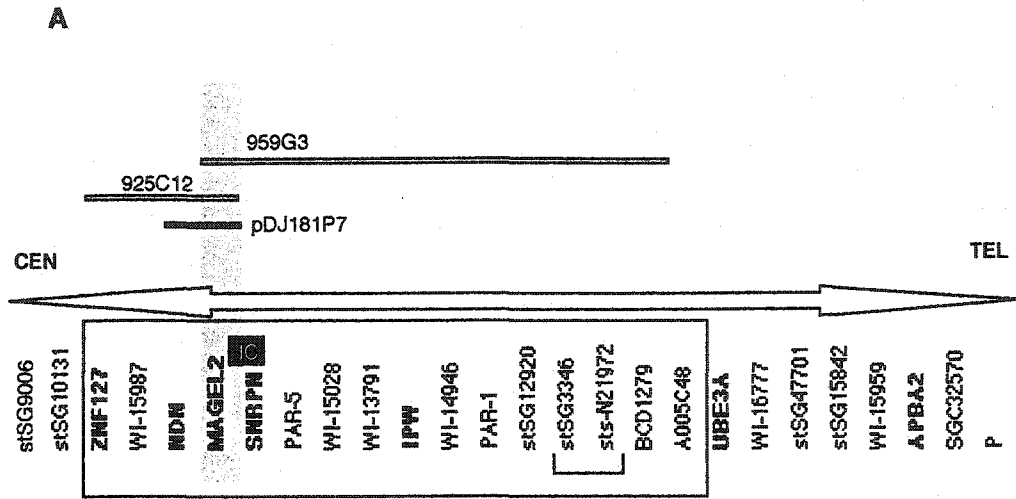


Table 4- 2. Localization of the *Magel2* gene within the mouse syntenic region on 7C.

Localization of *Magel2* PAC clones containing *Ndn* were analyzed for the presence (+) or absence (-) of *Mkrn3* and *Magel2* sequences by PCR with gene-specific primers.

PAC	GENE		
	<i>Mkrn3</i>	<i>Ndn</i>	<i>Magel2</i>
pDJ509A13	+	+	+
pDJ388B18	-	+	-
pDJ612H12	-	+	-
pDJ480A23	-	+	+
pDJ665K16	-	+	+

Expression profiles of human and mouse *MAGEL2*

Expression in tissues

The cDNAs in *MAGEL2* UniGene cluster Hs.141496 were derived from both adult and embryonic tissues, including total embryo/fetus, brain, uterus, lung and germ cells. To investigate the expression pattern of *MAGEL2* in a wider range of tissues, and to determine the relative expression levels, I examined a series of human tissues by northern blot analysis. *MAGEL2* expression was detectable, although at low levels in a variety of tissues. A human cDNA probe detected a 4.5 kb transcript in fetal kidney, fetal brain, fetal liver, and fetal lung (Figure 4-6 A). In the adult brain, the putamen, temporal lobe, frontal lobe, occipital lobe, medulla, and cerebral cortex expressed *MAGEL2*; lower levels were detected in the spinal cord. The size of the hybridization signal corresponded to the predicted minimum size of 4.3 kb based on RT-PCR experiments (Figure 4-2). The mouse ESTs corresponding to *Magel2* were derived only from late stage embryos. Dr. Serguei Kozlov showed that *Magel2* produced a moderately abundant 4.5 kb transcript in

mid to late embryonic stages, from E11, E15, and E17, while low levels of expression could be detected in adult brain by RT-PCR (see below).

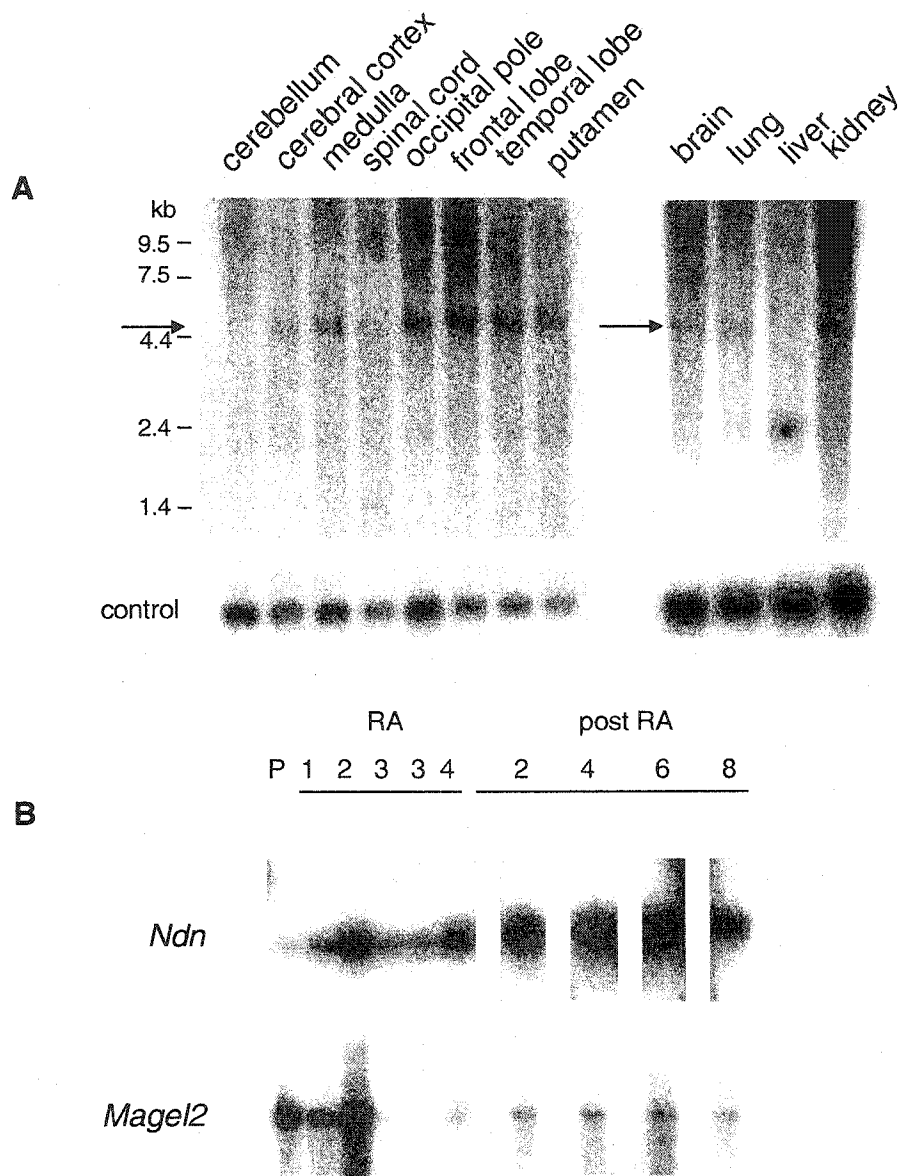


Figure 4- 6. Northern blot expression analysis of *MAGEL2/Magel2*.

(A) Northern blots of adult brain tissues (left) and of fetal tissues (right). The 4.5 kb *MAGEL2* transcript is indicated by the arrow. (B) Northern blot of RNA from murine P19 cells undergoing differentiation. RNA was collected from P19 cells before treatment, 1-4 days during retinoic acid (RA) treatment, and 1-8 days after RA withdrawal (post RA). The northern blot was hybridized with probes specific for *Ndn* and *Magel2*.

Expression in differentiating murine P19 cells

Ndn expression increases as P19 cells undergo differentiation from pluripotent cells to terminally differentiated neurons (Maruyama et al., 1991). Because *Magel2* shows sequence homology to *Ndn*, I hypothesized that it might also have functional parallels with *Ndn*. To determine if *Magel2* was involved in neurogenesis, I examined its expression in P19 cells undergoing neuronal differentiation.

P19 embryonal carcinoma cells were induced to undergo neuronal differentiation through the addition of RA. Cytosine arabinoside was used to select for terminally differentiated neurons among the differentiated cells. RNA collected throughout the induction process was electrophoresed on a denaturing agarose gel and visualized with ethidium bromide to estimate the relative levels of RNA in each lane. A northern blot was prepared and hybridized with probes specific for *Ndn* and *Magel2*. *Ndn* has been shown to be a marker of differentiated neurons in the P19 assay (Maruyama et al., 1991). Very low levels of *Ndn* expression were detected prior to the addition of RA (Figure 4-6B). *Ndn* expression levels increased immediately after the addition of RA, reached maximum levels 2 days after RA is withdrawn, and remained at these levels for the rest of the experiment. The induction of *Ndn* expression corroborated previous P19 differentiation experiments and confirmed that the cells were induced to become neurons.

Hybridization of the same blot with a *Magel2* specific probe produced an expression profile that was opposite to that of *Ndn* (Figure 4-6B). *Magel2* was strongly expressed in pluripotent P19 cells. Expression is downregulated in the third and fourth days of RA addition, and remained suppressed during neuronal growth and selection by cytosine arabinoside.

Imprinting of *MAGEL2/Magel2*

To be considered a candidate gene for PWS, *MAGEL2* must be preferentially expressed from the paternal allele. A similar assay to the one described in Chapter 2 was employed to determine the expression of *MAGEL2* in lymphoblast, fibroblast and brain of PWS, AS and control samples. RT-PCR showed no expression in any of the lymphoblast or fibroblast samples. *MAGEL2* expression was detected in the AS and control brain RNA, suggesting that the gene is paternally expressed (Figure 4-7A). To confirm uniparental expression in unaffected tissues, the RNA from 8 control brains was analyzed. DNA was sequenced from the 3' end of the *MAGEL2* gene and a single nucleotide polymorphism at position 73614 that abolishes a restriction enzyme recognition site for *Rsa I* was found. Five of the samples analyzed were heterozygous at this site. RNA was amplified from the control samples with the primers that span the polymorphism and the cDNA was digested with *Rsa I*. Samples with a heterozygous polymorphism in the DNA showed monoallelic expression in brain RNA (Figure 4-7B). This information combined with the absence of expression of *MAGEL2* in PWS brain suggested that the loss of *MAGEL2* expression in PWS was due to imprinting of the gene rather than being a direct consequence of the disease process.

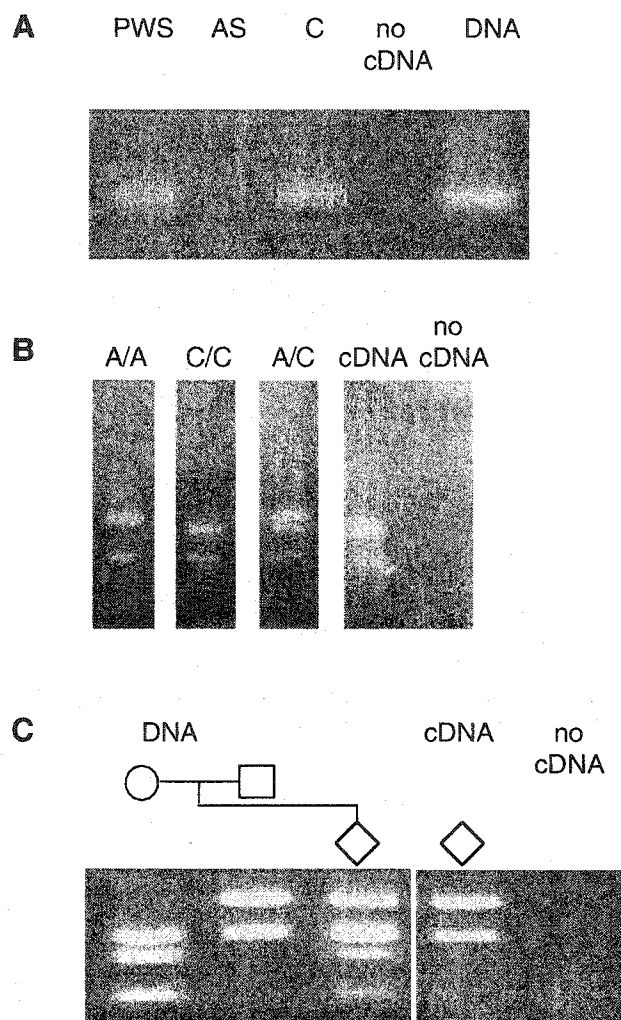


Figure 4- 7. Paternal origin of *MAGEL2/Magel2* gene expression.

(A) RT-PCR was performed on brain RNA from control (C), deletion Prader-Willi syndrome (PWS), and deletion Angelman syndrome (AS) individuals. The second last lane shows a PCR amplification with no cDNA added, and the last lane shows amplification with human genomic DNA. (B) Monoallelic expression of *MAGEL2* in human brain. A single nucleotide polymorphism produced an A/A, C/C or A/C genotype. RT-PCR performed on brain from a heterozygous A/C individual shows monoallelic expression of unknown parental origin. (C) The F1 offspring of an interspecies mouse cross is heterozygous for a single nucleotide polymorphism. RT-PCR performed on F1 brain RNA shows expression of the paternal allele.

To determine the imprinting status of *Magel2*, a single nucleotide polymorphism was found in the 3' UTR between *Mus Musculus* SPRET/Ei and *Mus Musculus* C57Bl/6. The polymorphism altered the recognition site for the restriction enzyme *Rsa I*. Brain RNA from an F1 cross between a male SPRET/Ei and female C57Bl/6 showed expression of only the paternally inherited allele by RT-PCR (Figure 4-7 C).

Discussion

In this chapter, I described the identification and expression profile of a novel type II MAGE gene, *MAGEL2*, and its mouse orthologue, *Magel2*. This gene was simultaneously identified and published by Boccaccio *et al.*, (Boccaccio *et al.*, 1999). In human adult tissues, *MAGEL2* had highest expression in brain, with wider expression in fetal tissues. *MAGEL2* was equally expressed in many parts of the human brain tested, although it showed only weak expression in spinal cord and cerebellum. The expression pattern and sequence similarity to *NDN* suggested that *MAGEL2* might have a general role in neural differentiation. Low-level expression in non-neural tissues such as in fetal kidney and lung suggested either a non-neural role in these tissues, or expression in the peripheral nervous system components of these tissues.

MAGEL2/Magel2 had highest sequence homology to *NDN/Ndn* within "region 2" of *neccin*. *Neccin* region 2 is the most highly conserved portion of the gene between mouse and humans (Nakada *et al.*, 1998). It has been shown to be important for protein interactions between *neccin* and the transcription factor E2F1, and *neccin*'s potential role as a growth suppressor. Because region 2 is strongly conserved in *MAGEL2/Magel2*, this novel gene may also interact with E2F1 or play a role in growth suppression.

Despite their sequence homologies, *Ndn* and *Magel2* show opposite patterns of expression when assayed in the P19 *in vitro* differentiation system. Their response to RA suggests that the two genes may have different roles during neuronal development. While it is known that *Ndn* is involved in the terminal differentiation of neurons, the expression of *Magel2* in P19 suggests that it could be important for the pluripotent state.

Alternatively, the genes may produce proteins of similar functions, but which act at different points during neuronal differentiation. *Magel2* could be expressed in early development prior to the formation of neurons, and could be replaced by *Ndn* once differentiation is initiated. Dr. Serguei Kozlov showed that *Magel2* expression was unaffected in an *Ndn*-deficient mouse, which suggested that the loss of *Ndn* did not have an effect on *Magel2* expression in these mice (Lee et al., 2000). A comparison of the endogenous expression of these two genes during early development would give more insight into their respective functions (see Chapter 5).

Since the completion of the Human Genome Project, it has been shown that *MAGEL2* is centromeric to *NDN*, and that *MAGEL2* and *NDN* are transcribed in the opposite orientation to *SNURF/SNRPN* (see Figure 3-4). The *MAGEL2* mapping results described in this chapter were obtained by content mapping of human YACs, which have a high rate of spontaneous deletions and rearrangements, and could potentially lead to misleading results. By content mapping of mouse bacterial artificial chromosomes (BACs), it has been shown that the correct gene order in mice is *Mkx3*, *Magel2*, *Ndn* and then *Snurf/Snrpn* (Stormy Chamberlain, in the laboratory of Dr. Cammilynn Brannan, University of Florida College of Medicine, personal communication). Because they contain smaller genomic inserts than PACs, content mapping with mouse BACs provides

a more refined gene location. This has been confirmed by the recently completed mouse genomic sequence spanning *Mkrn3* to *Ndn*.

Further work in the mouse system has shown that the imprinting mechanisms controlling the paternal expression of *Magel2* are similar to those of other PWS orthologues. Stormy Chamberlain showed that expression of *Magel2* was absent in the brains of newborn mice carrying a paternally inherited deletion of the mouse chromosome 7 IC (Lee et al., 2000). The mouse IC on chromosome 7 is homologous to the PWS IC, and a deletion spanning both the IC and the adjacent *Snrpn* gene has previously been shown to result in the loss of expression of *Mkrn3*, *Ndn*, *Snrpn* and *Ipw* (Yang et al., 1998). Evidence that the imprinting is erased and then reset between generations was shown by successive interspecies mouse crosses (Boccaccio et al., 1999). Allele specific expression was traced through three generations by following a polymorphism unique to SPRET/Ei mice. Exclusively paternal expression was seen in the RNA collected from the offspring of a female C57Bl/6 and male SPRET/Ei cross. F1 females were then mated with male C57Bl/6 mice, and the resulting offspring were shown to express the C57Bl/6 polymorphism. This work in mice suggests that the expression of *Magel2* is subject to regulation by the IC in a manner similar to that of *Mkrn3*, *Ndn* and *Ipw*.

In addition to significant homology to other MAGE genes, *MAGEL2* has also been found to have 64% amino acid similarity to the apoptosis-related protein 1, suggesting that *MAGEL2* may also be involved in the regulation of cell death or the cell cycle (Boccaccio et al., 1999). The 3' UTR of the *MAGEL2* gene has sequence features that are characteristic of mRNAs that encode for proto-oncogenes or nuclear transcription factors,

such as a non-canonical UAUAA poly(A) signal and AU-rich regions (Boccaccio et al., 1999). These sequences may target the RNA products for rapid and selective degradation. An AU-rich element has also been found in another PWS gene, *MKRN3/Mkrn3*, whose function is also unclear (Jong et al., 1999a).

MAGEL2 encodes a small protein of unknown function and has highest sequence similarity to necdin and the MAGE family of proteins. *NDN* and *MAGEL2* are simultaneously inactivated in PWS patients. Although loss of *MAGEL2* expression in PWS patients with IC mutations has yet to be shown, expression of *MAGEL2* is not affected in AS patients that have mutations in the IC (Boccaccio et al., 1999). This supports the hypothesis that the IC on chromosome 15 is bipartite and acts on two separate sets of genes (Horsthemke, 1997).

Because of its sequence similarity to *Ndn*, as well as its overlapping expression pattern by northern blot analysis in mouse tissue RNA and P19 cell RNA, *MAGEL2* may also play a role in neuronal development. As the loss of mouse *Ndn* does not fully recapitulate the PWS phenotype, the loss of both of these MAGE related genes may be more detrimental than the loss of *Ndn* alone. Likewise, in humans, the combined loss of both *NDN* and *MAGEL2* may be necessary for the development of the syndrome. Studies into the function of *MAGEL2* and *NDN* along with further gene targeting experiments in the mouse will yield insight into the pathophysiology of PWS and the normal development of the brain.

Chapter 5. Prader-Willi syndrome transcripts are expressed in phenotypically significant regions of the developing mouse brain.

Parts of this chapter are submitted or are in press.

Lee, S., Walker, C.L., and Wevrick, R. (2003). Prader-Willi syndrome transcripts are expressed in phenotypically significant regions of the developing mouse brain. Submitted.

Ren, J.*, Lee, S.*, Gerard, M., Pagliardini, S., Stewart, C. L., Greer, J. J. and Wevrick, R. (2003). Absence of Ndn, encoding the Prader-Willi syndrome deleted gene necdin, results in congenital deficiency of central respiratory drive in neonatal mice. *J Neurosci.* 23, 1569-1573 (Joint first authorship).

All of the results presented in this chapter were done by Syann Lee

Introduction

As neonatal lethality occurs in several of the PWS mouse models and perinatal complications are associated with human PWS, it is likely that the loss of PWS genes causes a prenatal developmental effect. Once all of the candidate genes have been identified in a microdeletion syndrome, an understanding of their expression patterns is imperative to establish correlations between individual genes and phenotypic traits.

Because of the difficulties inherent in examining PWS brain, it has been necessary to construct mouse models of the syndrome to understand its pathophysiology. As discussed in Chapter 1, none of the mouse models produced to date recapitulate the major PWS traits of hyperphagia or obesity. Because of the numerous differences between mice and humans, it may not be possible to create a mouse model that has all of the features of PWS. Furthermore, the syntenic region is not perfectly conserved and the species-specific genes *Frat3* in mice and *C15orf2* in humans may contribute to the overall phenotype. It is also possible that there are redundant genes in mice that can compensate for the loss of those in the PWS region, or alternatively, that the PWS genes have synergistic interactions in humans that are not present in mice (Wynshaw-Boris, 1996). Some human genes and their mouse homologues have also been shown to have differences in their embryonic expression patterns both temporally and spatially (Fougerousse et al., 2000). In order to interpret findings from existing mouse models for PWS, it is important to know where and when each PWS gene is expressed. Comparing the mouse and human expression patterns will be necessary to evaluate the current mouse models, and to determine how to evaluate each gene's contribution to healthy brain development. In order to evaluate the contribution of each PWS candidate gene to the

development of the brain and to the neuronal aspects of PWS, I utilized several complementary techniques to assess the expression pattern and functions of these genes in early and prenatal brain development.

RNA *in situ* hybridization

Temporal and spatial expression patterns of the PWS transcripts in the developing mouse brain were examined in serial sections of embryonic mice from E12.5, when most neurons begin to migrate and terminally differentiate, to E18.5, just prior to birth. RNA *in situ* hybridization allows multiple genes to be rapidly profiled at the same time. The technique also allows gene expression to be detected at the cellular level in morphologically preserved tissue samples. RNA *in situ* hybridization is particularly useful for examining the PWS candidate genes, as well as the downstream, untranslated exons of the *SNURF/SNRPN* transcript and the snoRNAs.

Using *Ndn* deficient mice to examine gene expression and function.

An *Ndn* deficient mouse was created by Dr. Matthieu Gérard, in the laboratory of our collaborator, Dr. Colin Stewart, at the National Cancer Institute in Frederick, Maryland, by replacing the open reading frame with a *lacZ* reporter gene fused in frame with the first 31 codons of the protein (Figure 5-1) (Gerard et al., 1999). Chimeric males derived from embryonic stem cell clones were mated with C57Bl/6 females. Offspring that inherited the *Ndn* deletion died due to respiratory failure. In the original targeted allele of Gérard *et al.*, there was approximately 70% lethality in the first 30 postnatal hours. Deletion of the PGK-neo cassette in the original targeted allele increased the lethality to 98% in the *Ndn*^{tm2Stw} necdin-deficient strain. The difference in survival may be due to an effect on nearby genes by the neomycin promoter in the original construct.

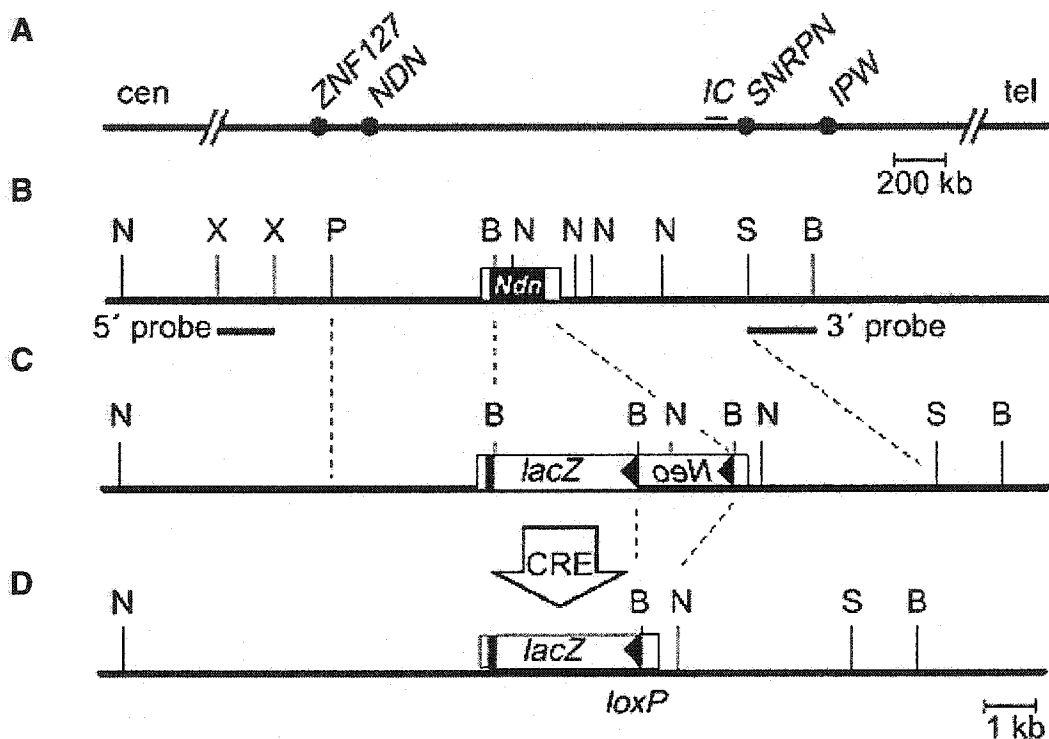


Figure 5- 1. Generation of the *Ndn*^{tm2Stw} allele.

(A) Map of human chromosome 15q11-q13 at the time the *Ndn* mouse was constructed, and which is syntenic to mouse chromosome 7C. *Znf127* has now been renamed as *Mkrn3*. (B) A partial restriction map of the mouse *Ndn* locus. *Ndn* is represented as rectangle with the ORF shown in black. The restriction sites shown are, B, BamH I; N, Nco I; X, Xba I; P, Pst I; and S, Spe I. (C). The *Ndn* locus after a homologous recombination. The *lacZ* reporter gene replaced the *Ndn* ORF. The floxed PGK-neo cassette is transcribed in the opposite direction to *Ndn*. (D). The *Ndn* allele after *in vivo* CRE-driven recombination. Figure taken from Gerard, M., Hernandez, L., Wevrick, R. and Stewart, C. L. (1999). Disruption of the mouse neccidin gene results in early post-natal lethality. *Nat Genet* 23, 199-202.

The transgenic mice express the *lacZ* reporter gene under the control of the *Ndn* promoter. Staining for the presence of β -galactosidase in tissue sections and embryos is reflective of *Ndn* promoter activity. The advantage of the *lacZ* reporter system over RNA *in situ* hybridization is that β -galactosidase is very stable, easily detectable even in low amounts, and requires minimal sample manipulation before detection. However, as β -galactosidase is stable for days, the detection of the protein product may not be reflective of endogenous transient gene activity. Furthermore, without knowledge of the target gene's expression in a wildtype embryo, it is difficult to determine if the β -galactosidase staining pattern has been influenced by loss of the coding region. Genes in which expression is regulated by auto-feedback mechanisms, whose regulatory regions are replaced by the *lacZ* gene, or whose gene products are essential for proper tissue development and morphology are situations that may result in β -galactosidase signals that differ from endogenous gene expression.

Preliminary insights into the function of *Ndn* were obtained by characterizing the respiratory defect that accompanies *Ndn* deficiency. Dr. Jun Ren, in the laboratory of our collaborator, Dr. John Greer at the University of Alberta, showed that the respiratory failure in *Ndn* deficient mice was due to the inability of the pre-Bötzinger complex within the respiratory center of the medulla to generate a respiratory rhythm (Ren et al., 2003). This suggests that *Ndn* is essential for the proper functioning of the pre-Bötzinger complex. A histological investigation of the medulla of *Ndn* deficient mice would provide additional insights into the function of *Ndn*.

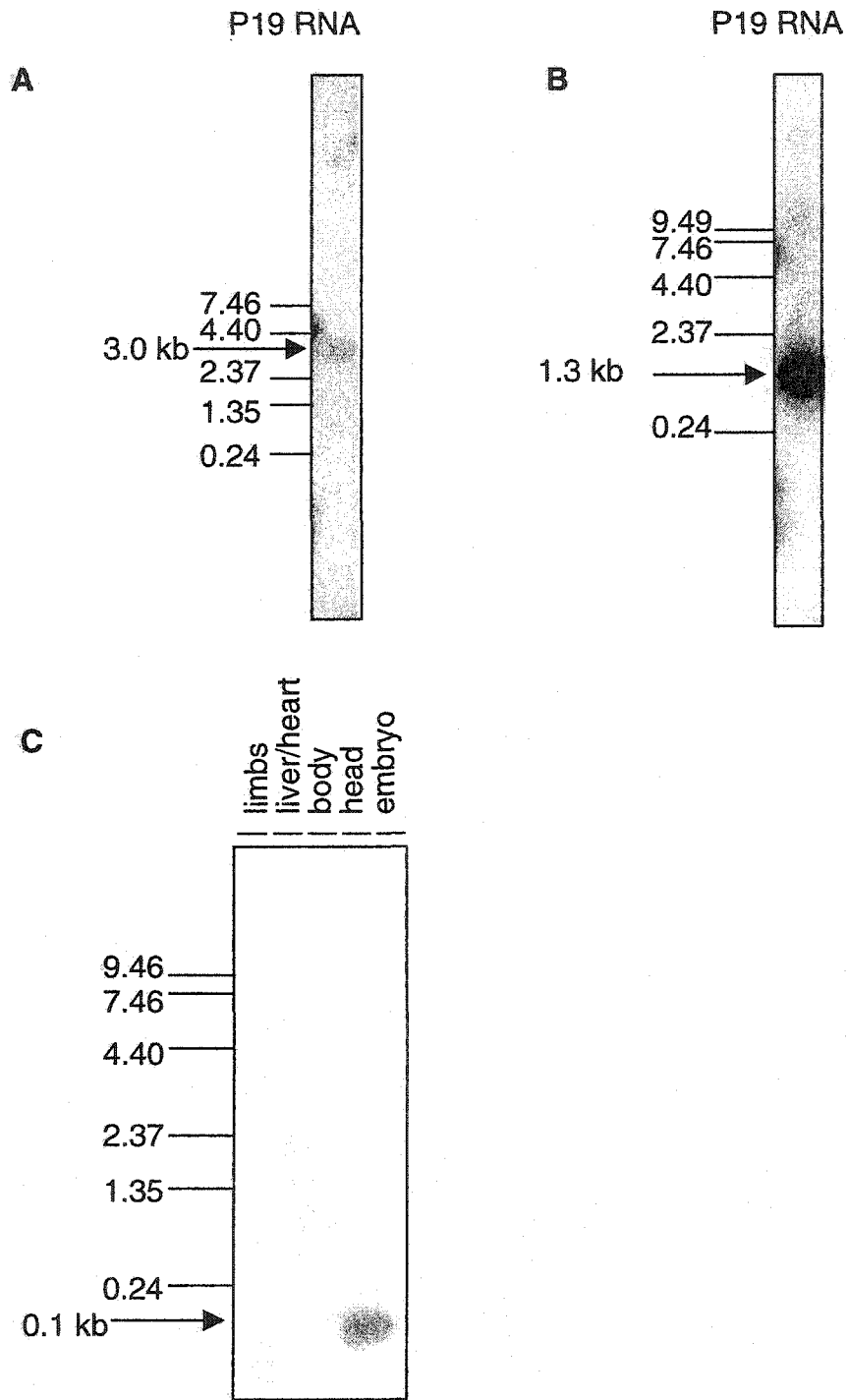
Results

RNA expression of the PWS candidate genes.

RNA *in situ* hybridization on wildtype mice and staining for β -galactosidase activity in *Ndn* deficient mice were used to survey the expression of the PWS orthologs during murine brain development. DNA probes for *Snrpn*, *Mkrn3*, and the snoRNA *MBII-85* transcriptional unit were developed and tested on northern blots to show that they hybridized to unique RNA products of the appropriate size (Figure 5-2). A previously published DNA fragment was used for the *Ipw* probe (Wevrick et al., 1996), while probes specific for *Magel2* and *Ndn* were described in Chapter 4. Among the snoRNAs, *MBII-85* was selected for analysis because it shows high levels of expression by northern blot analysis, is well conserved between humans and mice, and is implicated in translocation cases of PWS (Burger et al., 2002; Cavaille et al., 2000; de los Santos et al., 2000; Gallagher et al., 2002; Meguro et al., 2001b). RNA *in situ* hybridization with DIG-labeled probes was performed on serial cryosections of embryos at E12.5, E15.5 and E18.5, while β -galactosidase staining for *Ndn* promoter activity was used to examine whole embryos.

Figure 5- 2. Northern analysis of RNA *in situ* probes.

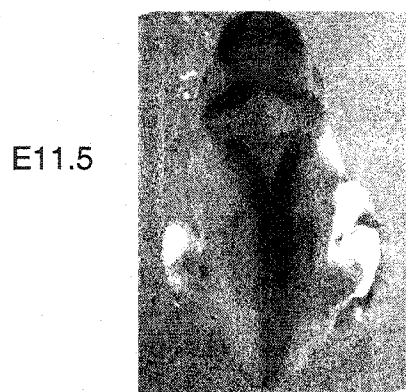
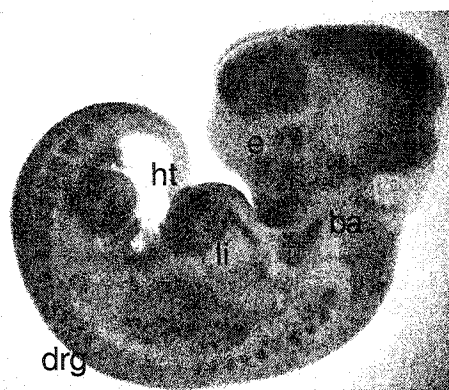
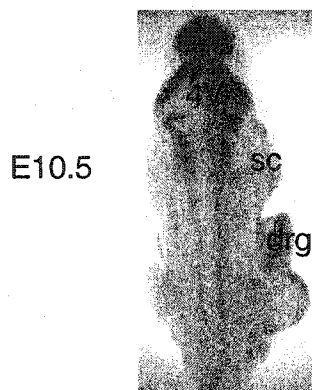
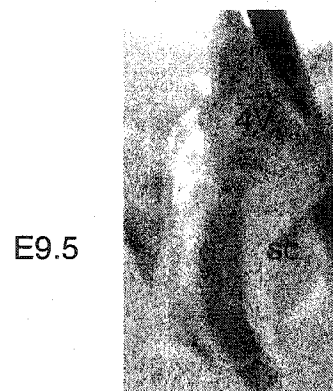
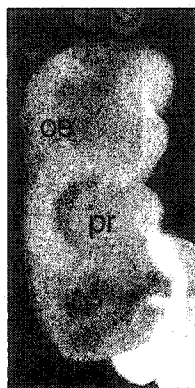
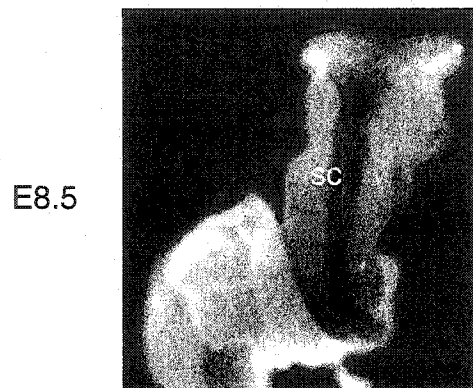
(A) A *Mkx3* specific probe was hybridized to a Northern blot containing mouse P19 embryonic carcinoma poly(A) RNA. A band approximately 3 kb in length was detected. (B) A *Snrpn* specific probe was hybridized to a Northern blot containing mouse P19 embryonic carcinoma poly(A) RNA. A band approximately 1.3 kb in length was detected. (C) A *MBII-85* specific probe was hybridized to a Northern blot containing mouse E12.5 total RNA. A band of approximately 0.1 kb was detected in the lane containing RNA from the head.



RNA *in situ* hybridization with *Magel2* and *Ndn* corroborated previously published expression studies and verified the specificity of these probes. Expression of *Magel2* had previously been detected by whole mount RNA *in situ* hybridization starting at E9 (Lee et al., 2000). β -galactosidase staining for *Ndn* promoter activity in E8.5 to E11.5 embryos produced similar staining patterns (Figure 5-3) as those seen in previously reported whole mount RNA *in situ* (Lee et al., 2000). Obtaining similar *Ndn* expression patterns using two parallel techniques confirmed the specificity of the RNA *in situ* hybridization probe. Furthermore, as the β -galactosidase pattern paralleled the expression pattern seen in wildtype embryos, the deletion of the *Ndn* open reading frame did not appear to result in gross morphological abnormalities in *Ndn* expressing neurons or in surrounding tissues. My *Ndn* RNA *in situ* hybridization results at E15.5 and E18.5 also confirmed previous studies of expression in postmitotic neurons (Aizawa et al., 1992; Uetsuki et al., 1996).

Figure 5- 3. Embryonic expression of *Ndn-lacZ*.

X-gal staining of heterozygous embryos from E8.5 to E11.5. Left: Dorsal views of embryos showing staining down the spinal cord. Right: Sagittal views showing staining throughout the embryo. 4V, fourth ventricle; ba, branchial arches; drg, dorsal root ganglion; e, eye; ht, heart; li, liver; oe, optic eminence; pr, pericardial region; sc, spinal cord.



After confirming that the *Magel2* and *Ndn* probes produced similar expression patterns to those previously reported, I examined the expression patterns of *Mkrn3*, *Snrpn*, *MBII-85* and *Ipw*. The pattern and expression levels of these genes in the neuronal structures implicated in the pathophysiology of PWS were compared. Overall, *Ndn*, *Snrpn*, and *Ipw* RNAs were strongly detected throughout most of the central nervous system, while *Mkrn3*, *Magel2*, and *MB85-II* were expressed at low levels throughout the brain, but were more highly expressed in specific structures.

PWS transcripts are expressed mainly in the mantle and ventricular cell layers

To examine expression in early cell layers, transverse sections of E12.5 embryos were processed for RNA *in situ* hybridization. Signals for the PWS transcripts were easily detected in the brain of E12.5 embryos (Figure 5-4). *Mkrn3* is ubiquitously expressed at low levels throughout the entire embryo, but expression is highest in the ventricular layers of the brain (Figure 5-4 A). At E12.5, *Magel2* is expressed at low levels in the mantle layers, but was highest in the developing hypothalamus (Figure 5-4 B). *Ndn*, *Snrpn*, and *Ipw* signals were detected predominantly in the mantle cell layers of the brain (Figure. 5-4 C, D, E). *Snrpn* transcripts were also detected at low levels in the ventricular cell layers. Throughout most of the brain, *Ipw* is expressed exclusively in the mantle layer, except in the pons and medulla where signals of equal intensities were seen in both mantle and ventricular cells. *MBII-85* signal is moderately stronger in the mantle layer than the ventricular layer (Figure 5-4 F).

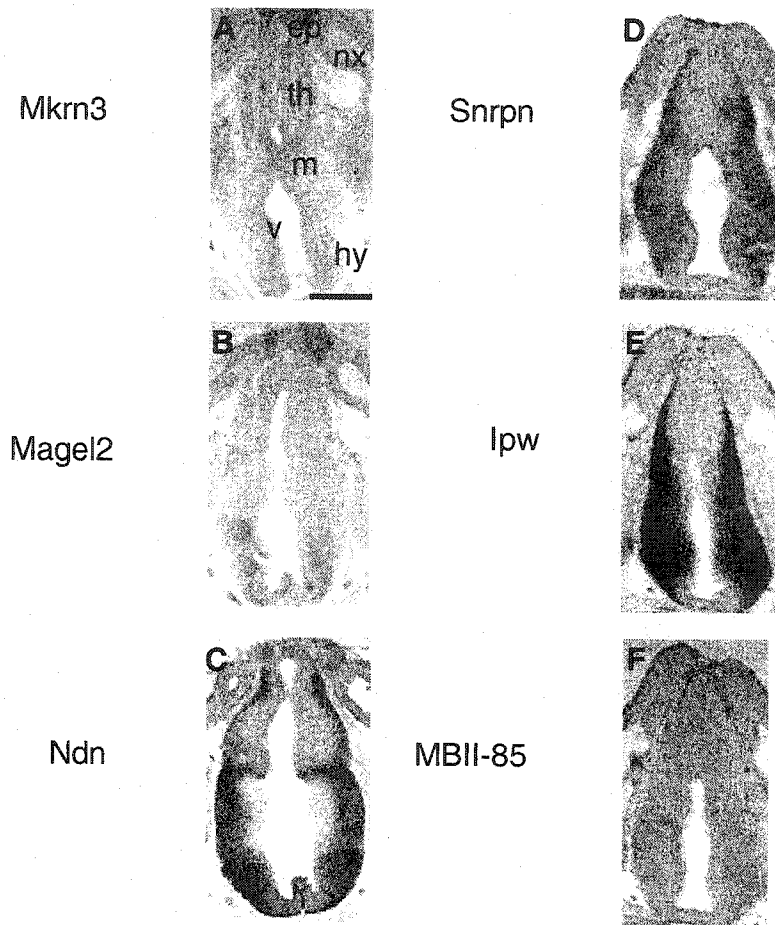


Figure 5- 4. PWS genes expressed in early development.

Transverse sections of E12.5 embryonic hypothalamus. Transcripts are detected primarily in the ventricular and mantle layers. ep, epithalamus; hy, hypothalamus; m, mantle layer, nx, neocortex; th, thalamus; v, ventricular layer. Scale bar: 500 μ m.

Expression in the forebrain.

While *Mkrn3*, *Magel2* and *MBII-85* are expressed at low levels throughout the forebrain, *Ndn*, *Snrpn*, and *Ipw* are highly expressed. Though the overall expression patterns are very similar, there are distinct differences in several regions. Expression is widespread throughout the orbitofrontal cortex but is restricted to the peripheral cells of the olfactory bulb (Figure 5-5 A, B, C). High levels of *Ndn* expression were detected around the cortical subplate. Neurons immediately dorsal to this showed weak levels of *Snrpn* and *Ndn*, but high levels of *Ipw*. Expression of all three probes was seen through most of the cingulate cortex, but only *Ipw* was detectable in the induseum griseum (Figure 5-5 D, E, F). In the caudoputamen, *Ndn* showed increased expression when compared to *Snrpn* and *Ipw* in the globus pallidus and cortical subplate (Figure 5-5 G,H, I).

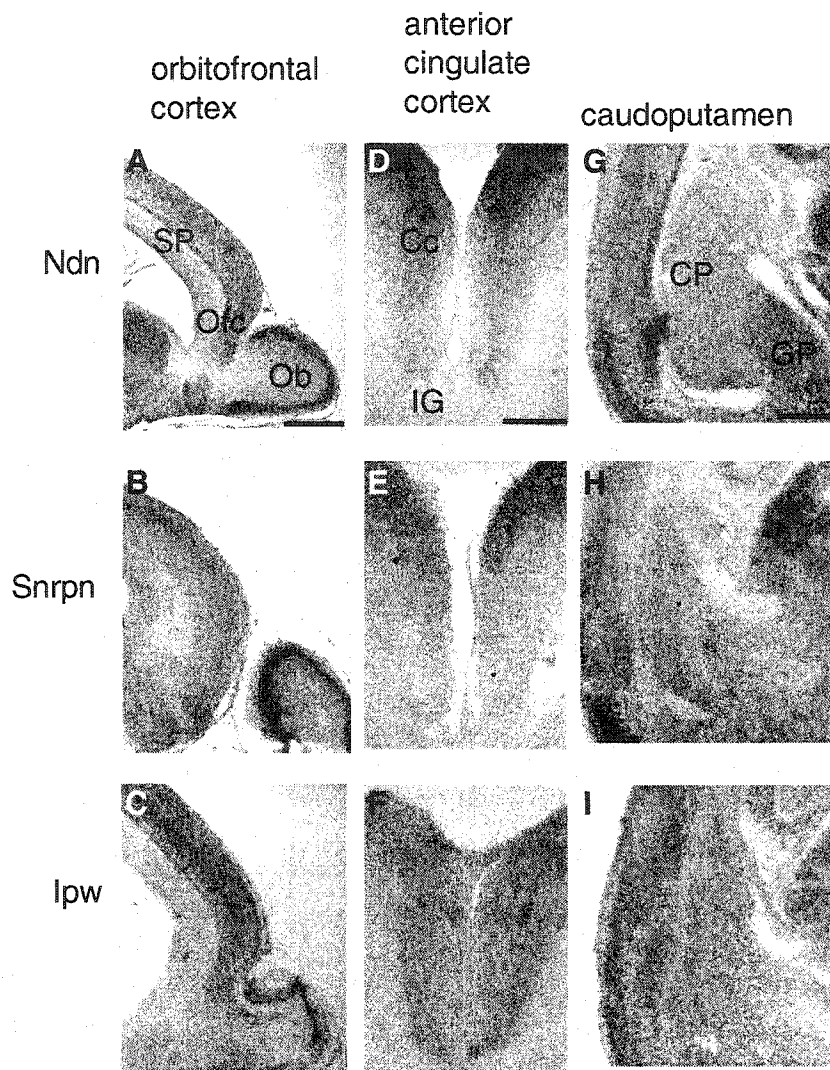


Figure 5- 5. *Ndn*, *Snrpn* and *Ipw* are highly expressed throughout the forebrain at E18.5.

(A-C) Sagittal sections of the orbitofrontal lobe. (D-F) Coronal sections of the cingulate cortex. Note the differential expression in the induseum griseum. (G-I) Coronal sections of the caudoputamen. CP, caudoputamen; Cc, cingulate cortex; GP, globus pallidus; IG, induseum griseum; Ob, olfactory bulb; Ofc, orbitofrontal cortex; SP, subplate. Scale bars: (A) 600 μm , (D) 250 μm , (G) 300 μm .

Several PWS transcripts are expressed in the developing pituitary at E12.5. Low levels of *Mkrn3*, *Magel2*, and *Ndn* expression are seen in the infundibulum, which becomes the posterior lobe, while *Mkrn3* and *Ndn* are also weakly expressed in Rathke's pouch, the future anterior pituitary (Figure 5-6).

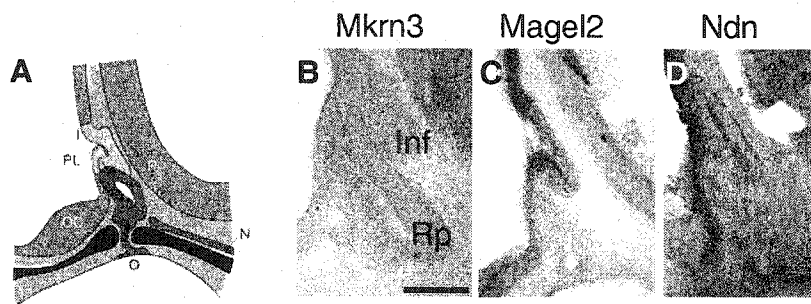


Figure 5- 6. *Mkrn3*, *Magel2* and *Ndn* are expressed in the developing pituitary gland.

Sagittal sections of E12.5 embryos hybridized with *Mkrn3*, *Magel2* and *Ndn* probes. (A) The pituitary gland at E12.5. Infundibulum is shown in yellow and Rathke's pouch in red. Figure adapted from Sheng, H. Z. and Westphal, H. (1999). Early steps in pituitary organogenesis. *Trends Genet* 15, 236-240. (B) *Mkrn3* is expressed in both the infundibulum and Rathke's pouch. (C) *Magel2* is expressed in the infundibulum. (D) *Ndn* is expressed in the infundibulum. Inf, infundibulum; N, neural plate; O, oral cavity; OC, optic chiasma; P, pontine flexure; PL, posterior lobe; Rp, Rathke's pouch. Scale bar: 100 μm .

Expression in the hypothalamic nuclei and arcuate nucleus

Because PWS is associated with hyperphagia and obesity, I examined the expression of the transcripts in the arcuate nucleus and hypothalamic nuclei associated with feeding behavior. *Mkrn3* and *MBII-85* RNAs were uniformly detectable at low levels in these structures, while *Magel2*, *Ndn*, *Snrpn* and *Ipw* produced discrete hybridization signals (Figure 5-7). I did not detect any significant differences in the RNA levels of *Ndn*, *Snrpn* or *Ipw* in the paraventricular nucleus that might correlate structural differences noted in PWS patients and *Ndn* deficient mice (Figure 5-7 A, B, C) (Muscatelli et al., 2000; Swaab et al., 1995). Similar expression levels of these three genes were also detected in the perifornical area, lateral hypothalamic area, and dorsal medial hypothalamus and arcuate nucleus. *Snrpn* expression is slightly higher in the ventral medial hypothalamus (Figure 5-7 E).

Magel2 is expressed at low levels throughout the brain during all of the stages surveyed. Transverse sections at E12.5 reveal intense levels of expression in the ventral thalamus, anterior hypothalamus, supraoptic, paraventricular, and presumptive suprachiasmatic areas (Figure 5-8, A, B, C). At E15.5 and E18.5, expression is highest in the dorsal medial suprachiasmatic nucleus, supraoptic nucleus and the preoptic area (Figure 5-8 D, E, F, G). Moderate levels of expression are also detected in the arcuate nucleus and paraventricular regions.

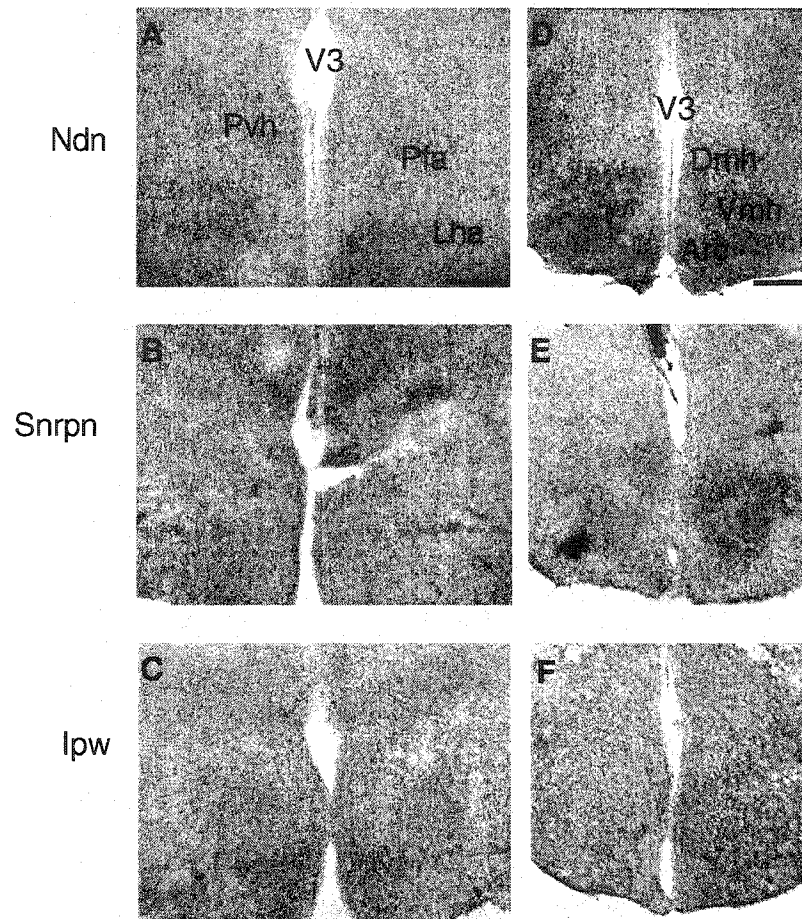


Figure 5- 7. *Ndn*, *Snrpn* and *Ipw* are highly expressed in regions regulating feeding at E18.5.

(A, B, C) Coronal sections of the paraventricular area. (D, E, F). Coronal sections of the arcuate nucleus. Arc, arcuate nucleus; Dmh, dorsal medial hypothalamic nucleus; Lha, lateral hypothalamic area; Pvh, paraventricular hypothalamic nucleus; Pfa, perifornical area; V3, third ventricle; Vmh, ventromedial hypothalamic nucleus. Scale bars: (A) 300 μ m, (D) 250 μ m.

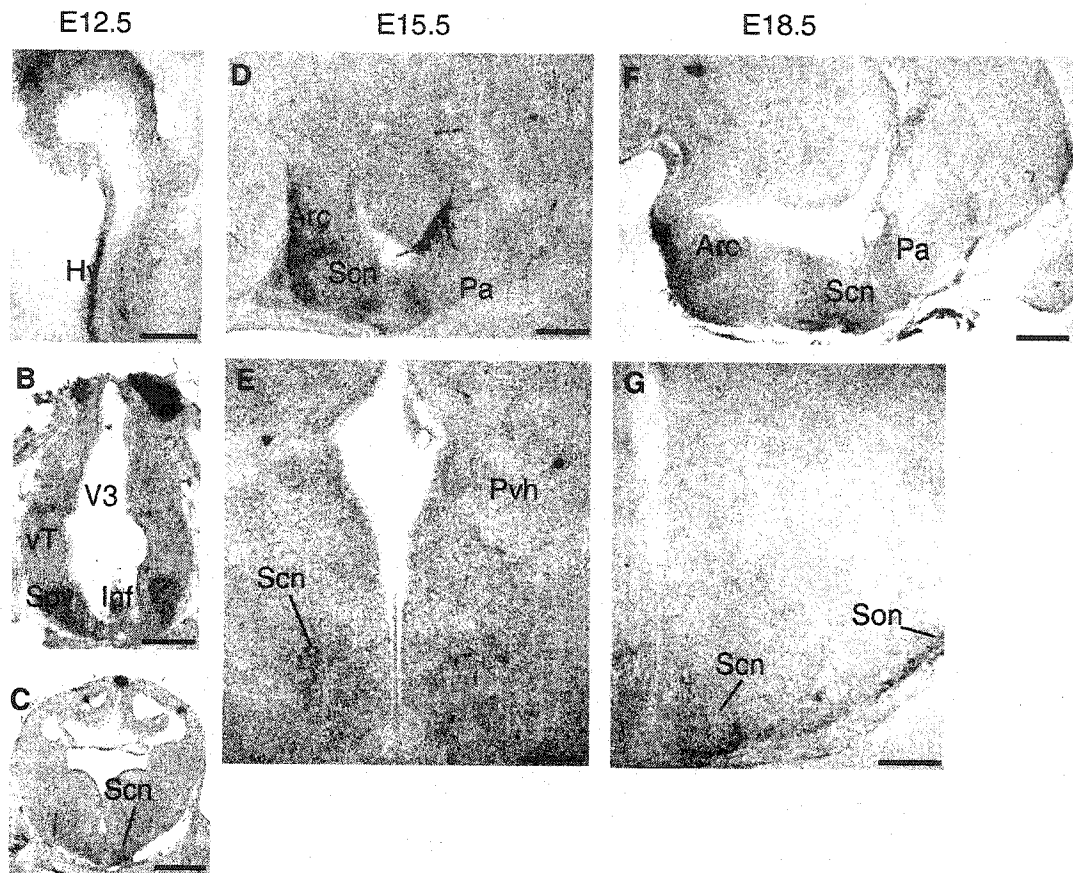


Figure 5- 8. *Magel2* is preferentially expressed in the suprachiasmatic nucleus and the supraoptic nucleus.

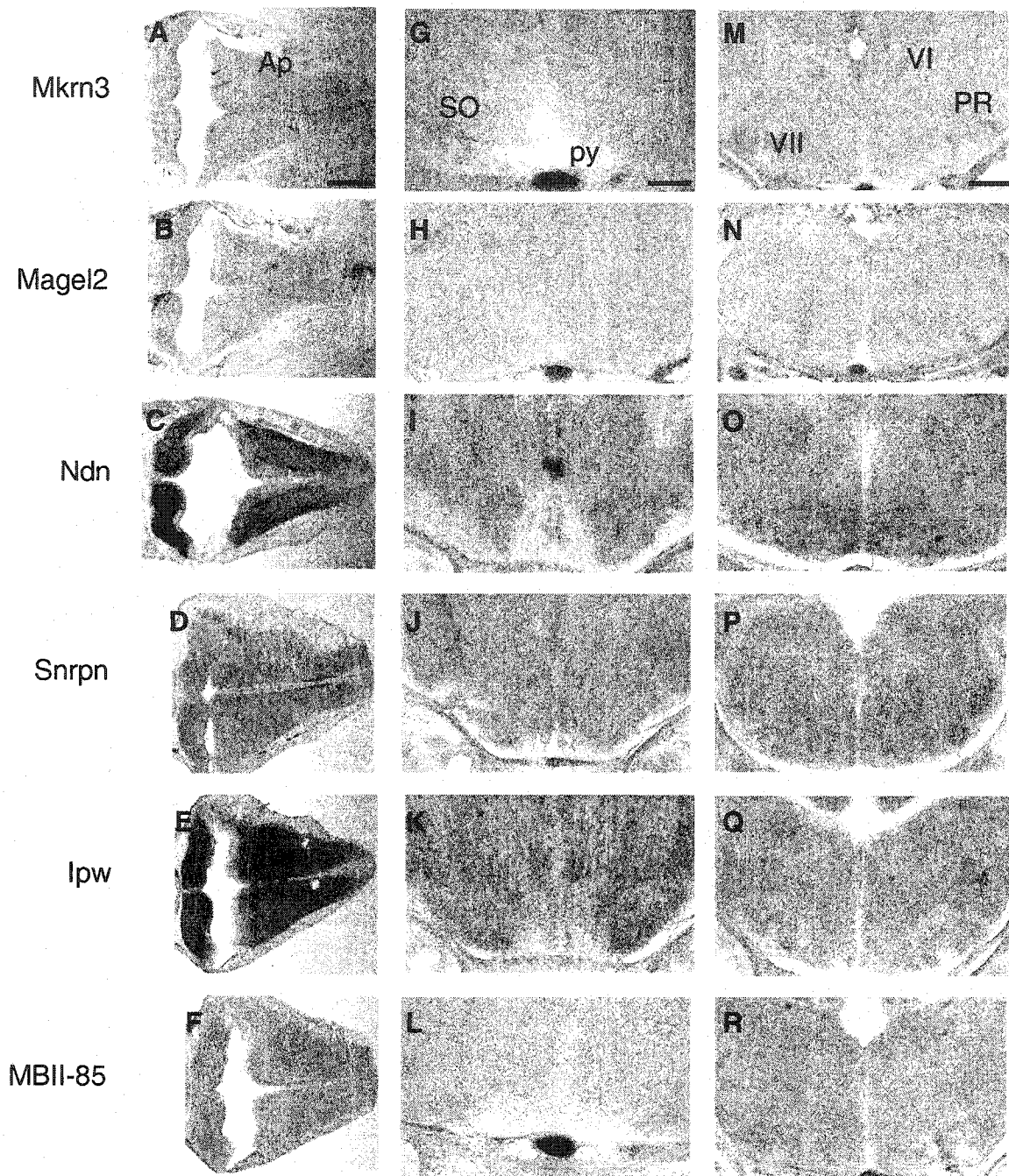
(A) Sagittal section of an E12.5 embryo showing strong staining in the anterior hypothalamus. (B, C) Transverse section at E12.5 embryo with expression in the mantle layer of the hypothalamus and ventral thalamus (B) and presumptive suprachiasmatic nucleus (C). (D, F) Sagittal section of E15.5 (D) and E18.5 (F) brains, oriented with anterior to the right, and posterior to the left. Strong staining is seen in the hypothalamus and extends into the preoptic area. (E) Coronal section of an E15.5 embryo showing signal in the suprachiasmatic nucleus. (G) Coronal section of an E18.5 embryo showing hybridization of *Magel2* in the suprachiasmatic nucleus and the supraoptic tract. Arc, arcuate nucleus; Hy, hypothalamus; Inf, infundibulum; Pa, preoptic area; Scn, suprachiasmatic nucleus; Son, supraoptic nucleus; Spv, supraoptic/paraventricular area; V3, third ventricle. Scale bars: (A) 250 μ m, (B) 400 μ m, (C,D,G) 500 μ m, (E) 150 μ m, (F) 250 μ m.

Expression in the hindbrain.

At E12.5, all transcripts were detected in the metencephalon, although *Mkrn3* and *Magel2* were detected at very low levels. (Figure 5-9 A, B). *Ndn*, *Snrpn*, and *Ipw* showed unique patterns of expression in the alar plate of the metencephalon. (Figure 5-9 C, D, E). At E15.5, *Mkrn3* and *MBII-85* were expressed at low levels throughout the brain with increased levels in the superior olive and facial nucleus. (Figure 5-9 G, L, M, R). *Mkrn3* was also more highly expressed in the region of the abducens nucleus (Figure 5-9 M). *Snrpn*, *Ndn* and *Ipw* were expressed at high levels in these structures as well as the reticular formation (Figure 5-9). Expression of *Snrpn*, *Ipw* and *Ndn* in the Raphe nuclei could be clearly seen at E18.5 (Figure 5-10).

Figure 5- 9. PWS genes are expressed in the hindbrain.

(A-F) Transverse sections of E12.5 metencephalon with anterior to the left, and posterior to the right. (G-L) Coronal sections of E15.5 brain showing the superior olive. Apparent staining below pyramidal tract is artifactual when visualized under higher magnification. (M-R) Coronal sections of E18.5 brain showing facial nucleus. Ap, alar plate; PR, parvicellular reticular nuclei; py, pyrimidal tract; SO, superior olive; VI, nucleus of the sixth nerve (abducens); VII, nucleus of the seventh nerve (facial). Scale bars: (A) 700 μm , (G, M) 300 μm .



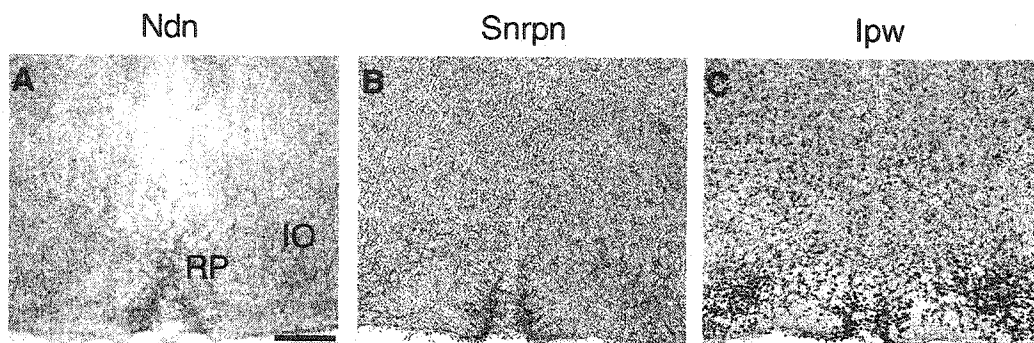


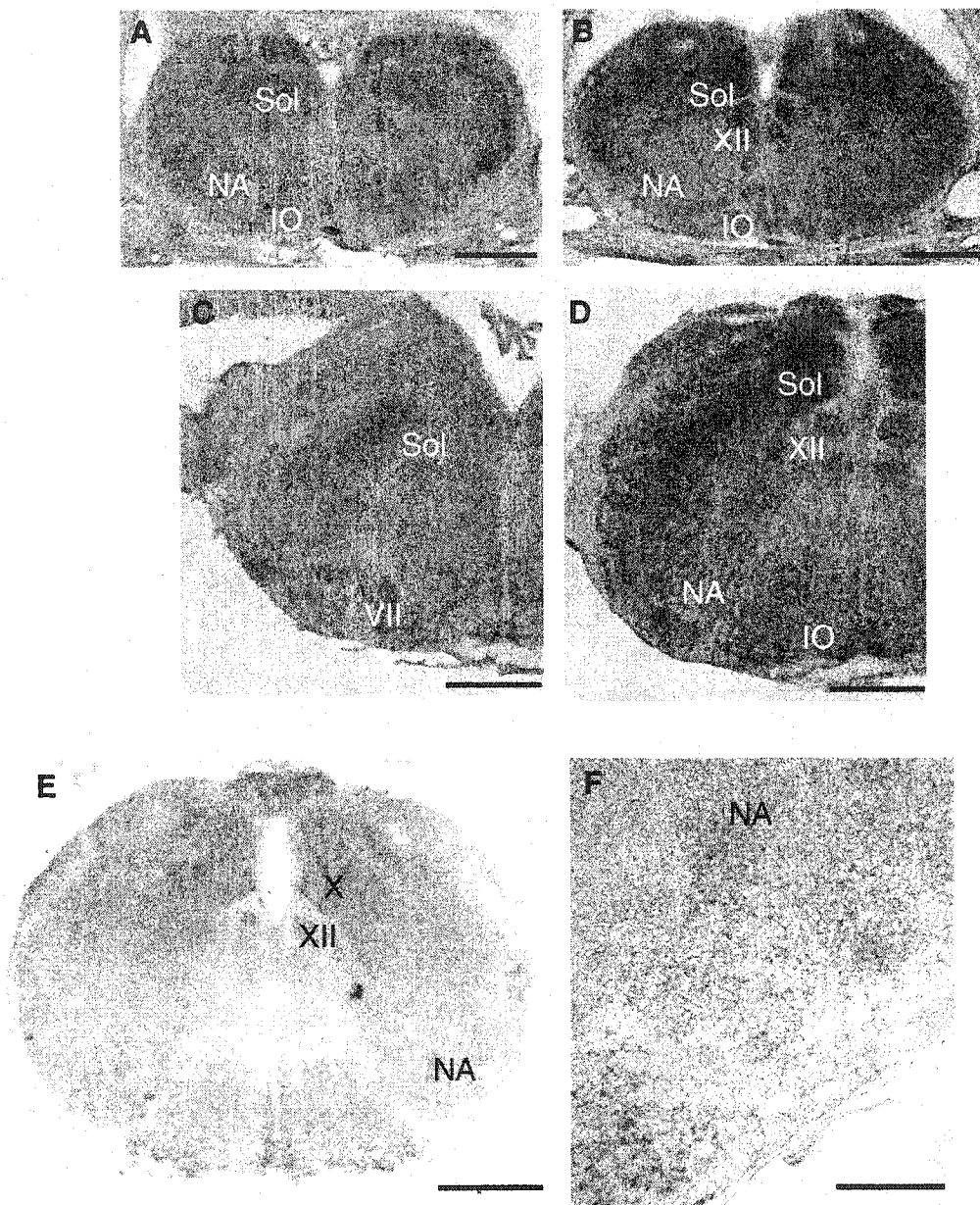
Figure 5- 10. *Ndn*, *Snrpn* and *Ipw* are expressed in the raphe nucleus.

Coronal sections of E18.5 brain. IO, inferior olive; RP, raphe pallidus. Scale bar: 500 μ m

Previous investigations of necdin gene expression by RNA *in situ* hybridization or immunohistochemistry had focused on the cerebrum, cerebellum, and the hypothalamus (Aizawa et al., 1992; Uetsuki et al., 1996). Expression of the *Ndn^{tm2Szw} lacZ* reporter gene had also been noted in the medulla, spinal cord and dorsal root ganglia in E17 embryos (Gerard et al., 1999). To further understand the respiratory phenotype seen in *Ndn* deficient mice, I examined the expression of necdin by RNA *in situ* hybridization in wildtype brainstem sections at E15.5, when respiratory activity commences, and at E18.5, the stage used for respiratory electrophysiological recordings by Dr. Jun Ren (Ren et al., 2003). RNA *in situ* was performed to determine whether differential levels of *Ndn* expression could be detected in subpopulations of medullary neurons. Necdin expression was evident in the ventrolateral medulla where the respiratory rhythm generator is located, but levels were not significantly different than in other medullary regions (Figure 5-11).

Figure 5- 11. *Ndn* is expressed in the fetal medulla.

Expression of *Ndn* in E15.5-E18.5 transverse medullary sections (A) Rostral medullary slice at E15.5. (B) Caudal medullary slice at E15.5 (C-E) Medullary sections from rostral to caudal at E18.5. (F) Higher power photo of the ventrolateral medulla in the region of the pre-Bötzinger complex. IO, inferior olive; NA, nucleus ambiguus; Sol, nucleus of the solitary tract; VII, nucleus of the seventh nerve (facial); X, nucleus of the tenth nerve (vagus); XII, nucleus of the twelfth nerve (hypoglossal). Scale bars: (A-E) 500 μm ; (F) 150 μm .



Histological characterization of *Ndn* deficient mice.

In litters of newborn mice born to a heterozygous *Ndn*^{tm2Stw} male and wildtype female, I observed that a subset of pups gasped for air, turned cyanotic and died over a postnatal time course of a few hours, as previously noted (Gerard et al., 1999; Muscatelli et al., 2000). Nudging the pups caused a transient increase in respiration and loss of cyanosis.

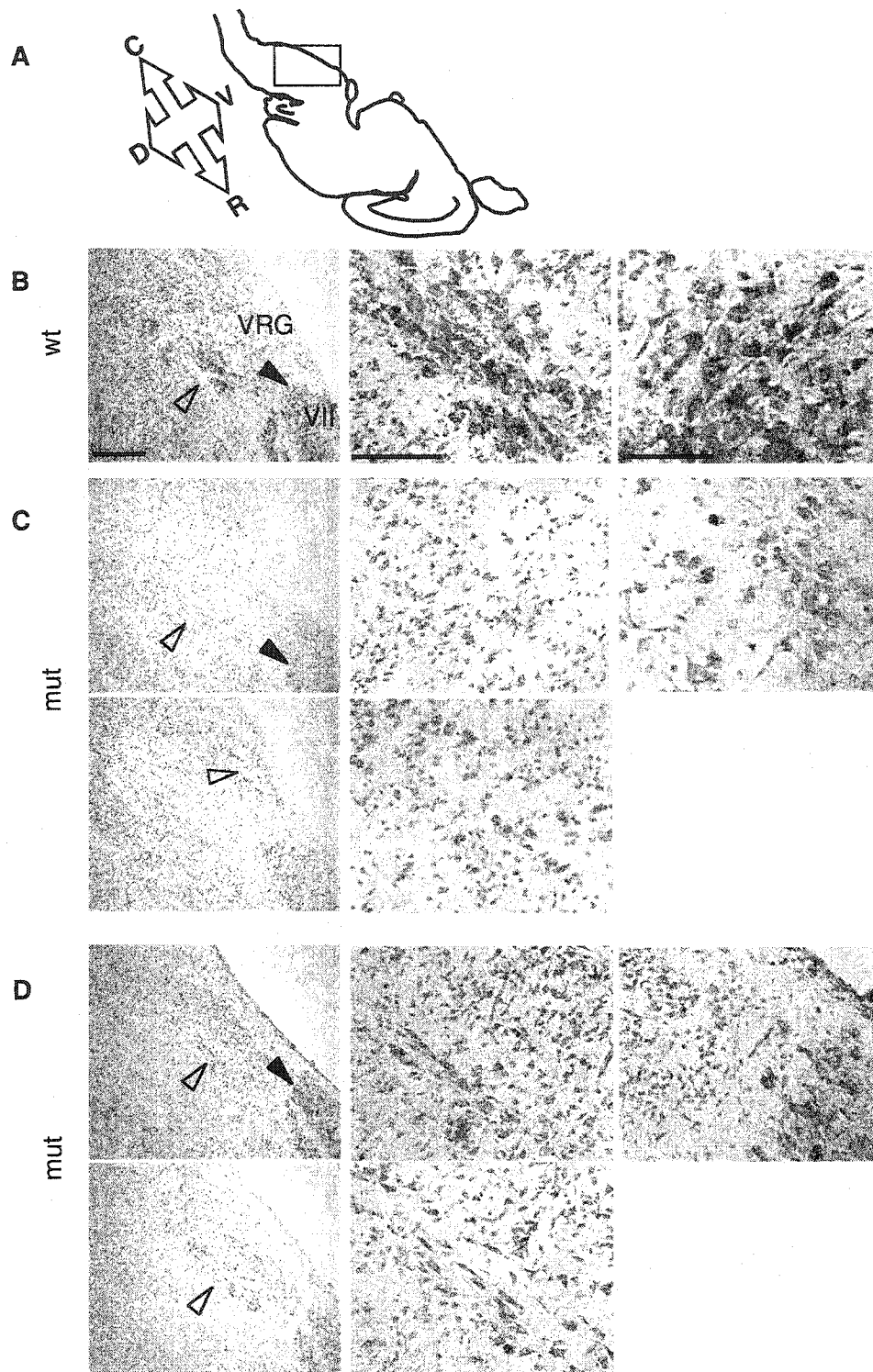
In the *Ndn*^{tm2Stw} line of *Ndn* deficient mice created by Gerard *et al.*, no gross morphological changes were observed in *Ndn* deficient mice by β -galactosidase staining (see above). A separate line of *Ndn* deficient mice created by Muscatelli *et al.*, was found to have decreased neurons in the PVH (Muscatelli et al., 2000). This suggested that a closer examination of the *Ndn*^{tm2Stw} line might reveal subtle neuronal changes. As Dr. Jun Ren showed that the *Ndn*^{tm2Stw} mutant mice were unable to generate a respiratory rhythm from the pre-Bötzinger complex (Ren et al., 2003), I hypothesized that these mice could have a subtle morphological alteration that would reflect the respiratory deficiency. To investigate the hindbrain morphology, *Ndn* deficient males on a C57Bl/6 background were mated with female C57Bl/6 mice. Hindbrains were removed from E18.5 embryos. Samples from the forebrain were used to genotype mice based on the ability to detect the presence of β -galactosidase activity. Serial 20 μ m sagittal cryosections were made on a total of 3 wildtype and 4 mutant mice from 2 separate litters. Sections were then thionin stained to examine neuronal morphology.

Based on a preliminary qualitative analysis of thionin stained sections, marked and variable dysmorphology of the motoneurons of the hindbrain were observed in the mutants, but not in wildtype littermates (Figure 5-12). In general, the neurons of the

mutant mice appeared less dense than their wildtype counterparts. There was pronounced and highly variable motoneuron loss between individual mutants. In one mutant, the facial nucleus appeared disorganized with a faint diffuse background staining. The motoneurons of the nucleus ambiguus were almost all absent. While a few residual large motoneurons were present, they were laterally displaced with respect to the nucleus ambiguus. These motoneurons could have been remnants of the nucleus ambiguus or part of a greatly reduced ventral respiratory group. In another mutant the facial nucleus was not grossly dysmorphic. Though the nucleus ambiguus was present, a qualitative examination suggested that the number of motoneurons nucleus was decreased.

Figure 5- 12. *Ndn* deficient mice show motoneuron loss in the hindbrain.

Thionin stained 20 μm sagittal sections of the medullary hindbrain of one wildtype and two mutant mice. (A) Outline of the mouse brain showing the orientation and location of the sections. C, caudal; D, dorsal; R, rostral; V, ventral. (B-D) Sections from three mice. Images on the left show the medullary region. Middle image is a magnification of the region indicated by the open triangle. Left image is a magnification of the region indicated by the black triangle. B) Wildtype mouse. (C) Mutant mouse 1. (D) Mutant mouse 2. The ventral surface is towards the top, rostral is to the right. NA, nucleus ambiguus; VII, nucleus of the seventh nerve (facial); VRG, ventral respiratory group. Scale bars: left: 250 μm , middle/right: 100 μm .



Conclusion

RNA localization patterns

The murine orthologues of PWS candidate genes are expressed throughout the developing mouse brain as early as E9.5. Expression of most of the PWS genes is widespread, although individual transcripts were more easily detected in certain regions. The expression patterns of the PWS genes in mice provide an insight into the structures that may be affected in the brain when these genes are absent in murine PWS models, and provide a reference point for studies of the human PWS genes.

Regulation of the Snurf-Snrpn transcription unit

Ipw and the snoRNAs are alternatively processed RNAs transcribed from the *Snurf/Snrpn* locus (Runte et al., 2001). I performed RNA *in situ* hybridization on adjacent tissue sections using probes from three portions of the *Snurf/Snrpn* transcriptional unit representing the protein coding *Snrpn*, untranslated RNA, *Ipw*, and the snoRNA *MBII-85*. The RNA *in situ* results showed pronounced differences in both levels and tissue distribution of the RNAs in early development, which became more subtle at E15.5 and E18.5. It is possible that some of the differences in the hybridization patterns from *Snrpn*, *Ipw* and *MBII-85* were due to the nature of the individual probes, with each probe having differing stability, hybridization affinity or tissue accessibility. However, *Ipw* and *Snrpn* often showed reciprocal expression intensities in different tissues. In the induseum griseum and in the neurons surrounding the cortical subplate, signals were stronger from the *Ipw* probe than *Snrpn*. Stronger signals were detected by *Snrpn* in the ventral medial hypothalamus and the dorsal root ganglia. Other studies have also shown differential spatial expression of RNA isoforms during embryogenesis (Hime et al., 2001). The

Snurf-Snrpn transcript may be spliced in a tissue-specific manner or the stability of the isoforms may be dependent on tissue-specific factors. Coordinately regulated transcripts may be important for the development of certain brain structures, or for the regulation of neurohormone production.

Implications for understanding the pathophysiology of PWS.

Despite the many differences between mice and humans, it is likely that the fundamental components of biological pathways are conserved, and that work in mice will provide information on the normal role of genes that are mutated in human disease (Wynshaw-Boris, 1996). Although correlations between gene expression in the mouse and human can be made, understanding how they relate to many aspects of human development, behavior and cognition is difficult to elucidate. However, the use of mouse models is necessary because of the difficulty of examining these tissues in humans.

One difficulty that arises when studying PWS is the heterogeneity seen in patients. Although several phenotypic characteristics are extremely common in PWS, there is no single feature that is present in all patients, probably due to differences in genetic modifiers. In this analysis, I have focused on the most common PWS characteristics as well as those that are implicated by the expression patterns seen in mice. Based on clinical data, the regions of the brain most implicated in PWS are the hypothalamus, pituitary, forebrain and brainstem.

The *Snurf/Snrpn* transcriptional unit and *Magel2* now join *Ndn* as imprinted PWS genes that are expressed in the developing hypothalamus, although *Magel2* is the only one that is exclusive to the hypothalamus (Gerard et al., 1999; Kaneko-Ishino et al., 1995; Kuroiwa et al., 1996; Muscatelli et al., 2000). The PVH, a major secretory nucleus best

known for its production of oxytocin and vasopressin, has been the focus of much PWS research. A 54% decrease in PVH oxytocin expressing neurons has been reported in PWS patients, and this has led to the suggestion that these neurons make up a satiety center (Swaab et al., 1995). My RNA *in situ* hybridization study shows that all of the PWS genes are expressed in the mouse PVH at low to moderate levels. Interestingly, mice that are deficient for *Ndn* have a 29% decrease in the number of oxytocin expressing neurons in the PVH (Muscatelli et al., 2000). My results show that *Ndn* is expressed throughout the hypothalamus and its levels in the PVH are similar to that seen in surrounding tissue. The *Ndn* knockout studies suggest that certain regions of the brain, such as the PVH, may be particularly sensitive to the loss of *Ndn*. Similarly, although *Ndn* expression is not unique to the brainstem, we have recently reported that medullary respiratory function is particularly sensitive to the loss of *Ndn* (Ren et al., 2003).

Although not as thoroughly investigated in relation to PWS as the PVH, there are several other hypothalamic nuclei that are also implicated in feeding and energy homeostasis. The ARC receives primary hormonal satiety signals, and generates secondary satiety signals to other neurons including the PVN, PFA, and LHA. (Batterham et al., 2002; Elmquist et al., 1998; Sawchenko, 1998; Schwartz et al., 2000; Swaab et al., 1993). Other regions implicated in feeding behavior include the DMH and VMH (Elmquist et al., 1998). *Ndn*, *Snrpn*, and *Ipw* are highly expressed in all of these nuclei.

Magel2 is expressed in the dorsomedial region of the developing SCN, which receives signals from the non-visual cortical and subcortical regions (Moore et al., 2002). A recent survey of mouse transcripts found that *Magel2* is expressed in the SCN in a

circadian fashion (Panda et al., 2002; Su et al., 2002). I confirmed that *Magel2* is expressed in the SCN and also found expression in the SON, which produces vasopressin along with oxytocin. The results in this chapter show a similar expression pattern to that of vasopressin within the SCN and SON, although further investigations are needed to confirm this (Moore et al., 2002; Schonemann et al., 1995). The SON is part of the hypothalamo-neurohypophyseal system, and neurons project to the posterior pituitary where vasopressin and oxytocin are released into the bloodstream (Reppert et al., 1987). Interestingly, decreased levels of hypothalamic vasopressin have been detected in several PWS subjects (Gabreels et al., 1998; Gabreels et al., 1994). Vasopressin production in the SCN is circadian, and independent of production in the SON, and may be involved in transmitting temporal information within the brain. There are many reports of PWS patients experiencing sleep disturbances, the most striking of which are excessive daytime sleepiness and rapid-eye movement sleep occurring at the onset of sleep (Vela-Bueno et al., 1984). The SCN in the hypothalamus is involved in establishing circadian rhythms, and also in promoting or facilitating wakefulness (Edgar et al., 1993). SCN function may be compromised in PWS, and there has been one post-mortem report of a woman with PWS with increased cell numbers in the SCN (Swaab et al., 1987).

At E12.5, *Magel2* expression is regionally restricted in the forebrain and is expressed in the migrating cells of the zona incerta of the ventral thalamus. Intense expression is detected in the SPV in the anterior hypothalamus, where parvocellular and magnocellular neuronal precursors of the PVH and SON are generated (Nakai et al., 1995). Cells that remain medial to the third ventricle become the PVH, while those that migrate laterally form the SON (Acampora et al., 1999). *Magel2* is the only known gene

that shows preferential expression in both the SCN and the SON. This expression precedes terminal differentiation of these neurons, and thus may be a marker for the development of hypothalamic vasopressin neurons.

Growth hormone (GH) deficiency is thought to be the cause of the short stature, high body fat mass, low muscle mass, higher incidence rates of osteoporosis, decreased bone marrow density and decreased insulin-like growth factor levels (Costeff et al., 1990; Hoybye et al., 2002; Lee, 1995). GH is produced in the pituitary but is regulated by GH releasing hormone (GHRH) produced in the arcuate nucleus, somatostatin produced in anterior pituitary, and ghrelin produced in the stomach. A 30% decrease in GHRH neurons has been found in the arcuate nuclei of PWS patients (Burman et al., 2001; Swaab, 1997). Elevated levels of plasma ghrelin have also been found in PWS, and may be involved in the obesity and GH deficiency (Cummings et al., 2002; DelParigi et al., 2002; Haqq et al., 2003). MRI analysis has found an absent or reduced posterior pituitary bright spot, the integrity of which is indicative of hypothalamic/pituitary function (Miller et al., 1996). Pituitary hypoplasia has also been seen in patients (Schmidt et al., 2000). The loss of PWS genes from the ARC or PVN may result in altered GH regulation. Furthermore, *Magel2*, *Mkrn3*, and *Ndn* are expressed in the developing mouse pituitary and may be important for the growth function of the pituitary in humans.

Behavioral problems have been reported in many PWS patients. Adaptive impairment related to compulsive behavior, hoarding, concerns over symmetry and exactness, need to ask or tell and skin picking are frequently seen in patients (Dykens et al., 1996; Warnock and Kestenbaum, 1992; Whitman and Accardo, 1987). Recently, it has been shown that the orbitofrontal cortex, cingulate cortex and the caudoputamen

make up the “obsessive compulsive disorder (OCD) circuit” (Graybiel and Rauch, 2000; Greer and Capecchi, 2002; Saxena et al., 1998). I found that *Ndn*, *Snrpn* and *Ipw* are expressed at high levels in the OCD circuit, and could potentially be involved in the behavioral problems seen in PWS patients. Furthermore, mice that are deficient for *Ndn* show increased skin scraping (Muscatelli et al., 2000), and the most recent investigations into the *Snrpn* deficient mice suggest that they might have dopamine imbalances and behavioral abnormalities suggestive of OCD (White et al., 2002). Most serotonergic neurons are located within the raphe nuclei and surrounding neurons, and *Ndn*, *Snrpn*, and *Ipw* are strongly expressed in these cells. Low levels of serotonin have been associated with impulsive, aggressive and self-injurious behavior (Hellings and Warnock, 1994). Treatment with selective serotonin inhibitors has been beneficial in cases of self-injurious skin picking, and some cases of OCD related behaviors in PWS patients (Dimitropoulos et al., 2000; Dykens et al., 1996; Hellings and Warnock, 1994). A defect in the reticular formation could result in the elevated hypercapnic arousal thresholds while sleeping, as well as lower resting diastolic blood pressure, abnormal pupil constriction, abnormal temperature regulation, increased pain tolerance, and thick, concentrated saliva seen in patients (Brandt and Rosen, 1998; DiMario et al., 1994; Hart, 1998; Livingston et al., 1995; Mason, 2001). High levels of *Ndn*, *Snrpn* and *Ipw* were detected in the reticular formation.

PWS patients experience difficulties with auditory discrimination and processing auditory information (Curfs et al., 1991; Gabel et al., 1986; Stauder et al., 2002; Warren and Junt, 1981). It is exciting to note that *Mkrn3* and *MBII-85* are expressed at very low levels throughout most of the mouse brain, but were upregulated in the superior olive,

which is known to be involved in auditory processing and sound localization (Spitzer and Semple, 1995). *Mkx3* was also specifically expressed in the abducens nucleus, suggesting that some of the eye abnormalities seen in PWS patients such as strabismus and esotropia could be due to a central defect (Butler et al., 2002; Engle, 2002; Holm et al., 1993). Although *Snrpn*, *Ipw* and *Ndn* were all expressed at high levels in these structures as well, the specific nature of the *Mkx3* and *MBII-85* expression pattern warrants further investigation.

Loss of *necdin* results in motoneuron dysmorphology

Abnormal ventilatory responses to hyperoxia, hypoxia and hypercapnia when awake and sleeping are noted in PWS patients (Arens et al., 1994; Gozal et al., 1994; Menendez, 1999; Schluter et al., 1997). There are also reports of sleep-related central and obstructive apnea (Clift et al., 1994; Manni et al., 2001; Nixon and Brouillette, 2002; Wharton and Loechner, 1996). A report of a 29-week premature infant with PWS who required prolonged ventilatory support suggests a prenatal onset of respiratory dysfunction in PWS (MacDonald and Camp, 2001). The sleep related breathing problems may also contribute significantly to the excessive daytime sleepiness in childhood and adulthood that is characteristic of PWS (Hertz et al., 1995). The RNA localization patterns of *Ndn* in the medulla, hindbrain dysmorphology in *Ndn* deficient mice, and the electrophysiological data of Dr. Jun Ren suggest that *Ndn* is involved in mouse respiration. I hypothesize that *NDN* deficiency in humans may be involved in the abnormal respiration seen in PWS infants, and that *NDN* may be important for normal respiratory activity in the human newborn hindbrain.

Despite the initial reports that an *Ndn* deficiency caused no overt morphological changes (Gerard et al., 1999), I found subtle changes in the hindbrains of mutant mice. Qualitative analysis of thionin stained sections suggested that the loss of *Ndn* affects the morphology and distribution of motoneurons of the NA and VRG which make up the respiratory center. Some mutant mice also showed disorganization of the facial nucleus, which is largely comprised of motoneurons, although it has only an accessory respiratory function (Champagnat and Fortin, 1997). The potential effects of a facial nucleus disruption may be masked by the respiratory distress. Neurons within the pre-Bötzinger complex could not be examined as there were no molecular markers available that defined that population of cells in neonatal mice. However, the motoneuron loss seen in other regions of the medulla may extend to the pre-Bötzinger complex and be the cause of its functional disruption.

Although the morphological changes were most evident in motoneurons, neuronal loss in the PVH (Muscatelli et al., 2000) suggests that *Ndn* may be essential for proper neuronal maintenance in specific cell populations. The loss of motoneurons from several physiologically defined clusters within the hindbrain of the mutant mice suggests that *Ndn* may be important for proper neurogenesis. Hindbrain motoneuron cell fate is determined early in mouse development when the hindbrain is partitioned into rhombomeres between developmental stages E8 and E12 (Champagnat and Fortin, 1997). In particular, rhombomeres r6-r8 give rise to the ventral respiratory group neurons. Furthermore, studies with chick embryos have suggested that the determination of ultimate neuronal phenotypes might occur in precursor cells, before final rhombomere formation, and before the end of mitotic expansion and dispersal. If *Ndn* is an important

regulator of such early events, its loss at these early stages could be reflected at E18 as a dysmorphology in several neuronal nuclei.

In vitro experiments have also suggested that *Ndn* is required for the correct terminal differentiation and survival of dorsal root ganglion cells (Takazaki et al., 2002). Cells in which *Ndn* is inhibited undergo apoptosis through the caspase 3 mediated pathway. The appearance of the cells in the region of the facial nucleus may be due to increased levels of cell death and suggest that further investigations with apoptosis markers are needed.

PWS is a global dysfunction involving multiple genes

RNA *in situ* hybridization provides a rapid means of profiling gene expression to gain insights into the function of individual protein coding genes and non-coding, functional RNAs. Although my results show that many of the PWS genes are widely expressed in the brain, they may be more regionally restricted at the protein level. For *necdin* at least, immunohistological studies with a polyclonal antibody show that the protein localization patterns parallel those of the RNA (Niinobe et al., 2000). *Snrpn* protein has previously been shown to be produced only postnatally (Grimaldi et al., 1993), suggesting that the prenatal expression of the RNA may have an alternative function to its postnatal role as a splicesomal factor.

Because the RNA *in situ* data presented in this chapter shows expression of the PWS candidate genes throughout most of the brain, it is difficult to determine which structures are most affected by their loss of function. Although the dogma is that PWS is primarily due to a hypothalamic deficiency, a broader view is that PWS may be due to dysfunctions in multiple neuronal systems that may include the hypothalamus, pituitary,

forebrain and brainstem. *Ndn* and *Magel2* are adjacent genes with high sequence similarities and overlapping expression patterns, suggesting that they may be functionally redundant, or have overlapping roles. A combined loss of these two genes may be responsible for neuronal dysfunction. The remaining genes may contribute to secondary features such behavior, auditory localization and ocular problems.

The results presented in this chapter suggest that multiple genes are responsible for various aspects of PWS, further supporting the idea that PWS is a multi-gene syndrome and that single gene mutations will not be seen in PWS patients. Construction of individual mouse gene knockouts, or the discovery of individual gene mutations in humans are still required to determine the contribution of each of these genes to PWS. Though there are some characteristics of PWS, such as articulation defects that cannot be studied in mice, I have shown that many of the PWS characteristics can be correlated with murine gene expression in structures that they are potentially involved in the syndrome.

Chapter 6. Conclusion

The PWS region contains at least 5 candidate genes

In this thesis, I have evaluated the role of the paternally expressed genes and transcripts within the 15q11-q13 imprinted domain for their role in the pathophysiology of PWS. I began by surveying the region for unidentified imprinted genes. Initially, I examined ESTs that were known to map to the region, and when partial sequence for the region was completed by the Human Genome Project, I used gene prediction programs to identify the gene *MAGEL2*. I then analyzed the expression patterns of the murine homologues for insights into their functional roles.

Initial estimates predicted approximately 100 genes within this 4 Mb deletion interval based on the overall gene frequency seen throughout the genome. Although the sequence is not entirely complete for the 15q11-q13 region or the mouse 7C region, the number of genes that can be identified *in silico* using gene prediction programs appears to be much less, with fewer than 20 genes identified. There are only 5 sets of transcripts in the PWS critical region that are paternally expressed in the brain, and can therefore be considered as candidates for PWS: *MKRN3*, *MAGEL2*, *NDN*, *SNURF/SNRPN*, and the snoRNAs.

Although *MAGEL2* remains the most recent gene identified in the PWS region, there may still be additional unidentified genes. Genomic sequence is still being generated to fill in the unsequenced gaps that remained after the initial phase of the Human Genome Project (see Figure 3-4). Gene prediction programs scan a sequence based on common gene elements such as open reading frames and splice sites between exons. However, there may be additional genes in this region that cannot be identified by standard gene prediction programs. Genes that function as regulatory RNAs, such as the

XIST gene (Brown et al., 1992), are not easily identified by standard gene prediction programs. Transcripts such as the snoRNAs are also difficult to predict as they have neither an open reading frame or a polyadenylation signal.

Some of the limitations of gene prediction programs can be overcome by analyzing EST clustering patterns by using databases like UniGene. In most cases, a UniGene cluster is reflective of a gene's overall expression level and tissue distribution. However, genes that are expressed in either a developmentally restricted or in a tissue specific manner may be under-represented in standard cDNA libraries and in the UniGene database. Furthermore, as cDNA clones are often selected based on transcript size and the presence of a poly(A) tail, small transcripts or those that do not become polyadenylated are also under-represented in UniGene. None of the snoRNAs in the PWS region can be found in the UniGene database for these reasons, despite their robust expression levels on northern blots.

Traditional methods of identifying novel genes based on protein coding regions and searching cDNA databases are nearing the limits of their usefulness as the definition of a functional gene evolves. The PWS region has many genes that do not have a classical gene structure. *MKRN3*, *MAGEL2*, *NDN* and *C15ORF2* are single exon genes and do not have splice acceptor/donor signals. *SNURF/SNRPN* appears to be bicistronic, encoding two proteins, a feature that is more reminiscent of the prokaryotic genome than a human gene. The downstream exons of this *SNURF/SNRPN* transcriptional unit do not have coding potential. Furthermore, the snoRNAs are located in the introns of this transcriptional unit, a region previously considered as "junk" DNA.

The PWS region shows that as our understanding of the human genome and gene structure increases, functional transcripts that do not fit the classical definition of a gene may be identified. The PWS region also suggests that functional, non-coding RNAs may have a large biological role in human gene regulation and hence human disease. Novel gene identification methods that take into account these new features will be needed.

Imprinting in 15q11-q13 is controlled as a domain

It has been proposed that most of the genes in the PWS region are a result of retrotranspositions because of the unusually high number of intronless genes and L1 repetitive retrotransposons (Chai et al., 2001). One model suggests that *SNRPN* is the original gene in the PWS critical region and is the result of a duplication event from the ancestral *SNRPB*' gene. Subsequent development of paternal expression and the IC may have conferred a postnatal growth advantage as both PWS newborns and mouse deletion models show failure to thrive immediately after birth. *Frat3*, *MKRN3*, *MAGEL2*, *NDN* and *C15ORF2* are intronless genes and proposed to be the result of retrotransposition events. In this "innocent bystander" model, functional genes that enter into the imprinting domain are affected by the epigenetic signals in the region and in turn become imprinted themselves. This model is supported by findings that suggest that *Frat3* is the result of a retrotransposition event into mouse 7C after the divergence of mice and humans. As *Frat3* is expressed only from the paternal allele, it appears to have become subject to the same imprinting mechanism as its neighboring genes (Chai et al., 2001).

The number of testis specific transcripts in the PWS region proximal to *SNURF/SNRPN* is striking (see Figure 3-4). The imprinting status of most of these testis-transcripts is not known, except for the *C15orf2* gene, which is biallelic and only

expressed in testis. A biallelically expressed gene would not violate the paternal only expression domain of the PWS region if the expression is restricted to post-meiotic sperm cells, a stage when the repressive maternal imprint has been erased (Farber et al., 2000; Nicholls and Knepper, 2001). This expression pattern is seen in *C15orf2*, which is expressed in testis, and remains silent and highly methylated in somatic tissues (Farber et al., 2000). Although the maternal and paternal alleles of *C15orf2* are not directly imprinted, its expression and unmethylated status in sperm would also ensure that the gene acquires a paternal-like imprint during spermatogenesis (Farber et al., 2000; Nicholls and Knepper, 2001).

The tissue distribution of transcripts in the PWS critical region suggests a model of gene acquisition, most likely by retrotransposition followed by the spreading of the imprinting mechanism to include the new genes. Recent evidence has suggested that the IC only functions in the somatic cells (Mann and Bartolomei, 2000) to maintain the imprint in post-zygotic cells (Bielinska et al., 2000). The ability of the IC to act on a newly acquired gene depends on the expression pattern of that gene and may not be able to act on a testis-specific transcript, resulting in the biallelic expression seen for *C15orf2*.

This model of gene acquisition followed by imprinting predicts that all somatically expressed genes in this region would be imprinted and only expressed from the paternal allele. Thus, the transcripts from Hs.279570, which are specific to lung, would be predicted to be derived only from the paternal allele.

PWS is a global brain dysfunction.

Because the brain utilizes many redundant and overlapping pathways, it is difficult to determine whether PWS is primarily a hypothalamic defect or is due to

dysfunctions in multiple neuronal systems. It has been proposed that PWS could be primarily a result of a hypothalamic disruption (Cassidy et al., 2000; Swaab, 1997), as hypothalamic nuclei control many aspects of biological homeostasis and exert control over many parts of the brain either through axonal connections or through hormone secretion.

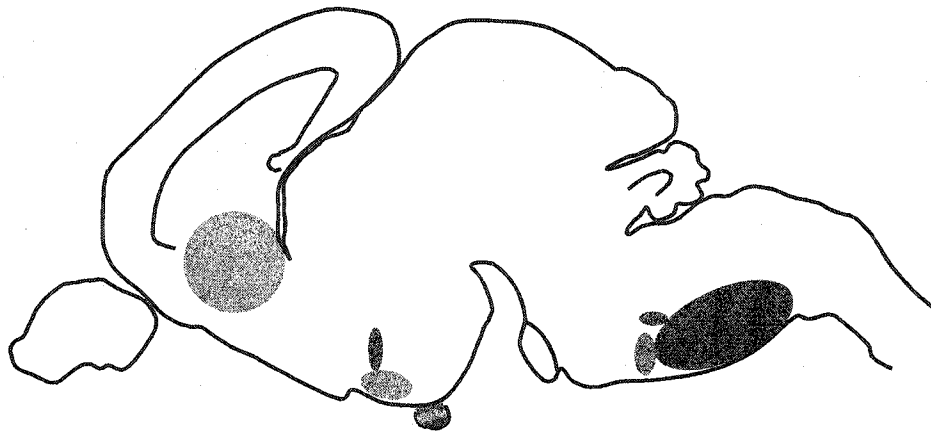
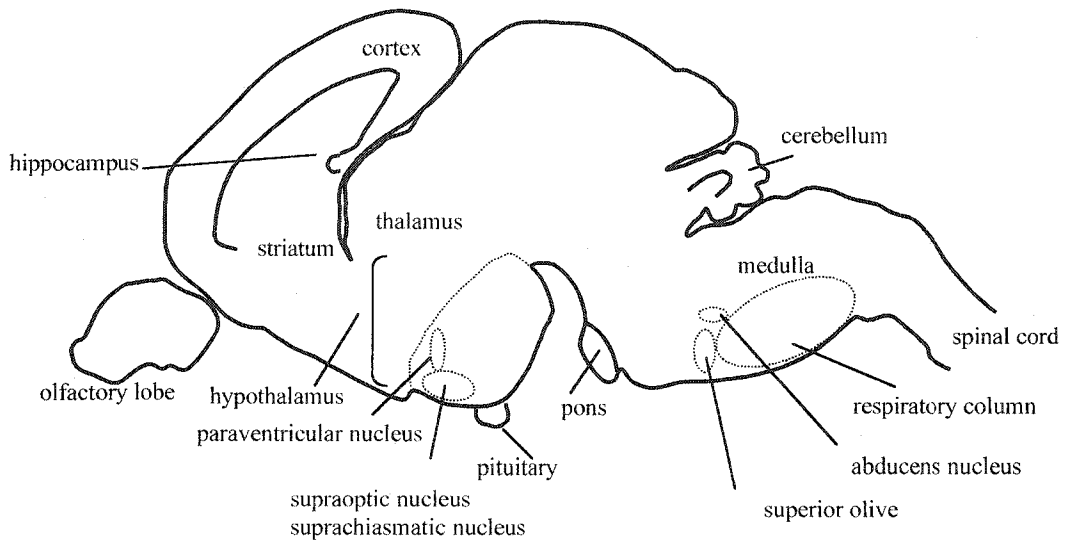
The RNA expression studies the data from the *Ndn* deficient mouse presented in Chapter 5 suggest that PWS may be a result of several regional deficiencies in the brain rather than a central hypothalamic defect. With the exception of *Magel2*, most of the PWS candidate genes are not expressed exclusively in the hypothalamus. Though strongly detected within the hypothalamus, *Ndn*, *Snrpn* and *Ipw* RNAs are also detected at high levels throughout the developing brain, suggesting that loss of expression of these genes may also have developmental consequences outside of the hypothalamus. Despite their global RNA distribution in the brain, post-transcriptional modifications could result in protein products with a more tissue specific localization pattern. Immunohistological studies show that, at least in the case of *Ndn*, the RNA expression pattern is reflective of the final product (Niinobe et al., 2000). Conversely, while the *Snrpn* transcript is highly expressed prenatally, its protein product is detectable only in postnatal brain when examined in rats (Grimaldi et al., 1993). Further protein and RNA comparison studies of the remaining PWS candidate genes will give more insights into the neuronal populations that may be affected in PWS.

Although transcripts from most of the PWS candidate genes can be detected throughout most of the developing mouse brain, I propose a model in which each of the PWS candidate genes has a critical role in the development of particular neuronal

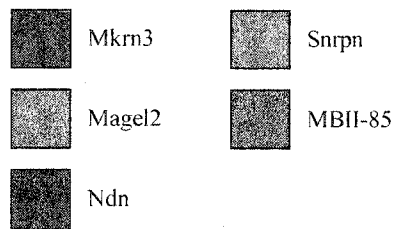
structures. Furthermore, the combined loss of several PWS genes in some structures could have a synergistic effect that is not seen when individual genes are silenced. A combined loss of *Magel2* and *Ndn* in the anterior hypothalamus may be responsible for the hypothalamic dysfunction, while loss of PWS genes in other regions of the brain could produce secondary effects such as respiratory failure and OCD. The potential role of each gene in the pathophysiology of PWS is outlined below and summarized in Figure 6-1.

Figure 6- 1. Hypothetical model of the effect of PWS genes the development of discrete regions of the brain.

(Top) An outline of an E18.5 mouse brain with the major structures labeled. (Bottom) The proposed regions of the brain that could be affected by the loss of the PWS genes based on RNA *in situ* data, morphological data from *Ndn* deficient mice, and behavioral data from *Snrpn* deficient mice. *Mkx3* expression data suggests that it may be important in the pituitary, superior olive, and abducens nucleus. *Magel2* expression implicates a role in the development of the supraoptic nucleus, suprachiasmatic nucleus and the pituitary. *Ndn* deficient mice suggest a role in paraventricular nucleus and medullary development, while RNA expression also suggests that it has a role in the formation of the pituitary. *Snrpn* deficient mice suggest that the gene is important for proper functioning of the striatum. *MBII-85* is expressed in the superior olive, and may be important for its functioning.



Genes and transcripts



Single gene effects.

Mkrn3 may have multiple roles throughout development.

Sequence from the *MKRN3* coding region suggests that it functions as a transcription factor (Jong et al., 1999b). Analysis of the open reading frame suggests that there are up to five different zinc-finger motifs and that *MKRN3* may be involved in the regulation of multiple target molecules (Jong et al., 1999b). Based on its expression pattern, it may have different roles during various developmental and cell cycle stages. *MKRN3/Mkrn3* is expressed in undifferentiated, mitotic neurons; differentiated, non-dividing neurons, and meiotic and post meiotic germ cells (Jong et al., 1999a; Jong et al., 1999b).

Mkrn3 is a member of the Makorin gene family, which consists of four functional transcription factors, and several pseudogenes (Gray et al., 2000). *Mkrn1* is the ancestral gene for the family, and expressed primarily in differentiated neuronal cells, while my data shows that *Mkrn3* is expressed in undifferentiated, dividing ventricular cells. The expression of *Mkrn3* and Makorin proteins in general, at early stages of development may be important for specifying neural identity.

At E15.5, *Mkrn3* is more highly detected in the superior olive, abducens nucleus, and facial nucleus. As these structures are not known to contain actively dividing cells, the role of *Mkrn3* at E15.5 may differ from that at E12.5. One function of late embryonic stage *Mkrn3* may be to maintain the integrity of certain neuronal structures such as the abducens nucleus. Loss of the abducens nucleus may result in improper innervation of the lateral rectus muscle of the eye, which would present as strabismus. A hypoplastic or absent abducens nucleus is the proposed cause for the congenital strabismus seen in

Duane syndrome (Engle, 2002). Strabismus is one of the minor diagnostic criteria for PWS (Table 1-1), and was previously thought to be secondary to the general muscle hypotonia seen in patients (Butler et al., 2002). The expression pattern of *Mkrn3* suggests that the strabismus in PWS may be due to a primary defect in the abducens nucleus.

A role for Magel2 in the development and functions of the SCN and SON.

Magel2 shows a unique pattern of expression in the P19 cell induction system, it is expressed at high levels in untreated mouse embryonic cells and then is down-regulated after the addition of RA. Very few genes have been identified that are down-regulated in response to RA, and many, like the transcription factors, *Oct-3* and *Otx-2*, control lineage commitment (Bain et al., 1994; Niwa et al., 2000; Simeone et al., 1995)

RNA *in situ* analysis shows expression of *Magel2* in the non-dividing, differentiated mantle layer of the hypothalamus at E12.5. Overall expression in the mouse brain as determined by northern blot analysis shows highest levels from E15-E17. Taken together, the results from the P19 induction and the RNA *in situ* experiments suggest that *Magel2* is down-regulated in response to RA. *Magel2* may be expressed in differentiated cells that respond to the anterior-posterior RA gradient present in the developing embryo. RA levels are highest at the posterior end, and are important for anterior-posterior identity within the embryo (Maden, 1999). In addition to providing anterior-posterior information along the entire embryo, RA concentrations also provide patterning information within structures such as the developing eye. Transcriptional control in response to RA levels is known to be important for hindbrain development (Maden, 1999), and may also be important for development of the hypothalamus.

In mid and late gestation embryos, *Magel2* is most strongly detected in the SON and SCN. These two nuclei, along with the PVH, are the major sites for VP production. The neurons of the SCN can be further divided based on their expression of neuropeptides, and interestingly, *Magel2* shows a similar localization pattern as VP producing neurons. It is tempting to speculate that the loss of *MAGEL2* may disrupt production of VP from the SCN and SON. This may be related to preliminary reports of PWS patients with defects in VP processing (Gabreels et al., 1998). *MAGEL2* may also be responsible for the proper development of the SCN, as there has been a report of a PWS patient with increased cell numbers within the SCN (Swaab et al., 1987). Although PWS patients do not have a severe disruption in their circadian rhythm, like the inverted rhythm seen in Smith-Magenis syndrome (De Leersnyder et al., 2001), it may manifest as excessive daytime sleepiness and abnormal rapid eye movement sleep, and which are seen in some PWS patients.

Magel2 is the only gene that is expressed at high levels in both the SCN and SON, and at lower levels in the PVH. Many genes that are involved in the early development of the hypothalamic-pituitary axis are co-expressed in both the SON and PVH as the two structures are derived from the same precursor population and contain magnocellular neurons (Michaud, 2001). The expression of *Magel2* in early development is most similar to that seen for the Orthopedia (*Otp*) gene. *Otp* is a highly conserved homeobox-containing transcription factor that is expressed in the developing anterior hypothalamus, paraventricular, retrochiasmatic and ventral tuberal regions, which later develop into the anterior periventricular nucleus (aPV), PVH, SON and ARC (Acampora et al., 1999). *Otp* regulates both the proliferation and differentiation of the precursor cells. Similar to

Magel2, *Otp* is highly expressed in the anterior hypothalamus at E12.5. By E15.5, *Otp* expression is mainly detected in the PVH and SON, with no detectable expression in the SCN. *Otp* deficient mice are neonatal lethal and show decreased cell proliferation, as well as abnormalities in cell migration and terminal differentiation of both magnocellular and parvocellular neurons. Interestingly, although *Otp* is not expressed in the SCN, some *Otp* deficient mice showed increased VP expression in the SCN. *Otp* may affect SCN development indirectly through the regulation of downstream target genes. Very little is known about the development of the SCN, but *Magel2* is one of the only genes shown to be expressed throughout the development of the SCN. *Otp* could potentially influence SCN development through *Magel2*.

Magel2 expression is strongest in the dorsomedial SCN, which not only receives non-visual input from the hypothalamus, basal forebrain, limbic cortical areas, thalamus and brainstem; but also projects to other neurons throughout the brain. Based on its expression pattern, *Magel2*, is an excellent candidate gene for the obesity phenotype seen in PWS patients. Recent work has shown that there is an association between the SCN and feeding behavior and metabolism regulation through two major, but opposing mechanisms. Firstly, the SCN enforces the cessation of eating by releasing anorexigenic signals (Kalra et al., 1999). Evidence for this comes from rats that develop hyperphagia after the SCN is lesioned. The SCN is also involved in food intake and energy metabolism through controlling the release of orexigenic signals. The axons of the SCN extend to the VMN, DMN, LH and ARC, which are all components of the feeding pathway. Moderate levels of *Magel2* were also seen in the ARC and the PVH, a putative center of satiety. Circadian patterns have been demonstrated for the orexigenic

neuropeptides galanin, neuropeptide Y, and proopiomelanocortin. Cyclic levels of leptin in serum and adipocytes, as well as leptin receptor in the hypothalamus have also been reported (Kalra et al., 1999). Thus, abnormal development of the SCN could result in an imbalance in the anorexigenic and orexigenic signals in the brain.

Ndn is essential for terminal differentiation and survival of specific neurons.

Experiments on P19 cell cultures suggest that *Ndn* is most highly expressed in differentiated cells. This is supported by the RNA *in situ* data in Chapter 5, which shows expression in the mantle layer of E12.5 embryos. *Ndn* is expressed throughout the developing nervous system, and at low levels throughout the body. Unlike *Magel2*, expression of *Ndn* does not appear to be in response to the anterior-posterior RA gradient, but is expressed in most post-mitotic neurons throughout the embryo.

Mouse models have shown that the loss of *Ndn* results in a decrease in the number of OT and lutenizing hormone producing neurons in the PVH of the hypothalamus (Muscatelli et al., 2000). This is paralleled in studies of PWS patients that also show a decrease in OT neurons in the PVH. Interestingly, mice deficient for the transcription factor *Sim1* show a similar reduction in neurons in the PVH as well as obesity. A translocation through human *SIMI* has been shown to result in profound obesity (Holder et al., 2000). Human *SIMI* maps to chromosome 6q, and there are 5 case reports of interstitial deletions of this region that result in a PWS-like phenotype (Faivre et al., 2002). Patients with the 6q deletion have obesity, hypotonia, short extremities and developmental delay. However, excessive appetite is not always seen, while cardiac defects, neurological problems such as seizures and hearing loss are reported in some 6q patients, but are not features of PWS. The similarities between PWS and the 6q deletion

suggest that they may have defects in the same biochemical or developmental pathway. Necdin is a strong candidate for a downstream target of *Sim1*, as both the *Ndn* and the *Sim1* mice show similar histological abnormalities in the PVH. The possibility that *Ndn* and *Sim1* interact is supported by data that shows a binding site in the *Ndn* promoter for the Pas transcription factor family, of which *Sim1* is a member (Uetsuki et al., 1996).

In collaboration with the laboratory of Dr. John Greer, I have shown that the loss of mouse *Ndn* also results in the loss of and disorganization of motoneurons in the hindbrain. It has been shown that neurons that are deficient for necdin through antisense oligonucleotide silencing undergo apoptosis (Takazaki et al., 2002). Furthermore, silencing of *Ndn* in primary dorsal root ganglion cultures resulted in a decrease in the number of terminally differentiated neurons. Because *Ndn* knockout mice show selective neuronal loss, particularly in the OT and lutenizing neurons of the PVH and in the motoneurons of the hindbrain, *Ndn* appears to be essential for the proper development or maintenance of specific classes of neurons. *Ndn* may be one of the many transcription factors that are involved in defining the final identity of differentiating neurons. If differentiation is inhibited in *Sim1* expressing cells, the cells either die or assume a different fate (Michaud et al., 1998). A similar process may occur in the motoneurons of the brainstem of *Ndn* deficient mice. Although *Ndn* is expressed throughout the developing brain, there may be other genes in the Necdin/MAGE family that can compensate for loss of necdin in unaffected brain regions.

The Snurf/Snrpn transcript has multiple functions.

The *Snurf/Snrpn* locus is highly complex and has multiple functions. The transcript is heavily processed, and the resulting RNA species and protein products show

differing localization patterns. Firstly, the locus contains the IC, which is important for setting the imprint and maintaining the imprint in early development.

Secondly, the locus encodes two proteins, SNURF and SmN, the protein product of the *SNRPN* gene. The function of SNURF is unknown, however, the minimal defined region of the IC includes the promoter and the first exon of the SNURF protein (Gray et al., 1999a). Translation of SNURF is highest in prenatal and neonatal brain. Postnatally, the transcript is translated into the SmN protein, and functions as a splicesomal factor (Grimaldi et al., 1993; Schmauss et al., 1989). Presumably, the loss of an essential neuronal splicesomal factor would be lethal, and in PWS patients, the embryonic form, SmB/B', is up-regulated to compensate (Gray et al., 1999b). Recently, it has been shown that mice with a deletion spanning *Snrpn* have striatal imbalances in their levels of dopamine and dopamine metabolites (White et al., 2002). The authors noted that OCD is often associated with right striatal over-activity in humans. Interestingly, by RNA *in situ*, I found that mouse *Snrpn* showed strikingly high levels of expression in a region containing the dopaminergic bundles of the metencephalon. There are two possible models for *SNRPN* dysfunction. In the first model, SmN and SmB/B' have overlapping, but not identical functions, and thus the up-regulation of SmB/B' is not sufficient to fully compensate for the loss of *SNRPN*, resulting in OCD. Alternatively, SmB/B' and SmN are fully interchangeable, but up-regulation of SmB/B' may not be able to compensate for the loss of the downstream noncoding exons as well as the snoRNAs. As snoRNAs function to process target RNAs through sequence complementarity, it is intriguing to note that *HBII-52* has a 18 nucleotide complementarity to a segment of the serotonin 2C receptor mRNA (Cavaille et al., 2000). It has recently been proposed that OCD is a result

of disruption of both the serotonergic and dopaminergic systems (Stein and Ludik, 2000). Selective serotonin reuptake inhibitors are used most commonly to treat OCD, and have been effective for some of the behavioral problems seen in PWS patients. Thus, the behavioral problems seen in PWS patients may be due to the combined disruption of both serotonin and dopamine systems.

In addition to *HBII-52* mentioned above, the *SNURF/SNRPN* locus is also host to the snoRNAs *HBII-13*, *HBII-85*, *HBII-436*, *HBII-437*, *HBII-438A*, and *HBII-438B* (Cavaille et al., 2000; de los Santos et al., 2000; Meguro et al., 2001b; Runte et al., 2001). Although most of the snoRNAs show expression in multiple tissues by northern blot analysis, *HBII-52* is restricted to brain in mouse and humans, and *HBII-85* is expressed only in murine brain, but is more widespread in humans. There are parallels between *HBII-85* and *HBII-52* and a set of recently identified snoRNAs on human 14q32/mouse 12 that are also part of an imprinted gene cluster and processed from the noncoding exons of a larger transcript (Cavaille et al., 2002). Although the functions of the snoRNAs from the PWS region and 14q32 are not known, both are in regions associated with imprinted disorders. Maternal UPD of chromosome 14 is clinically distinct from Prader-Willi, although patients do have several features in common, including, hypotonia, short stature, poor sucking during the neonatal period, obesity, skill with jigsaw puzzles, and skin picking (Shimoda et al., 2002).

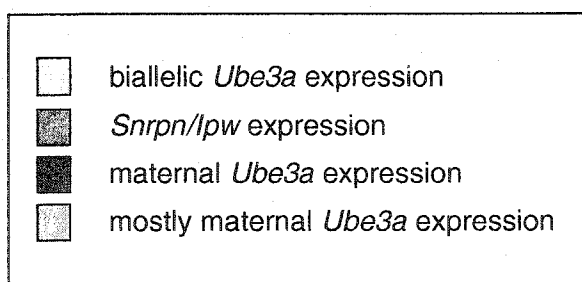
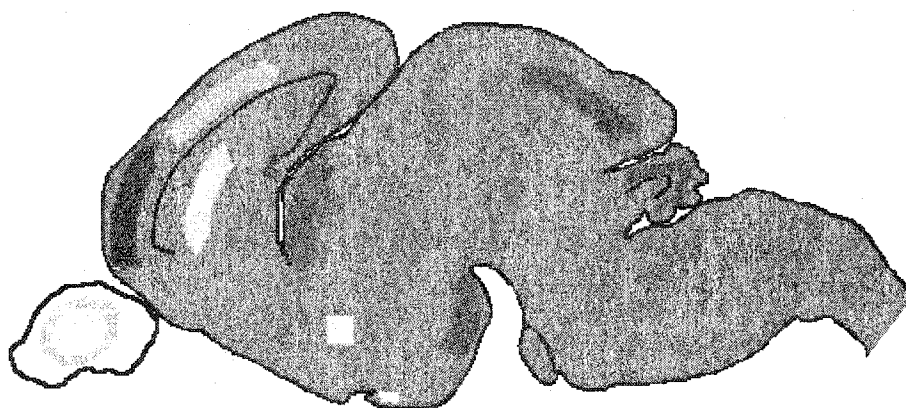
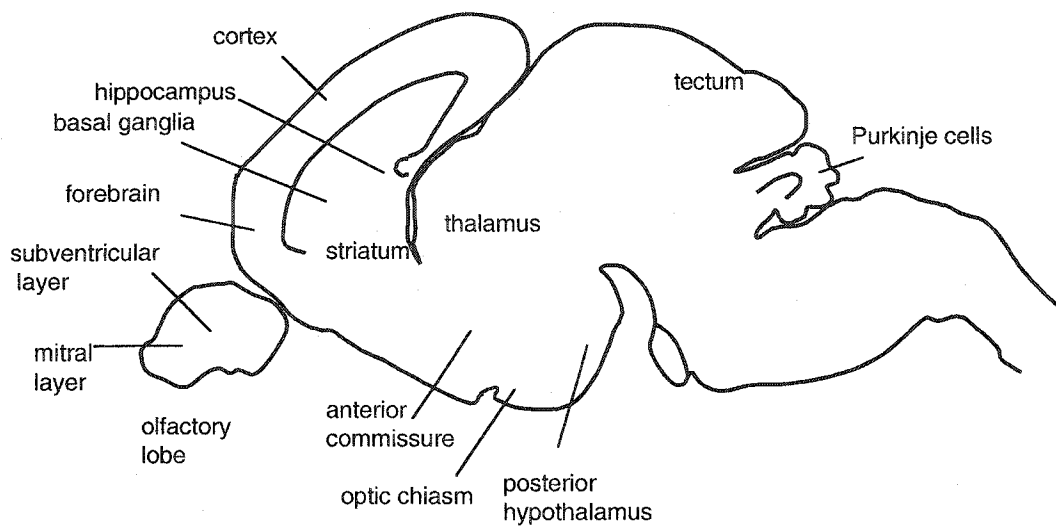
The *SNURF/SNRPN* transcript regulates the uniparental expression of *UBE3A* and most likely, *ATPIOC*, although this has yet to be shown. The EST SGC32610 was shown to be preferentially expressed from the maternal allele as described in Chapter 3. This result has been confirmed by another group that compared the expression levels of

control samples with PWS patient samples using a custom designed microarray chip containing transcripts in the 15q11-q13 region (Bittel et al., 2002). As there is no evidence for an independent mechanism for maternal expression, selective silencing of the paternal allele by the *SNURF/SNRPN* transcript may also regulate SGC32610. SGC32610 is located in the repeated clusters on either end of the 15q11-q13 domain, and regulation by *SNURF/SNRPN* would require that the transcript extends to the 15q13 boundary. SGC32610 is present in multiple copies because it is part of the repeated clusters flanking the deletion region, but it is not known if all of the copies are expressed. Expression from multiple copies, but paternal silencing of only the one at the distal end of the PWS/AS region could result in the pattern of preferential maternal expression seen in Chapter 3 and by Bittel *et. al.*

The *Snurf-Snrpn* transcript acts as an antisense RNA to silence the paternal allele of *Ube3a* in specific regions of the brain where it is expressed (Runte et al., 2001). Accordingly, the regions expressing *Snrpn* and/or *Ipw* have very similar expression patterns at E15.5 and, so that comparing the expression of these two RNAs, representing the antisense product, with the expression pattern of the protein coding, *Ube3a*, is important for understanding *Ube3a* imprinting regulation (summarized in Figure 6-2 and below).

Figure 6- 2. Comparison of transcripts from the *Snurf/Snrpn* and *Ube3a* promoters.

Comparing the expression patterns of probes from the *Snurf/Snrpn* locus with a *Ube3a* locus supports the model that an untranslated transcript driven by the *Snurf/Snrpn* promoter silences the maternal allele of *Ube3a* in specific neuronal structures. (Top) An outline of an E18.5 mouse brain with the major structures labeled. (Bottom) A compilation of data from RNA *in situ* expression studies on E15. 5 and E18.5 mice using probes for *Snrpn*, *Ipw* (see chapter 5 for details) and *Ube3a* by Albrecht, U., Sutcliffe, J. S., Cattanach, B. M., Beechey, C. V., Armstrong, D., Eichele, G. and Beaudet, A. L. (1997). Imprinted expression of the murine Angelman syndrome gene, *Ube3a*, in hippocampal and Purkinje neurons. *Nat Genet* **17**, 75-78.. Yellow neuronal structures: only *Ube3a* RNA was detected in wildtype mice and maternal UPD mice, but not *Snrpn* or *Ipw*. Blue neuronal structures: expression detected from *Snrpn* and *Ipw* only. Dark green regions: transcripts detected using *Snrpn*, *Ipw* and *Ube3a* probes in wildtype mice, as well as structures which show complete loss of *Ube3a* signal in paternal UPD mice. Light green regions: expression of *Ube3a* is decreased in maternal UPD mice while *Snrpn* and *Ipw* are strongly expressed.



Ube3a expression has been studied by RNA *in situ* hybridization in wildtype embryos and in mice with partial paternal uniparental disomy encompassing *Ube3a* (Albrecht et al., 1997). In wildtype E15.5 embryos, expression of *Ube3a* transcripts was detected in the basal ganglia region ventral to the lateral ventricle and the subventricular zone of the olfactory bulb (Albrecht et al., 1997). I did not detect significant levels of *Snrpn* or *Ipw* in these structures, suggesting that expression from *Ube3a* should be biallelic in these tissues. On the other hand, expression in the forebrain, thalamus, hypothalamus and central gray of the tectum was seen for all *Snrpn*-related probes, suggesting that the *Ube3a* probe would only be detecting expression from the maternal allele in these regions. In adult mice with partial paternal UPD, expression of *Ube3a* in Purkinje cells, hippocampal neurons and mitral cells of the olfactory bulb was markedly reduced presumably because of antisense regulation by the *Snurf/Snrpn* transcript on both alleles. The data from Albrecht, *et al.*, also suggests that the extent of silencing of the paternal allele of *Ube3a* by the *Snurf/Snrpn* transcript is variable between tissues. The hippocampus and cerebellum show a strong hybridization signal when an *Ube3a* probe is used to detect RNA in wildtype mice, while a greatly reduced signal is detected in the same tissues of paternal UPD mice (Albrecht et al., 1997). This suggests that the silencing of the paternal allele is complete in the hippocampus and cerebellum. In the olfactory bulb and cerebral cortex, the UPD mice show a slight reduction in signal intensity. This suggests that silencing of the paternal allele is incomplete or variable, possibly because only specific classes of neurons express the *Snurf/Snrpn* transcript, or that all of the neurons are capable of expressing *Snurf/Snrpn*, but that the extent of the transcript, or even the initiation of transcription is highly variable between individual

cells of this region. Finally, the anterior commissure and optic chiasm show high levels of *Ube3a* expression in both wildtype and mutant mice. My *in situ* data parallels these findings, with strong expression of *Snrpn*-related transcripts in the hippocampus, cerebellum, olfactory bulb, and cerebral cortex, while no signal was detected in the anterior commissure and optic chiasm. My results also support the model that monoallelic *Ube3a* expression is dependent on transcription from the *Snurf/Snrpn* locus (Runte et al., 2001). In tissues in which *Snurf/Snrpn* transcription is detected, but which do have expression from the *Ube3a* promoter, the transcript may have a function other than silencing the paternal allele of *Ube3a*. Transcription from the *Snurf/Snrpn* promoter may also be required for the functioning of the IC, production of the SNURF protein, or transcription of the snoRNAs.

Additive effects of losing multiple PWS genes.

The absence of any known mutations that disrupt a single PWS candidate gene suggests that several of these genes may interact in a synergistic manner, and that the loss of several genes would be required to produce a disease phenotype. Genes may have redundant functions, be members of the same developmental or biochemical pathway, or be involved in other types of synergistic interactions. The combined effect of losing several interacting genes would be greater than would be expected based on the effects of single gene mutations.

Several of the PWS genes may be involved in synergistic gene interactions. Individual knockouts of the *Mkrn3*, *Ndn*, and *Snrpn* do not produce an obvious phenotypic effect. *Ndn* is the only gene that has produced a physiological effect when absent. Thus, the development of PWS may require the loss of at least two of the

candidate genes simultaneously. Synergistic interactions among the PWS candidate genes could be investigated by constructing a series of transgenic mice with different combinations of deletions.

Mkrn3 and MBII-85 may be important for auditory discrimination

Several of the PWS genes are expressed in the superior olive. *Snrpn* and *Ipw* are highly expressed, while *Ndn* shows low levels of expression. *Mkrn3* and *MBII-85* are the only transcripts that are up-regulated in the superior olive. *Mkrn3* by itself, or in combination with another of the PWS transcripts such as *MBII-85*, may be important in the development of this structure, the loss of which may result in the defects in auditory discrimination and auditory information processing seen in PWS patients (Curfs et al., 1991; Gabel et al., 1986; Stauder et al., 2002).

Magel2 and Ndn may be important for development of hypothalamic-pituitary axis

Magel2 and *Ndn* are adjacent genes with high sequence similarities and overlapping expression patterns, suggesting that they may be the result of a gene duplication event with a subsequent divergence in function and expression. Alternatively, the genes could be derivatives of the same founder gene through separate retrotransposition events.

The terminal differentiation of neurons involves the expression of a series of transcription factors that progressively define neuronal identity. The transcription factors involved in the development of the PVH, SON and aPV are well characterized (Michaud, 2001). Two parallel pathways, controlled by *Sim1* and *Otp* are responsible for the proper development of the anterior hypothalamus. Evidence from *Ndn* deficient mice, as well as

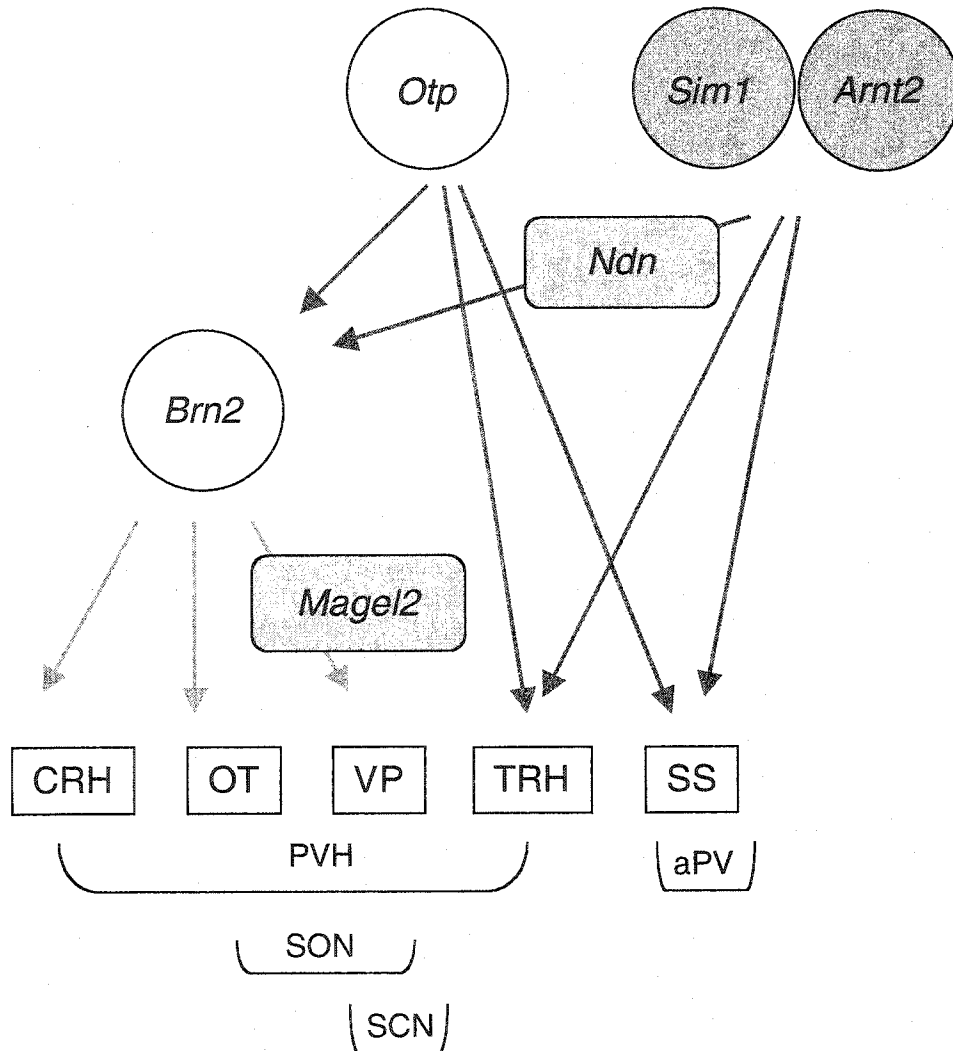
phenotypic similarities between PWS and *SIM1* patients implicate *Ndn* as a member of the *Sim1* pathway. Parallels in the RNA expression patterns between *Otp* and *Magel2* suggest that these two genes may also function in the same developmental pathway. Both *Sim1*, which acts with its heterodimerization partner, *Arnt2*, as well as *Otp* are required for the maintenance of the transcription factor *Brn2*. *Brn2* controls the differentiation of CRH, AVP and OT expressing neurons.

I hypothesize that both *Magel2* and *Ndn* may be involved in the proliferation and differentiation of the anterior hypothalamus through the *Sim1* and *Otp* transcription factor cascades (Figure 6-3). Both *Sim1* and *Otp* are key regulators in the anterior hypothalamic developmental pathway (Michaud, 2001), whereas *Magel2* and *Ndn* may be downstream targets in their respective activation cascades. Thus, the loss of either *Magel2* or *Ndn* individually may not be sufficient to completely disrupt hypothalamic development and recapitulate the *Sim1* deficiency phenotype. Conversely, a simultaneous loss of expression from both *Magel2* and *Ndn* may affect the development of the PVH, SON and SCN, and produce a more severe phenotype. Although both *Ndn* (Muscatelli et al., 2000) and *Sim1* deficient (Michaud et al., 2001) mice showed similar patterns of neuronal loss in the PVH, only the *Sim1* deficient mouse developed hyperphagia and obesity. Although none of the existing mouse models for PWS develop obesity, the mutant mice generally do not survive past the neonatal period (Cattanach et al., 1992; Gabriel et al., 1999; Yang et al., 1998). Mice which have a deletion spanning *Snrpn* and *Ube3a* did survive into adulthood, but did not develop obesity at 14 months of age (Tsai et al., 1999b), suggesting a locus for hyperphagia and obesity located upstream of *Snrpn*. Based on their expression patterns, *Magel2* and *Ndn* are both strong candidates for genes involved in the

hypothalamic control of food intake and metabolism. Despite the loss of PVH neurons, the loss of *Ndn* does not appear to have an effect on food intake or overall body weight in the mutants that do survive past the neonatal period. Thus the combined loss of *Magel2* and *Ndn* may be required for the development of obesity.

Figure 6- 3. *Magel2* and *Ndn* may act in transcription factor cascades controlling hypothalamic development.

Transcription factor cascade controlling the development of magnocellular and parvocellular neurons in the hypothalamus. *Sim1/Arnt2* and *Otp* control the development of neurons expressing corticotropin releasing hormone (CRH), oxytocin (OT), vasopressin (VP) by maintaining *Brn2* expression. *Sim1/Arnt2* also regulates the differentiation of neurons expressing thyrotropin-releasing hormone (TRH), and somatostatin (SS). The arrows represent the targets of the transcription factors. The cell types found in several hypothalamic nuclei are shown in brackets. *Magel2* is expressed in the SCN and SON in a pattern similar to that of VP, suggesting that it is downstream of both *Otp* and *Brn2*. *Ndn* may be a target of *Sim1/Arnt2*. *Ndn* deficient mice show a loss of OT neurons in the PVH, suggesting that *Ndn* may act along the pathway that defines those cell types. Figure adapted from Michaud, J. L. (2001). The developmental program of the hypothalamus and its disorders. *Clin Genet* 60, 255-263.



It has been proposed that the magnocellular neurons of the PVH and SON project to the posterior lobe of the pituitary where they release trophic factors for the pituicytes (Michaud et al., 1998). A loss of *Magel2* and *Ndn* may also affect the development of the pituitary. A pituitary defect has been proposed to be the cause of the GH deficiency seen in PWS patients (Miller et al., 1996). *Magel2* and *Ndn* expression was also detected in pituitary precursor cells by RNA *in situ* hybridization.

Directions for further study

The identification and characterization of any remaining genes in the PWS critical region is required before the pathophysiology of the syndrome can be understood.

Although there do not appear to be any additional genes that are expressed in the brain, peripherally expressed genes may be important in the health of PWS patients.

Furthermore, the identification of all genes along 15q11-q13 will be important for understanding how imprinting is regulated.

Although much work still needs to be done on all of the candidate genes and transcripts in the PWS region, I will mainly describe experiments relating to *Magel2* and *Ndn*, as they were the focus of my thesis. *Magel2* is the only gene known to show high levels of RNA expression in both the developing SCN and SON. Immunohistology with an antibody raised against *Magel2* will show whether protein localization correlates with RNA expression patterns. Immunohistological detection will also reveal whether *Magel2* protein levels also fluctuate in a circadian fashion.

To further understand the role of *Magel2* in the development of the SCN, it will be essential to develop mice that have a paternally inherited deletion of the gene. Mice can be examined for alterations in circadian rhythm, metabolism and VP processing. As

circadian rhythms are present before birth, it will be important to assess these mice pre- and postnatally.

The *Ndn* deficient mouse provides an *in vivo* system for dissecting the role of *Ndn* in neuronal survival and differentiation, and more specifically, its role in respiratory rhythmogenesis. It has been shown in cell culture experiments that the loss of *Ndn* results in a failure of neurons to terminally differentiate and to undergo apoptosis (Uetsuki et al., 1996). Whether this is the mechanism for the motoneuron loss seen in the *Ndn* mice remains to be determined. *Ndn* deficient embryos can be examined at various stages of development with histological stains that identify motoneurons, such as acetylcholinesterase; immunohistological markers that identify respiratory cells, such as neurokinin-1 receptor; and apoptosis assays, such as TUNEL labeling. Examining *Ndn* deficient mice throughout development will determine whether precursor cells are developing into motoneurons prior to undergoing apoptosis or whether differentiation along that cell lineage is blocked, and the stages during development that these events take place. The development of the mouse hindbrain is well understood, and the expression patterns of many transcription factors involved in specifying hindbrain identity are well characterized. Transcription factors that define specific cell populations can be used to follow the development of motoneurons in a *Ndn* deficient background. Downstream targets of *Ndn* can be identified by comparing RNA from hindbrains of wildtype and *Ndn* deficient littermates on microchip cDNA arrays. Genes identified from a microchip survey could be examined in further detail using additional molecular techniques such as RNA *in situ* hybridization on a *Ndn* deficient background.

The hypothesis that both *Magel2* and *Ndn* are both involved in the development of the anterior hypothalamus can be investigated with a more thorough expression analysis in the embryo. Co-localization of expression with genes involved in the development of the PVH and SON, such as *Sim1*, *Arnt2*, *Otp*, *Brn2/Pou3* (Michaud, 2001), will provide molecular markers to further identify the cell lineages that express *Magel2* and *Ndn*. Mice deficient in *Sim1*, *Otp* and *Brn2* have been constructed and the analysis expression of both *Magel2* and *Ndn* in these mice will be of interest (Acampora et al., 1999; Michaud et al., 1998; Nakai et al., 1995; Schonemann et al., 1995). Comparing the phenotypes of *Magel2* deficient mice with *Sim1*, *Otp* and *Brn2* mice will provide insights into the role of *Magel2* in hypothalamic development.

Possible synergistic interactions between *Magel2* and *Ndn* could be investigated through the construction of a mouse that is deficient in both genes. The initial paper describing the construction of the *Ndn* deficient line showed that the perinatal phenotype was less penetrant in a first generation interspecies cross between FVB mice and C57Bl/6 mice (Gerard et al., 1999). As the *Ndn* phenotype is influenced by genetic modifiers, mice deficient for both *Magel2* and *Ndn* will also need to be evaluated in several mouse strains.

As the hyperphagia, obesity, developmental delay and behavioral problems associated with PWS are most likely due to prenatal errors in brain development, further research into the function of the PWS candidate genes may not provide a cure for PWS. However, research will greatly enhance the understanding of the biological pathways that are affected in the syndrome, and provide the basis for more effective therapies for patients. Although GH therapy is currently the most effective treatment for the short

stature and hypotonia associated with PWS, it has not been as successful in regulating the hyperphagia, metabolism or behavioral problems. Furthermore, knowledge gained from studying PWS genes will provide a greater understanding of developmental neurobiology. PWS genes are involved in metabolism, neuronal survival, respiration and circadian rhythms, and thus have clinical significance outside of the syndrome. An understanding of the pathways that are affected in PWS will enable future investigators to design therapies that specifically target these systems.

References

- Acampora, D., Postiglione, M. P., Avantaggiato, V., Di Bonito, M., Vaccarino, F. M., Michaud, J. and Simeone, A.** (1999). Progressive impairment of developing neuroendocrine cell lineages in the hypothalamus of mice lacking the Orthopedia gene. *Genes Dev* **13**, 2787-2800.
- Aizawa, T., Maruyama, K., Kondo, H. and Yoshikawa, K.** (1992). Expression of neccdin, an embryonal carcinoma-derived nuclear protein, in developing mouse brain. *Brain Res Dev Brain Res* **68**, 265-274.
- Albrecht, U., Sutcliffe, J. S., Cattanaach, B. M., Beechey, C. V., Armstrong, D., Eichele, G. and Beaudet, A. L.** (1997). Imprinted expression of the murine Angelman syndrome gene, Ube3a, in hippocampal and Purkinje neurons. *Nat Genet* **17**, 75-78.
- Amos-Landgraf, J. M., Ji, Y., Gottlieb, W., Depinet, T., Wandstrat, A. E., Cassidy, S. B., Driscoll, D. J., Rogan, P. K., Schwartz, S. and Nicholls, R. D.** (1999). Chromosome breakage in the Prader-Willi and Angelman syndromes involves recombination between large, transcribed repeats at proximal and distal breakpoints. *Am J Hum Genet* **65**, 370-386.
- Arens, R., Gozal, D., Omlin, K. J., Livingston, F. R., Liu, J., Keens, T. G. and Ward, S. L.** (1994). Hypoxic and hypercapnic ventilatory responses in Prader-Willi syndrome. *J Appl Physiol* **77**, 2224-2230.
- Bain, G., Ray, W. J., Yao, M. and Gottlieb, D. I.** (1994). From embryonal carcinoma cells to neurons: the P19 pathway. *Bioessays* **16**, 343-348.
- Barker, P. A. and Salehi, A.** (2002). The MAGE proteins: emerging roles in cell cycle progression, apoptosis, and neurogenetic disease. *J Neurosci Res* **67**, 705-712.
- Barlow, D. P.** (1997). Competition--a common motif for the imprinting mechanism? *Embo J* **16**, 6899-6905.
- Barton, S. C., Surani, M. A. and Norris, M. L.** (1984). Role of paternal and maternal genomes in mouse development. *Nature* **311**, 374-376.
- Batterham, R. L., Cowley, M. A., Small, C. J., Herzog, H., Cohen, M. A., Dakin, C. L., Wren, A. M., Brynes, A. E., Low, M. J., Ghatei, M. A. et al.** (2002). Gut hormone PYY(3-36) physiologically inhibits food intake. *Nature* **418**, 650-654.
- Bi, W., Yan, J., Stankiewicz, P., Park, S. S., Walz, K., Boerkoel, C. F., Potocki, L., Shaffer, L. G., Devriendt, K., Nowaczyk, M. J. et al.** (2002). Genes in a refined Smith-Magenis syndrome critical deletion interval on chromosome 17p11.2 and the syntenic region of the mouse. *Genome Res* **12**, 713-728.

- Bielinska, B., Blaydes, S. M., Buiting, K., Yang, T., Krajewska-Walasek, M., Horsthemke, B. and Brannan, C. I. (2000).** De novo deletions of SNRPN exon 1 in early human and mouse embryos result in a paternal to maternal imprint switch. *Nat Genet* **25**, 74-78.
- Bittel, D. C., Kibiryeve, N., Talebizadeh, Z. and Butler, M. G. (2002).** Microarray analysis of gene/transcript expression in Prader-Willi syndrome: Deletion versus UPD. *Am. J. Hum. Genet.* **71**, A1884.
- Boccaccio, I., Glatt-Deeley, H., Watrin, F., Roeckel, N., Lalande, M. and Muscatelli, F. (1999).** The human MAGEL2 gene and its mouse homologue are paternally expressed and mapped to the Prader-Willi region. *Hum Mol Genet* **8**, 2497-2505.
- Boguski, M. S. and Schuler, G. D. (1995).** ESTablishing a human transcript map. *Nat Genet* **10**, 369-371.
- Brandt, B. R. and Rosen, I. (1998).** Impaired peripheral somatosensory function in children with Prader-Willi syndrome. *Neuropediatrics* **29**, 124-126.
- Bressler, J., Tsai, T. F., Wu, M. Y., Tsai, S. F., Ramirez, M. A., Armstrong, D. and Beaudet, A. L. (2001).** The SNRPN promoter is not required for genomic imprinting of the Prader-Willi/Angelman domain in mice. *Nat Genet* **28**, 232-240.
- Brown, C. J., Hendrich, B. D., Rupert, J. L., Lafreniere, R. G., Xing, Y., Lawrence, J. and Willard, H. F. (1992).** The human XIST gene: analysis of a 17 kb inactive X-specific RNA that contains conserved repeats and is highly localized within the nucleus. *Cell* **71**, 527-542.
- Budarf, M. L. and Emanuel, B. S. (1997).** Progress in the autosomal segmental aneusomy syndromes (SASs): single or multi-locus disorders? *Hum Mol Genet* **6**, 1657-1665.
- Buiting, K., Gross, S., Lich, C., Gillessen-Kaesbach, G., El-Maarri, O. and Horsthemke, B. (2003).** Epimutations in Prader-Willi and Angelman Syndromes: A Molecular Study of 136 Patients with an Imprinting Defect. *Am J Hum Genet* **72**, 3.
- Buiting, K., Saitoh, S., Gross, S., Dittrich, B., Schwartz, S., Nicholls, R. D. and Horsthemke, B. (1995).** Inherited microdeletions in the Angelman and Prader-Willi syndromes define an imprinting centre on human chromosome 15. *Nat Genet* **9**, 395-400.
- Burge, C. and Karlin, S. (1997).** Prediction of complete gene structures in human genomic DNA. *J Mol Biol* **268**, 78-94.

- Burger, J., Horn, D., Tonnie, H., Neitzel, H. and Reis, A.** (2002). Familial interstitial 570 kbp deletion of the UBE3A gene region causing Angelman syndrome but not Prader-Willi syndrome. *Am J Med Genet* **111**, 233-237.
- Burman, P., Ritzen, E. M. and Lindgren, A. C.** (2001). Endocrine dysfunction in Prader-Willi syndrome: a review with special reference to GH. *Endocr Rev* **22**, 787-799.
- Butler, J. V., Whittington, J. E., Holland, A. J., Boer, H., Clarke, D. and Webb, T.** (2002). Prevalence of, and risk factors for, physical ill-health in people with Prader-Willi syndrome: a population-based study. *Dev Med Child Neurol* **44**, 248-255.
- Butler, M. G., Meaney, F. J. and Palmer, C. G.** (1986). Clinical and cytogenetic survey of 39 individuals with Prader-Labhart-Willi syndrome. *Am J Med Genet* **23**, 793-809.
- Carrel, A. L., Myers, S. E., Whitman, B. Y. and Allen, D. B.** (2002). Benefits of long-term GH therapy in Prader-Willi syndrome: a 4-year study. *J Clin Endocrinol Metab* **87**, 1581-1585.
- Cassidy, S. B.** (1997). Prader-Willi syndrome. *J Med Genet* **34**, 917-923.
- Cassidy, S. B., Dykens, E. and Williams, C. A.** (2000). Prader-Willi and Angelman syndromes: sister imprinted disorders. *Am J Med Genet* **97**, 136-146.
- Cattanach, B. M., Barr, J. A., Evans, E. P., Burtenshaw, M., Beechey, C. V., Leff, S. E., Brannan, C. I., Copeland, N. G., Jenkins, N. A. and Jones, J.** (1992). A candidate mouse model for Prader-Willi syndrome which shows an absence of Snrpn expression. *Nat Genet* **2**, 270-274.
- Cavaille, J., Buiting, K., Kieffmann, M., Lalande, M., Brannan, C. I., Horsthemke, B., Bachelier, J. P., Brosius, J. and Huttenhofer, A.** (2000). Identification of brain-specific and imprinted small nucleolar RNA genes exhibiting an unusual genomic organization. *Proc Natl Acad Sci U S A* **97**, 14311-14316.
- Cavaille, J., Seitz, H., Paulsen, M., Ferguson-Smith, A. C. and Bachelier, J. P.** (2002). Identification of tandemly-repeated C/D snoRNA genes at the imprinted human 14q32 domain reminiscent of those at the Prader-Willi/Angelman syndrome region. *Hum Mol Genet* **11**, 1527-1538.
- Chai, J. H., Locke, D. P., Ohta, T., Greally, J. M. and Nicholls, R. D.** (2001). Retrotransposed genes such as Frat3 in the mouse Chromosome 7C Prader-Willi syndrome region acquire the imprinted status of their insertion site. *Mamm Genome* **12**, 813-821.

- Chaillet, J. R., Knoll, J. H., Horsthemke, B. and Lalande, M.** (1991). The syntenic relationship between the critical deletion region for the Prader-Willi/Angelman syndromes and proximal mouse chromosome 7. *Genomics* **11**, 773-776.
- Chamberlain, S. J. and Brannan, C. I.** (2001). The Prader-Willi syndrome imprinting center activates the paternally expressed murine Ube3a antisense transcript but represses paternal Ube3a. *Genomics* **73**, 316-322.
- Champagnat, J. and Fortin, G.** (1997). Primordial respiratory-like rhythm generation in the vertebrate embryo. *Trends Neurosci* **20**, 119-124.
- Choi, S. and Dallman, M. F.** (1999). Hypothalamic obesity: multiple routes mediated by loss of function in medial cell groups. *Endocrinology* **140**, 4081-4088.
- Chomez, P., De Backer, O., Bertrand, M., De Plaen, E., Boon, T. and Lucas, S.** (2001). An overview of the MAGE gene family with the identification of all human members of the family. *Cancer Res* **61**, 5544-5551.
- Christian, S. L., Bhatt, N. K., Martin, S. A., Sutcliffe, J. S., Kubota, T., Huang, B., Mutirangura, A., Chinault, A. C., Beaudet, A. L. and Ledbetter, D. H.** (1998). Integrated YAC contig map of the Prader-Willi/Angelman region on chromosome 15q11-q13 with average STS spacing of 35 kb. *Genome Res* **8**, 146-157.
- Christian, S. L., Fantes, J. A., Mewborn, S. K., Huang, B. and Ledbetter, D. H.** (1999). Large genomic duplicons map to sites of instability in the Prader-Willi/Angelman syndrome chromosome region (15q11-q13). *Hum Mol Genet* **8**, 1025-1037.
- Christian, S. L., Robinson, W. P., Huang, B., Mutirangura, A., Line, M. R., Nakao, M., Surti, U., Chakravarti, A. and Ledbetter, D. H.** (1995). Molecular characterization of two proximal deletion breakpoint regions in both Prader-Willi and Angelman syndrome patients. *Am J Hum Genet* **57**, 40-48.
- Clift, S., Dahlitz, M. and Parkes, J. D.** (1994). Sleep apnoea in the Prader-Willi syndrome. *J Sleep Res* **3**, 121-126.
- Conroy, J. M., Grebe, T. A., Becker, L. A., Tsuchiya, K., Nicholls, R. D., Buiting, K., Horsthemke, B., Cassidy, S. B. and Schwartz, S.** (1997). Balanced translocation 46,XY,t(2;15)(q37.2;q11.2) associated with atypical Prader-Willi syndrome. *Am J Hum Genet* **61**, 388-394.
- Constancia, M., Pickard, B., Kelsey, G. and Reik, W.** (1998). Imprinting mechanisms. *Genome Res* **8**, 881-900.
- Cordes, S. P.** (2001). Molecular genetics of cranial nerve development in mouse. *Nat Rev Neurosci* **2**, 611-623.

- Costeff, H., Holm, V. A., Ruvalcaba, R. and Shaver, J. (1990). Growth hormone secretion in Prader-Willi syndrome. *Acta Paediatr Scand* **79**, 1059-1062.
- Cowley MA, Smith RG, Diano S, Tschop M, Pronchuk N, Grove KL, Strasburger CJ, Bidlingmaier M, Esterman M, Heiman ML, Garcia-Segura LM, Nillni EA, Mendez P, Low MJ, Sotonyi P, Friedman JM, Liu H, Pinto S, Colmers WF, Cone RD, Horvath TL. (2003). The distribution and mechanism of action of ghrelin in the CNS demonstrates a novel hypothalamic circuit regulating energy homeostasis. *Neuron* **37**, 649-661.
- Cummings, D. E., Clement, K., Purnell, J. Q., Vaisse, C., Foster, K. E., Frayo, R. S., Schwartz, M. W., Basdevant, A. and Weigle, D. S. (2002). Elevated plasma ghrelin levels in Prader Willi syndrome. *Nat Med* **8**, 643-644.
- Cummings, D. E., Purnell, J. Q., Frayo, R. S., Schmidova, K., Wisse, B. E. and Weigle, D. S. (2001). A preprandial rise in plasma ghrelin levels suggests a role in meal initiation in humans. *Diabetes* **50**, 1714-1719.
- Curfs, L. M., Wieggers, A. M., Sommers, J. R., Borghgraef, M. and Fryns, J. P. (1991). Strengths and weaknesses in the cognitive profile of youngsters with Prader-Willi syndrome. *Clin Genet* **40**, 430-434.
- Dao, D., Frank, D., Qian, N., O'Keefe, D., Vosatka, R. J., Walsh, C. P. and Tycko, B. (1998). IMPT1, an imprinted gene similar to polyspecific transporter and multi-drug resistance genes. *Hum Mol Genet* **7**, 597-608.
- Dattani, M. T. and Robinson, I. C. (2000). The molecular basis for developmental disorders of the pituitary gland in man. *Clin Genet* **57**, 337-346.
- De Leersnyder, H., De Blois, M. C., Claustrat, B., Romana, S., Albrecht, U., Von Kleist-Retzow, J. C., Delobel, B., Viot, G., Lyonnet, S., Vekemans, M. et al. (2001). Inversion of the circadian rhythm of melatonin in the Smith-Magenis syndrome. *J Pediatr* **139**, 111-116.
- de los Santos, T., Schweizer, J., Rees, C. A. and Francke, U. (2000). Small evolutionarily conserved RNA, resembling C/D box small nucleolar RNA, is transcribed from PWCR1, a novel imprinted gene in the Prader-Willi deletion region, which is highly expressed in brain. *Am J Hum Genet* **67**, 1067-1082.
- De Plaen, E., Arden, K., Traversari, C., Gaforio, J. J., Szikora, J. P., De Smet, C., Brasseur, F., van der Bruggen, P., Lethe, B., Lurquin, C. et al. (1994). Structure, chromosomal localization, and expression of 12 genes of the MAGE family. *Immunogenetics* **40**, 360-369.

- Deloukas, P., Schuler, G. D., Gyapay, G., Beasley, E. M., Soderlund, C., Rodriguez-Tome, P., Hui, L., Matise, T. C., McKusick, K. B., Beckmann, J. S. et al.** (1998). A physical map of 30,000 human genes. *Science* **282**, 744-746.
- DelParigi, A., Tschop, M., Heiman, M. L., Salbe, A. D., Vozarova, B., Sell, S. M., Bunt, J. C. and Tataranni, P. A.** (2002). High circulating ghrelin: a potential cause for hyperphagia and obesity in prader-willi syndrome. *J Clin Endocrinol Metab* **87**, 5461-5464.
- Descheemaeker, M. J., Vogels, A., Govers, V., Borghgraef, M., Willekens, D., Swillen, A., Verhoeven, W. and Fryns, J. P.** (2002). Prader-Willi syndrome: new insights in the behavioural and psychiatric spectrum. *J Intellect Disabil Res* **46**, 41-50.
- Dhar, M., Webb, L. S., Smith, L., Hauser, L., Johnson, D. and West, D. B.** (2000). A novel ATPase on mouse chromosome 7 is a candidate gene for increased body fat. *Physiol Genomics* **4**, 93-100.
- Diez del Corral, R. and Storey, K. G.** (2001). Markers in vertebrate neurogenesis. *Nat Rev Neurosci* **2**, 835-839.
- DiMario, F. J., Jr., Dunham, B., Burleson, J. A., Moskovitz, J. and Cassidy, S. B.** (1994). An evaluation of autonomic nervous system function in patients with Prader-Willi syndrome. *Pediatrics* **93**, 76-81.
- Dimitropoulos, A., Feurer, I. D., Roof, E., Stone, W., Butler, M. G., Sutcliffe, J. and Thompson, T.** (2000). Appetitive behavior, compulsivity, and neurochemistry in Prader-Willi syndrome. *Ment Retard Dev Disabil Res Rev* **6**, 125-130.
- Dittrich, B., Buiting, K., Korn, B., Rickard, S., Buxton, J., Saitoh, S., Nicholls, R. D., Poustka, A., Winterpacht, A., Zabel, B. et al.** (1996). Imprint switching on human chromosome 15 may involve alternative transcripts of the SNRPN gene. *Nat Genet* **14**, 163-170.
- Donnai, D. and Karmiloff-Smith, A.** (2000). Williams syndrome: from genotype through to the cognitive phenotype. *Am J Med Genet* **97**, 164-171.
- Dykens, E. M., Leckman, J. F. and Cassidy, S. B.** (1996). Obsessions and compulsions in Prader-Willi syndrome. *J Child Psychol Psychiatry* **37**, 995-1002.
- Dyomin, V. G., Rao, P. H., Dalla-Favera, R. and Chaganti, R. S.** (1997). BCL8, a novel gene involved in translocations affecting band 15q11-13 in diffuse large-cell lymphoma. *Proc Natl Acad Sci U S A* **94**, 5728-5732.

- Edgar, D. M., Dement, W. C. and Fuller, C. A.** (1993). Effect of SCN lesions on sleep in squirrel monkeys: evidence for opponent processes in sleep-wake regulation. *J Neurosci* **13**, 1065-1079.
- Eiholzer, U., l'Allemand, D., van der Sluis, I., Steinert, H., Gasser, T. and Ellis, K.** (2000). Body composition abnormalities in children with Prader-Willi syndrome and long-term effects of growth hormone therapy. *Horm Res* **53**, 200-206.
- El-Maarri, O., Buiting, K., Peery, E. G., Kroisel, P. M., Balaban, B., Wagner, K., Urman, B., Heyd, J., Lich, C., Brannan, C. I. et al.** (2001). Maternal methylation imprints on human chromosome 15 are established during or after fertilization. *Nat Genet* **27**, 341-344.
- Elmqvist, J. K., Maratos-Flier, E., Saper, C. B. and Flier, J. S.** (1998). Unraveling the central nervous system pathways underlying responses to leptin. *Nat Neurosci* **1**, 445-450.
- Engle, E. C.** (2002). Applications of molecular genetics to the understanding of congenital ocular motility disorders. *Ann N Y Acad Sci* **956**, 55-63.
- Ewart, A. K., Morris, C. A., Atkinson, D., Jin, W., Sternes, K., Spallone, P., Stock, A. D., Leppert, M. and Keating, M. T.** (1993). Hemizygoty at the elastin locus in a developmental disorder, Williams syndrome. *Nat Genet* **5**, 11-16.
- Ewing, B. and Green, P.** (2000). Analysis of expressed sequence tags indicates 35,000 human genes. *Nat Genet* **25**, 232-234.
- Faivre, L., Cormier-Daire, V., Lapierre, J. M., Colleaux, L., Jacquemont, S., Genevieve, D., Saunier, P., Munnich, A., Turleau, C., Romana, S. et al.** (2002). Deletion of the SIM1 gene (6q16.2) in a patient with a Prader-Willi-like phenotype. *J Med Genet* **39**, 594-596.
- Farber, C., Dittrich, B., Buiting, K. and Horsthemke, B.** (1999). The chromosome 15 imprinting centre (IC) region has undergone multiple duplication events and contains an upstream exon of SNRPN that is deleted in all Angelman syndrome patients with an IC microdeletion. *Hum Mol Genet* **8**, 337-343.
- Farber, C., Gross, S., Neesen, J., Buiting, K. and Horsthemke, B.** (2000). Identification of a testis-specific gene (C15orf2) in the Prader-Willi syndrome region on chromosome 15. *Genomics* **65**, 174-183.
- Ferguson-Smith, A. C. and Surani, M. A.** (2001). Imprinting and the epigenetic asymmetry between parental genomes. *Science* **293**, 1086-1089.
- Fields, C., Adams, M. D., White, O. and Venter, J. C.** (1994). How many genes in the human genome? *Nat Genet* **7**, 345-346.

- Fougerousse, F., Bullen, P., Herasse, M., Lindsay, S., Richard, I., Wilson, D., Suel, L., Durand, M., Robson, S., Abitbol, M. et al. (2000).** Human-mouse differences in the embryonic expression patterns of developmental control genes and disease genes. *Hum Mol Genet* **9**, 165-173.
- Francke, U. (1999).** Williams-Beuren syndrome: genes and mechanisms. *Hum Mol Genet* **8**, 1947-1954.
- Frangiskakis, J. M., Ewart, A. K., Morris, C. A., Mervis, C. B., Bertrand, J., Robinson, B. F., Klein, B. P., Ensing, G. J., Everett, L. A., Green, E. D. et al. (1996).** LIM-kinase1 hemizygoty implicated in impaired visuospatial constructive cognition. *Cell* **86**, 59-69.
- Gabel, S., Tarter, R. E., Gavalier, J., Golden, W. L., Hegedus, A. M. and Maier, B. (1986).** Neuropsychological capacity of Prader-Willi children: general and specific aspects of impairment. *Appl Res Ment Retard* **7**, 459-466.
- Gabreels, B. A., Swaab, D. F., de Kleijn, D. P., Seidah, N. G., Van de Loo, J. W., Van de Ven, W. J., Martens, G. J. and van Leeuwen, F. W. (1998).** Attenuation of the polypeptide 7B2, prohormone convertase PC2, and vasopressin in the hypothalamus of some Prader-Willi patients: indications for a processing defect. *J Clin Endocrinol Metab* **83**, 591-599.
- Gabreels, B. A., Swaab, D. F., Seidah, N. G., van Duijnhoven, H. L., Martens, G. J. and van Leeuwen, F. W. (1994).** Differential expression of the neuroendocrine polypeptide 7B2 in hypothalamus of Prader-(Labhart)-Willi syndrome patients. *Brain Res* **657**, 281-293.
- Gabriel, J. M., Higgins, M. J., Gebuhr, T. C., Shows, T. B., Saitoh, S. and Nicholls, R. D. (1998).** A model system to study genomic imprinting of human genes. *Proc Natl Acad Sci U S A* **95**, 14857-14862.
- Gabriel, J. M., Merchant, M., Ohta, T., Ji, Y., Caldwell, R. G., Ramsey, M. J., Tucker, J. D., Longnecker, R. and Nicholls, R. D. (1999).** A transgene insertion creating a heritable chromosome deletion mouse model of Prader-Willi and Angelman syndromes. *Proc Natl Acad Sci U S A* **96**, 9258-9263.
- Gallagher, R. C., Pils, B., Albalwi, M. and Francke, U. (2002).** Evidence for the Role of PWCR1/HBII-85 C/D Box Small Nucleolar RNAs in Prader-Willi Syndrome. *Am J Hum Genet* **71**, 3.
- Gerard, M., Hernandez, L., Wevrick, R. and Stewart, C. L. (1999).** Disruption of the mouse necdin gene results in early post-natal lethality. *Nat Genet* **23**, 199-202.

- Gerhold, D. and Caskey, C. T.** (1996). It's the genes! EST access to human genome content. *Bioessays* **18**, 973-981.
- Gozal, D., Arens, R., Omlin, K. J., Ward, S. L. and Keens, T. G.** (1994). Absent peripheral chemosensitivity in Prader-Willi syndrome. *J Appl Physiol* **77**, 2231-2236.
- Graham, D. A., Abbott, G. D., Suzuki, Y., Suzuki, H. and Shimoda, S.** (1992). Neuroendocrine protein 7B2 in Prader-Willi syndrome. *Aust N Z J Med* **22**, 455-457.
- Gray, T. A., Hernandez, L., Carey, A. H., Schaldach, M. A., Smithwick, M. J., Rus, K., Marshall Graves, J. A., Stewart, C. L. and Nicholls, R. D.** (2000). The ancient source of a distinct gene family encoding proteins featuring RING and C(3)H zinc-finger motifs with abundant expression in developing brain and nervous system. *Genomics* **66**, 76-86.
- Gray, T. A., Saitoh, S. and Nicholls, R. D.** (1999a). An imprinted, mammalian bicistronic transcript encodes two independent proteins. *Proc Natl Acad Sci U S A* **96**, 5616-5621.
- Gray, T. A., Smithwick, M. J., Schaldach, M. A., Martone, D. L., Graves, J. A., McCarrey, J. R. and Nicholls, R. D.** (1999b). Concerted regulation and molecular evolution of the duplicated SNRPN/B and SNRPN loci. *Nucleic Acids Res* **27**, 4577-4584.
- Graybiel, A. M. and Rauch, S. L.** (2000). Toward a neurobiology of obsessive-compulsive disorder. *Neuron* **28**, 343-347.
- Greer, J. M. and Capecchi, M. R.** (2002). Hoxb8 is required for normal grooming behavior in mice. *Neuron* **33**, 23-34.
- Greger, V., Woolf, E. and Lalonde, M.** (1993). Cloning of the breakpoints of a submicroscopic deletion in an Angelman syndrome patient. *Hum Mol Genet* **2**, 921-924.
- Grimaldi, K., Horn, D. A., Hudson, L. D., Terenghi, G., Barton, P., Polak, J. M. and Latchman, D. S.** (1993). Expression of the SmN splicing protein is developmentally regulated in the rodent brain but not in the rodent heart. *Dev Biol* **156**, 319-323.
- Gunay-Aygun, M., Schwartz, S., Heeger, S., O'Riordan, M. A. and Cassidy, S. B.** (2001). The changing purpose of Prader-Willi syndrome clinical diagnostic criteria and proposed revised criteria. *Pediatrics* **108**, E92.

- Hall, B. D. and Smith, D. W.** (1972). Prader-Willi syndrome. A resume of 32 cases including an instance of affected first cousins, one of whom is of normal stature and intelligence. *J Pediatr* **81**, 286-293.
- Hamabe, J., Kuroki, Y., Imaizumi, K., Sugimoto, T., Fukushima, Y., Yamaguchi, A., Izumikawa, Y. and Niikawa, N.** (1991). DNA deletion and its parental origin in Angelman syndrome patients. *Am J Med Genet* **41**, 64-68.
- Haqq, A. M., Farooqi, I. S., O'Rahilly, S., Stadler, D. D., Rosenfeld, R. G., Pratt, K. L., LaFranchi, S. H. and Purnell, J. Q.** (2003). Serum ghrelin levels are inversely correlated with body mass index, age, and insulin concentrations in normal children and are markedly increased in prader-willi syndrome. *J Clin Endocrinol Metab* **88**, 174-178.
- Harmer, S. L., Panda, S. and Kay, S. A.** (2001). Molecular bases of circadian rhythms. *Annu Rev Cell Dev Biol* **17**, 215-253.
- Hart, P. S.** (1998). Salivary abnormalities in Prader-Willi syndrome. *Ann N Y Acad Sci* **842**, 125-131.
- Hayashi, Y., Matsuyama, K., Takagi, K., Sugiura, H. and Yoshikawa, K.** (1995). Arrest of cell growth by necdin, a nuclear protein expressed in postmitotic neurons. *Biochem Biophys Res Commun* **213**, 317-324.
- Hellings, J. A. and Warnock, J. K.** (1994). Self-injurious behavior and serotonin in Prader-Willi syndrome. *Psychopharmacol Bull* **30**, 245-250.
- Hertz, G., Cataletto, M., Feinsilver, S. H. and Angulo, M.** (1995). Developmental trends of sleep-disordered breathing in Prader-Willi syndrome: the role of obesity. *Am J Med Genet* **56**, 188-190.
- Herzing, L. B., Kim, S. J., Cook, E. H., Jr. and Ledbetter, D. H.** (2001). The human aminophospholipid-transporting ATPase gene ATP10C maps adjacent to UBE3A and exhibits similar imprinted expression. *Am J Hum Genet* **68**, 1501-1505.
- Hime, G. R., Abud, H. E., Garner, B., Harris, K. L. and Robertson, H.** (2001). Dynamic expression of alternate splice forms of D-cbl during embryogenesis. *Mech Dev* **102**, 235-238.
- Hochstrasser, M.** (1996). Ubiquitin-dependent protein degradation. *Annu Rev Genet* **30**, 405-439.
- Hogan, B., Beddington, R., Costantini, F. and Lacy, E.** (1994). *Manipulating the Mouse Embryo*. Plainview: Cold Spring Harbor Laboratory Press.

- Holder, J. L., Jr., Butte, N. F. and Zinn, A. R.** (2000). Profound obesity associated with a balanced translocation that disrupts the SIM1 gene. *Hum Mol Genet* **9**, 101-108.
- Holm, V. A., Cassidy, S. B., Butler, M. G., Hanchett, J. M., Greenswag, L. R., Whitman, B. Y. and Greenberg, F.** (1993). Prader-Willi syndrome: consensus diagnostic criteria. *Pediatrics* **91**, 398-402.
- Hoogenraad, C. C., Koekkoek, B., Akhmanova, A., Krugers, H., Dortland, B., Miedema, M., Van Alphen, A., Kistler, W. M., Jaegle, M., Koutsourakis, M. et al.** (2002). Targeted mutation of Cyln2 in the Williams syndrome critical region links CLIP-115 haploinsufficiency to neurodevelopmental abnormalities in mice. *Nat Genet* **32**, 116-127.
- Horsthemke, B.** (1997). Structure and function of the human chromosome 15 imprinting center. *J Cell Physiol* **173**, 237-241.
- Hoybye, C., Hilding, A., Jacobsson, H. and Thoren, M.** (2002). Metabolic profile and body composition in adults with Prader-Willi syndrome and severe obesity. *J Clin Endocrinol Metab* **87**, 3590-3597.
- Huang, B., Crolla, J. A., Christian, S. L., Wolf-Ledbetter, M. E., Macha, M. E., Papenhausen, P. N. and Ledbetter, D. H.** (1997). Refined molecular characterization of the breakpoints in small inv dup(15) chromosomes. *Hum Genet* **99**, 11-17.
- Itoh, K., Hayashi, A., Nakao, M., Hoshino, T., Seki, N. and Shichijo, S.** (1996). Human tumor rejection antigens MAGE. *J Biochem (Tokyo)* **119**, 385-390.
- Jacobowitz, D. M. and Abbott, L. C.** (1998). Chemoarchitectonic atlas of the developing mouse brain. Boca Raton: CRC Press.
- Jay, P., Rougeulle, C., Massacrier, A., Moncla, A., Mattei, M. G., Malzac, P., Roeckel, N., Taviaux, S., Lefranc, J. L., Cau, P. et al.** (1997). The human necdin gene, NDN, is maternally imprinted and located in the Prader-Willi syndrome chromosomal region. *Nat Genet* **17**, 357-361.
- Ji, Y., Walkowicz, M. J., Buiting, K., Johnson, D. K., Tarvin, R. E., Rinchik, E. M., Horsthemke, B., Stubbs, L. and Nicholls, R. D.** (1999). The ancestral gene for transcribed, low-copy repeats in the Prader-Willi/Angelman region encodes a large protein implicated in protein trafficking, which is deficient in mice with neuromuscular and spermiogenic abnormalities. *Hum Mol Genet* **8**, 533-542.

- Jiang, Y. H., Armstrong, D., Albrecht, U., Atkins, C. M., Noebels, J. L., Eichele, G., Sweatt, J. D. and Beaudet, A. L.** (1998). Mutation of the Angelman ubiquitin ligase in mice causes increased cytoplasmic p53 and deficits of contextual learning and long-term potentiation. *Neuron* **21**, 799-811.
- Johnson, D. K., Stubbs, L. J., Culiati, C. T., Montgomery, C. S., Russell, L. B. and Rinchik, E. M.** (1995). Molecular analysis of 36 mutations at the mouse pink-eyed dilution (p) locus. *Genetics* **141**, 1563-1571.
- Jong, M. T., Carey, A. H., Caldwell, K. A., Lau, M. H., Handel, M. A., Driscoll, D. J., Stewart, C. L., Rinchik, E. M. and Nicholls, R. D.** (1999a). Imprinting of a RING zinc-finger encoding gene in the mouse chromosome region homologous to the Prader-Willi syndrome genetic region. *Hum Mol Genet* **8**, 795-803.
- Jong, M. T., Gray, T. A., Ji, Y., Glenn, C. C., Saitoh, S., Driscoll, D. J. and Nicholls, R. D.** (1999b). A novel imprinted gene, encoding a RING zinc-finger protein, and overlapping antisense transcript in the Prader-Willi syndrome critical region. *Hum Mol Genet* **8**, 783-793.
- Kalra, S. P., Dube, M. G., Pu, S., Xu, B., Horvath, T. L. and Kalra, P. S.** (1999). Interacting appetite-regulating pathways in the hypothalamic regulation of body weight. *Endocr Rev* **20**, 68-100.
- Kaneko-Ishino, T., Kuroiwa, Y., Miyoshi, N., Kohda, T., Suzuki, R., Yokoyama, M., Vville, S., Barton, S. C., Ishino, F. and Surani, M. A.** (1995). Peg1/Mest imprinted gene on chromosome 6 identified by cDNA subtraction hybridization. *Nat Genet* **11**, 52-59.
- Kelly, M., Edgar, A. J. and Wevrick, R.** (2001). Analysis of DEXI/Dexi refines the organization of the mouse 7C and human 15q11-->q13 imprinting clusters. *Cytogenet Cell Genet* **92**, 149-152.
- Kent, G. C.** (1992). Comparative Anatomy of the Vertebrates. St. Louis: Mosby-YearBook, Inc.
- Kishino, T., Lalonde, M. and Wagstaff, J.** (1997). UBE3A/E6-AP mutations cause Angelman syndrome. *Nat Genet* **15**, 70-73.
- Kojima, M., Hosoda, H., Date, Y., Nakazato, M., Matsuo, H. and Kangawa, K.** (1999). Ghrelin is a growth-hormone-releasing acylated peptide from stomach. *Nature* **402**, 656-660.
- Kozak, M.** (1989). The scanning model for translation: an update. *J Cell Biol* **108**, 229-241.

- Kremer, H. P. H.** (1992). The hypothalamic lateral tuberal nucleus: normal anatomy and changes in neurological diseases. In *The Human Hypothalamus in Health and Disease*, vol. 93 (ed. D. F. Swaab, M. A. Hofman, M. Mirmiran, R. Ravid and F. W. Van Leeuwen), pp. 249-261. Amsterdam: Elsevier Science Publishers.
- Kupfermann, I.** (1991). Hypothalamus and Limbic System: Peptidergic Neurons, Homeostasis, and Emotional Behaviour. In *Principles of Neural Science*, (ed. E. R. Kandel, J. H. Schwartz and T. M. Jessell), pp. 735-749. New York: Elsevier Science Publishing Co.
- Kuroiwa, Y., Kaneko-Ishino, T., Kagitani, F., Kohda, T., Li, L. L., Tada, M., Suzuki, R., Yokoyama, M., Shiroishi, T., Wakana, S. et al.** (1996). Peg3 imprinted gene on proximal chromosome 7 encodes for a zinc finger protein. *Nat Genet* **12**, 186-190.
- Kuslich, C. D., Kobori, J. A., Mohapatra, G., Gregorio-King, C. and Donlon, T. A.** (1999). Prader-Willi syndrome is caused by disruption of the SNRPN gene. *Am J Hum Genet* **64**, 70-76.
- Ledbetter, D. H., Riccardi, V. M., Airhart, S. D., Strobel, R. J., Keenan, B. S. and Crawford, J. D.** (1981). Deletions of chromosome 15 as a cause of the Prader-Willi syndrome. *N Engl J Med* **304**, 325-329.
- Lee, J. T., Davidow, L. S. and Warshawsky, D.** (1999a). Tsix, a gene antisense to Xist at the X-inactivation centre. *Nat Genet* **21**, 400-404.
- Lee, M. P., DeBaun, M. R., Mitsuya, K., Galonek, H. L., Brandenburg, S., Oshimura, M. and Feinberg, A. P.** (1999b). Loss of imprinting of a paternally expressed transcript, with antisense orientation to KVLQT1, occurs frequently in Beckwith-Wiedemann syndrome and is independent of insulin-like growth factor II imprinting. *Proc Natl Acad Sci U S A* **96**, 5203-5208.
- Lee, P. D. K.** (1995). Endocrine and metabolic aspects of Prader-Willi syndrome. In *Management of Prader-Willi syndrome*, (ed. L. R. Greenswag and R. C. Alexander), pp. 32-57. New York: Springer-Verlag.
- Lee, S., Kozlov, S., Hernandez, L., Chamberlain, S. J., Brannan, C. I., Stewart, C. L. and Wevrick, R.** (2000). Expression and imprinting of MAGEL2 suggest a role in Prader-Willi syndrome and the homologous murine imprinting phenotype. *Hum Mol Genet* **9**, 1813-1819.
- Lee, S. T., Nicholls, R. D., Bunday, S., Laxova, R., Musarella, M. and Spritz, R. A.** (1994). Mutations of the P gene in oculocutaneous albinism, ocular albinism, and Prader-Willi syndrome plus albinism. *N Engl J Med* **330**, 529-534.

- Lindgren, A. C., Hellstrom, L. G., Ritzen, E. M. and Milerad, J. (1999).** Growth hormone treatment increases CO₂ response, ventilation and central inspiratory drive in children with Prader-Willi syndrome. *Eur J Pediatr* **158**, 936-940.
- Livingston, F. R., Arens, R., Bailey, S. L., Keens, T. G. and Ward, S. L. (1995).** Hypercapnic arousal responses in Prader-Willi syndrome. *Chest* **108**, 1627-1631.
- MacDonald, H. R. and Wevrick, R. (1997).** The necdin gene is deleted in Prader-Willi syndrome and is imprinted in human and mouse. *Hum Mol Genet* **6**, 1873-1878.
- MacDonald, J. T. and Camp, D. (2001).** Prolonged but reversible respiratory failure in a newborn with Prader-Willi syndrome. *J Child Neurol* **16**, 153-154.
- Maden, M. (1999).** Heads or tails? Retinoic acid will decide. *Bioessays* **21**, 809-812.
- Mann, M. R. and Bartolomei, M. S. (2000).** Maintaining imprinting. *Nat Genet* **25**, 4-5.
- Manni, R., Politini, L., Nobili, L., Ferrillo, F., Livieri, C., Veneselli, E., Biancheri, R., Martinetti, M. and Tartara, A. (2001).** Hypersomnia in the Prader Willi syndrome: clinical-electrophysiological features and underlying factors. *Clin Neurophysiol* **112**, 800-805.
- Martin, J. H. and Jessell, T. M. (1991).** Development as a Guide to the Regional Anatomy of the Brain. In *Principles of Neural Science*, (ed. E. R. Kandel, J. H. Schwartz and T. M. Jessell), pp. 296-308. New York: Elsevier Science Publishing Co.
- Maruyama, K., Usami, M., Aizawa, T. and Yoshikawa, K. (1991).** A novel brain-specific mRNA encoding nuclear protein (necdin) expressed in neurally differentiated embryonal carcinoma cells. *Biochem Biophys Res Commun* **178**, 291-296.
- Mascari, M. J., Gottlieb, W., Rogan, P. K., Butler, M. G., Waller, D. A., Armour, J. A., Jeffreys, A. J., Ladda, R. L. and Nicholls, R. D. (1992).** The frequency of uniparental disomy in Prader-Willi syndrome. Implications for molecular diagnosis. *N Engl J Med* **326**, 1599-1607.
- Mason, P. (2001).** Contributions of the medullary raphe and ventromedial reticular region to pain modulation and other homeostatic functions. *Annu Rev Neurosci* **24**, 737-777.
- Matsumoto, K., Taniura, H., Uetsuki, T. and Yoshikawa, K. (2001).** Necdin acts as a transcriptional repressor that interacts with multiple guanosine clusters. *Gene* **272**, 173-179.

- Matsuura, T., Sutcliffe, J. S., Fang, P., Galjaard, R. J., Jiang, Y. H., Benton, C. S., Rommens, J. M. and Beaudet, A. L. (1997).** De novo truncating mutations in E6-AP ubiquitin-protein ligase gene (UBE3A) in Angelman syndrome. *Nat Genet* **15**, 74-77.
- Mattei, M. G., Mbikay, M., Sylla, B. S., Lenoir, G., Mattei, J. F., Seidah, N. G. and Chretien, M. (1990).** Assignment of the gene for neuroendocrine protein 7B2 (SGNE1 locus) to mouse chromosome region 2[E3-F3] and to human chromosome region 15q11-q15. *Genomics* **6**, 436-440.
- McBurney, M. W. (1993).** P19 embryonal carcinoma cells. *Int J Dev Biol* **37**, 135-140.
- Meguro, M., Kashiwagi, A., Mitsuya, K., Nakao, M., Kondo, I., Saitoh, S. and Oshimura, M. (2001a).** A novel maternally expressed gene, ATP10C, encodes a putative aminophospholipid translocase associated with Angelman syndrome. *Nat Genet* **28**, 19-20.
- Meguro, M., Mitsuya, K., Nomura, N., Kohda, M., Kashiwagi, A., Nishigaki, R., Yoshioka, H., Nakao, M., Oishi, M. and Oshimura, M. (2001b).** Large-scale evaluation of imprinting status in the Prader-Willi syndrome region: an imprinted direct repeat cluster resembling small nucleolar RNA genes. *Hum Mol Genet* **10**, 383-394.
- Meguro, M., Mitsuya, K., Sui, H., Shigenami, K., Kugoh, H., Nakao, M. and Oshimura, M. (1997).** Evidence for uniparental, paternal expression of the human GABAA receptor subunit genes, using microcell-mediated chromosome transfer. *Hum Mol Genet* **6**, 2127-2133.
- Menendez, A. A. (1999).** Abnormal ventilatory responses in patients with Prader-Willi syndrome. *Eur J Pediatr* **158**, 941-942.
- Michaud, J. L. (2001).** The developmental program of the hypothalamus and its disorders. *Clin Genet* **60**, 255-263.
- Michaud, J. L., Boucher, F., Melnyk, A., Gauthier, F., Goshu, E., Levy, E., Mitchell, G. A., Himms-Hagen, J. and Fan, C. M. (2001).** Sim1 haploinsufficiency causes hyperphagia, obesity and reduction of the paraventricular nucleus of the hypothalamus. *Hum Mol Genet* **10**, 1465-1473.
- Michaud, J. L., Rosenquist, T., May, N. R. and Fan, C. M. (1998).** Development of neuroendocrine lineages requires the bHLH-PAS transcription factor SIM1. *Genes Dev* **12**, 3264-3275.
- Miller, A. P. and Willard, H. F. (1998).** Chromosomal basis of X chromosome inactivation: identification of a multigene domain in Xp11.21-p11.22 that escapes X inactivation. *Proc Natl Acad Sci U S A* **95**, 8709-8714.

- Miller, L., Angulo, M., Price, D. and Taneja, S.** (1996). MR of the pituitary in patients with Prader-Willi syndrome: size determination and imaging findings. *Pediatr Radiol* **26**, 43-47.
- Mitsuya, K., Meguro, M., Lee, M. P., Katoh, M., Schulz, T. C., Kugoh, H., Yoshida, M. A., Niikawa, N., Feinberg, A. P. and Oshimura, M.** (1999). LIT1, an imprinted antisense RNA in the human KvLQT1 locus identified by screening for differentially expressed transcripts using monochromosomal hybrids. *Hum Mol Genet* **8**, 1209-1217.
- Moore, R. Y.** (1992). The organization of the human circadian timing system. In *The Human Hypothalamus in Health and Disease*, (ed. D. F. Swaab, M. A. Hofman, M. Mirmiran, R. Ravid and F. W. van Leeuwen), pp. 101-118. Amsterdam: Elsevier Science Publishers.
- Moore, R. Y., Speh, J. C. and Leak, R. K.** (2002). Suprachiasmatic nucleus organization. *Cell Tissue Res* **309**, 89-98.
- Muller, J.** (1997). Hypogonadism and endocrine metabolic disorders in Prader-Willi syndrome. *Acta Paediatr Suppl* **423**, 58-59.
- Muscатели, F., Abrous, D. N., Massacrier, A., Boccaccio, I., Le Moal, M., Cau, P. and Cremer, H.** (2000). Disruption of the mouse *Necdin* gene results in hypothalamic and behavioral alterations reminiscent of the human Prader-Willi syndrome. *Hum Mol Genet* **9**, 3101-3110.
- Nakada, Y., Taniura, H., Uetsuki, T., Inazawa, J. and Yoshikawa, K.** (1998). The human chromosomal gene for *necdin*, a neuronal growth suppressor, in the Prader-Willi syndrome deletion region. *Gene* **213**, 65-72.
- Nakai, S., Kawano, H., Yudate, T., Nishi, M., Kuno, J., Nagata, A., Jishage, K., Hamada, H., Fujii, H., Kawamura, K. et al.** (1995). The POU domain transcription factor *Brn-2* is required for the determination of specific neuronal lineages in the hypothalamus of the mouse. *Genes Dev* **9**, 3109-3121.
- Nakao, M., Sutcliffe, J. S., Durtschi, B., Mutirangura, A., Ledbetter, D. H. and Beaudet, A. L.** (1994). Imprinting analysis of three genes in the Prader-Willi/Angelman region: *SNRPN*, E6-associated protein, and *PAR-2* (D15S225E). *Hum Mol Genet* **3**, 309-315.
- Nakazato, M., Murakami, N., Date, Y., Kojima, M., Matsuo, H., Kangawa, K. and Matsukura, S.** (2001). A role for ghrelin in the central regulation of feeding. *Nature* **409**, 194-198.

- Nicholls, R. D. and Knepper, J. L.** (2001). Genome organization, function, and imprinting in Prader-Willi and Angelman syndromes. *Annu Rev Genomics Hum Genet* **2**, 153-175.
- Nicholls, R. D., Saitoh, S. and Horsthemke, B.** (1998). Imprinting in Prader-Willi and Angelman syndromes. *Trends Genet* **14**, 194-200.
- Niinobe, M., Koyama, K. and Yoshikawa, K.** (2000). Cellular and subcellular localization of neudin in fetal and adult mouse brain. *Dev Neurosci* **22**, 310-319.
- Ning, Y., Roschke, A., Christian, S. L., Lesser, J., Sutcliffe, J. S. and Ledbetter, D. H.** (1996). Identification of a novel paternally expressed transcript adjacent to snRPN in the Prader-Willi syndrome critical region. *Genome Res* **6**, 742-746.
- Niwa, H., Miyazaki, J. and Smith, A. G.** (2000). Quantitative expression of Oct-3/4 defines differentiation, dedifferentiation or self-renewal of ES cells. *Nat Genet* **24**, 372-376.
- Nixon, G. M. and Brouillette, R. T.** (2002). Sleep and breathing in Prader-Willi syndrome. *Pediatr Pulmonol* **34**, 209-217.
- Odent, S., Atti-Bitach, T., Blayau, M., Mathieu, M., Aug, J., Delezo de, A. L., Gall, J. Y., Le Marec, B., Munnich, A., David, V. et al.** (1999). Expression of the Sonic hedgehog (SHH) gene during early human development and phenotypic expression of new mutations causing holoprosencephaly. *Hum Mol Genet* **8**, 1683-1689.
- Ohta, T., Gray, T. A., Rogan, P. K., Buiting, K., Gabriel, J. M., Saitoh, S., Muralidhar, B., Bilienska, B., Krajewska-Walasek, M., Driscoll, D. J. et al.** (1999). Imprinting-mutation mechanisms in Prader-Willi syndrome. *Am J Hum Genet* **64**, 397-413.
- Osborne, L. and Pober, B.** (2001). Genetics of childhood disorders: XXVII. Genes and cognition in Williams syndrome. *J Am Acad Child Adolesc Psychiatry* **40**, 732-735.
- Ozcelik, T., Leff, S., Robinson, W., Donlon, T., Lalande, M., Sanjines, E., Schinzel, A. and Francke, U.** (1992). Small nuclear ribonucleoprotein polypeptide N (SNRPN), an expressed gene in the Prader-Willi syndrome critical region. *Nat Genet* **2**, 265-269.
- Panda, S., Antoch, M. P., Miller, B. H., Su, A. I., Schook, A. B., Straume, M., Schultz, P. G., Kay, S. A., Takahashi, J. S. and Hogenesch, J. B.** (2002). Coordinated transcription of key pathways in the mouse by the circadian clock. *Cell* **109**, 307-320.

- Potocki, L., Glaze, D., Tan, D. X., Park, S. S., Kashork, C. D., Shaffer, L. G., Reiter, R. J. and Lupski, J. R.** (2000). Circadian rhythm abnormalities of melatonin in Smith-Magenis syndrome. *J Med Genet* **37**, 428-433.
- Prader, A., Labhart, A. and H., W.** (1956). Ein Syndrom von Adipositas, Kleinwuchs, Krptorchismus und Oligophrenic nach myatonieartigem Zustand im Neugeborenenalter. *Schweiz Med Wochenschr* **86**, 1260-1261.
- Reik, W. and Walter, J.** (1998). Imprinting mechanisms in mammals. *Curr Opin Genet Dev* **8**, 154-164.
- Ren, J., Lee, S., Gerard, M., Pagliardini, S., Stewart, C. L., Greer, J. J. and Wevrick, R.** (2003). Absence of Ndn, encoding the Prader-Willi syndrome deleted gene neccdin, results in congenital deficiency of central respiratory drive in neonatal mice. *J Neurosci* **23**, 1569-1573.
- Reppert, S. M., Schwartz, W. J. and Uhl, G. R.** (1987). Arginine vasopressin: a novel peptide rhythm in cerebrospinal fluid. *Trends Neurosci* **10**, 76-80.
- Richter, D. W. and Spyer, K. M.** (2001). Studying rhythmogenesis of breathing: comparison of in vivo and in vitro models. *Trends Neurosci* **24**, 464-472.
- Rinchik, E. M., Bultman, S. J., Horsthemke, B., Lee, S. T., Strunk, K. M., Spritz, R. A., Avidano, K. M., Jong, M. T. and Nicholls, R. D.** (1993). A gene for the mouse pink-eyed dilution locus and for human type II oculocutaneous albinism. *Nature* **361**, 72-76.
- Robinson, W. P., Bottani, A., Xie, Y. G., Balakrishnan, J., Binkert, F., Machler, M., Prader, A. and Schinzel, A.** (1991). Molecular, cytogenetic, and clinical investigations of Prader-Willi syndrome patients. *Am J Hum Genet* **49**, 1219-1234.
- Role, L. W. and Kelly, J. P.** (1991). The Brain Stem: Cranial Nerve Nuclei and the Monoaminergic Systems. In *Principles of Neural Science*, (ed. E. R. Kandel, J. H. Schwartz and T. M. Jessell), pp. 683-699. New York: Elsevier Science Publishing Co.
- Rougeulle, C., Cardoso, C., Fontes, M., Colleaux, L. and Lalande, M.** (1998). An imprinted antisense RNA overlaps UBE3A and a second maternally expressed transcript. *Nat Genet* **19**, 15-16.
- Rougeulle, C., Glatt, H. and Lalande, M.** (1997). The Angelman syndrome candidate gene, UBE3A/E6-AP, is imprinted in brain. *Nat Genet* **17**, 14-15.
- Rougeulle, C. and Lalande, M.** (1998). Angelman syndrome: how many genes to remain silent? *Neurogenetics* **1**, 229-237.

- Rudnicki, M. A. and McBurney, M. W.** (1987). Cell culture methods and induction of differentiation of embryonal carcinoma cell lines. In *Embryonic Stem Cells: A Practical Approach*, (ed. E. J. Robertson), pp. 19-49. Oxford: IRL Press.
- Rugh, R.** (1968). *The Mouse. Its Reproduction and Development*. Minneapolis: Burgess Publishing Company.
- Runte, M., Huttenhofer, A., Gross, S., Kiefmann, M., Horsthemke, B. and Buiting, K.** (2001). The IC-SNURF-SNRPN transcript serves as a host for multiple small nucleolar RNA species and as an antisense RNA for UBE3A. *Hum Mol Genet* **10**, 2687-2700.
- Sambrook, J. and Russell, D. W.** (2001). *Molecular Cloning: A laboratory manual*. New York: Cold Spring Harbour Press.
- Sawchenko, P. E.** (1998). Toward a new neurobiology of energy balance, appetite, and obesity: the anatomists weigh in. *J Comp Neurol* **402**, 435-441.
- Saxena, S., Brody, A. L., Schwartz, J. M. and Baxter, L. R.** (1998). Neuroimaging and frontal-subcortical circuitry in obsessive-compulsive disorder. *Br J Psychiatry Suppl*, 26-37.
- Scherer, S. and Tsui, L.-C.** (1991). Cloning and Analysis of Large DNA Molecules. In *Advanced Techniques in Chromosome Research*, (ed. K. Adolph), pp. . New York: Marcel Dekker Inc.
- Schluter, B., Buschatz, D., Trowitzsch, E., Aksu, F. and Andler, W.** (1997). Respiratory control in children with Prader-Willi syndrome. *Eur J Pediatr* **156**, 65-68.
- Schmauss, C., McAllister, G., Ohosone, Y., Hardin, J. A. and Lerner, M. R.** (1989). A comparison of snRNP-associated Sm-autoantigens: human N, rat N and human B/B'. *Nucleic Acids Res* **17**, 1733-1743.
- Schmidt, H., Bechtold, S. and Schwarz, H. P.** (2000). Prader-Labhart-Willi syndrome: auxological response to a conventional dose of growth hormone in patients with classical growth hormone deficiency. *Eur J Med Res* **5**, 307-310.
- Schonemann, M. D., Ryan, A. K., McEvelly, R. J., O'Connell, S. M., Arias, C. A., Kalla, K. A., Li, P., Sawchenko, P. E. and Rosenfeld, M. G.** (1995). Development and survival of the endocrine hypothalamus and posterior pituitary gland requires the neuronal POU domain factor Brn-2. *Genes Dev* **9**, 3122-3135.

- Schulze, A., Hansen, C., Skakkebaek, N. E., Brondum-Nielsen, K., Ledbeter, D. H. and Tommerup, N. (1996). Exclusion of SNRPN as a major determinant of Prader-Willi syndrome by a translocation breakpoint. *Nat Genet* **12**, 452-454.
- Schwartz, M. W., Woods, S. C., Porte, D., Jr., Seeley, R. J. and Baskin, D. G. (2000). Central nervous system control of food intake. *Nature* **404**, 661-671.
- Shemer, R., Hershko, A. Y., Perk, J., Mostoslavsky, R., Tsuberi, B., Cedar, H., Buiting, K. and Razin, A. (2000). The imprinting box of the Prader-Willi/Angelman syndrome domain. *Nat Genet* **26**, 440-443.
- Sheng, H. Z. and Westphal, H. (1999). Early steps in pituitary organogenesis. *Trends Genet* **15**, 236-240.
- Shimoda, M., Morita, S., Obata, Y., Sotomaru, Y., Kono, T. and Hatada, I. (2002). Imprinting of a small nucleolar RNA gene on mouse chromosome 12. *Genomics* **79**, 483-486.
- Simeone, A., Avantaggiato, V., Moroni, M. C., Mavilio, F., Arra, C., Cotelli, F., Nigro, V. and Acampora, D. (1995). Retinoic acid induces stage-specific antero-posterior transformation of rostral central nervous system. *Mech Dev* **51**, 83-98.
- Smit, A. F. (1996). The origin of interspersed repeats in the human genome. *Curr Opin Genet Dev* **6**, 743-748.
- Smith, A. C., Dykens, E. and Greenberg, F. (1998). Behavioral phenotype of Smith-Magenis syndrome (del 17p11.2). *Am J Med Genet* **81**, 179-185.
- Smith, J. C., Ellenberger, H. H., Ballanyi, K., Richter, D. W. and Feldman, J. L. (1991). Pre-Botzinger complex: a brainstem region that may generate respiratory rhythm in mammals. *Science* **254**, 726-729.
- Southern, E. M. (1975). Detection of specific sequences among DNA fragments separated by gel electrophoresis. *J Mol Biol* **98**, 503-517.
- Spitzer, M. W. and Semple, M. N. (1995). Neurons sensitive to interaural phase disparity in gerbil superior olive: diverse monaural and temporal response properties. *J Neurophysiol* **73**, 1668-1690.
- Stauder, J. E., Brinkman, M. J. and Curfs, L. M. (2002). Multi-modal P3 deflation of event-related brain activity in Prader-Willi syndrome. *Neurosci Lett* **327**, 99-102.
- Stein, D. J. and Ludik, J. (2000). A neural network of obsessive-compulsive disorder: modelling cognitive disinhibition and neurotransmitter dysfunction. *Med Hypotheses* **55**, 168-176.

- Stoykova, A., Fritsch, R., Walther, C. and Gruss, P.** (1996). Forebrain patterning defects in Small eye mutant mice. *Development* **122**, 3453-3465.
- Su, A. I., Cooke, M. P., Ching, K. A., Hakak, Y., Walker, J. R., Wiltshire, T., Orth, A. P., Vega, R. G., Sapinoso, L. M., Moqrich, A. et al.** (2002). Large-scale analysis of the human and mouse transcriptomes. *Proc Natl Acad Sci U S A* **99**, 4465-4470.
- Sun, Y., Nicholls, R. D., Butler, M. G., Saitoh, S., Hainline, B. E. and Palmer, C. G.** (1996). Breakage in the SNRPN locus in a balanced 46,XY,t(15;19) Prader-Willi syndrome patient. *Hum Mol Genet* **5**, 517-524.
- Surani, M. A. and Barton, S. C.** (1983). Development of gynogenetic eggs in the mouse: implications for parthenogenetic embryos. *Science* **222**, 1034-1036.
- Sutcliffe, J. S., Han, M., Christian, S. L. and Ledbetter, D. H.** (1997). Neuronally-expressed necdin gene: an imprinted candidate gene in Prader-Willi syndrome. *Lancet* **350**, 1520-1521.
- Sutcliffe, J. S., Nakao, M., Christian, S., Orstavik, K. H., Tommerup, N., Ledbetter, D. H. and Beaudet, A. L.** (1994). Deletions of a differentially methylated CpG island at the SNRPN gene define a putative imprinting control region. *Nat Genet* **8**, 52-58.
- Swaab, D. F.** (1995). Development of the human hypothalamus. *Neurochem Res* **20**, 509-519.
- Swaab, D. F.** (1997). Prader-Willi syndrome and the hypothalamus. *Acta Paediatr Suppl* **423**, 50-54.
- Swaab, D. F., Hofman, M. A., Lucassen, P. J., Purba, J. S., Raadsheer, F. C. and Van de Nes, J. A.** (1993). Functional neuroanatomy and neuropathology of the human hypothalamus. *Anat Embryol (Berl)* **187**, 317-330.
- Swaab, D. F., Purba, J. S. and Hofman, M. A.** (1995). Alterations in the hypothalamic paraventricular nucleus and its oxytocin neurons (putative satiety cells) in Prader-Willi syndrome: a study of five cases. *J Clin Endocrinol Metab* **80**, 573-579.
- Swaab, D. F., Roozendaal, B., Ravid, R., Velis, D. N., Gooren, L. and Williams, R. S.** (1987). Suprachiasmatic nucleus in aging, Alzheimer's disease, transsexuality and Prader-Willi syndrome. *Prog Brain Res* **72**, 301-310.
- Takazaki, R., Nishimura, I. and Yoshikawa, K.** (2002). Necdin is required for terminal differentiation and survival of primary dorsal root ganglion neurons. *Exp Cell Res* **277**, 220-232.

- Taniura, H., Matsumoto, K. and Yoshikawa, K.** (1999). Physical and functional interactions of neuronal growth suppressor necdin with p53. *J Biol Chem* **274**, 16242-16248.
- Taniura, H., Taniguchi, N., Hara, M. and Yoshikawa, K.** (1998). Necdin, a postmitotic neuron-specific growth suppressor, interacts with viral transforming proteins and cellular transcription factor E2F1. *J Biol Chem* **273**, 720-728.
- Tassabehji, M., Metcalfe, K., Karmiloff-Smith, A., Carette, M. J., Grant, J., Dennis, N., Reardon, W., Splitt, M., Read, A. P. and Donnai, D.** (1999). Williams syndrome: use of chromosomal microdeletions as a tool to dissect cognitive and physical phenotypes. *Am J Hum Genet* **64**, 118-125.
- Tilghman, S. M.** (1999). The sins of the fathers and mothers: genomic imprinting in mammalian development. *Cell* **96**, 185-193.
- Trainor, P. A. and Krumlauf, R.** (2000). Patterning the cranial neural crest: hindbrain segmentation and Hox gene plasticity. *Nat Rev Neurosci* **1**, 116-124.
- Tsai, T. F., Armstrong, D. and Beaudet, A. L.** (1999a). Necdin-deficient mice do not show lethality or the obesity and infertility of Prader-Willi syndrome. *Nat Genet* **22**, 15-16.
- Tsai, T. F., Jiang, Y. H., Bressler, J., Armstrong, D. and Beaudet, A. L.** (1999b). Paternal deletion from Snrpn to Ube3a in the mouse causes hypotonia, growth retardation and partial lethality and provides evidence for a gene contributing to Prader-Willi syndrome. *Hum Mol Genet* **8**, 1357-1364.
- Tschop, M., Smiley, D. L. and Heiman, M. L.** (2000). Ghrelin induces adiposity in rodents. *Nature* **407**, 908-913.
- Tschop, M., Wawarta, R., Riepl, R. L., Friedrich, S., Bidlingmaier, M., Landgraf, R. and Folwaczny, C.** (2001). Post-prandial decrease of circulating human ghrelin levels. *J Endocrinol Invest* **24**, RC19-21.
- Uetsuki, T., Takagi, K., Sugiura, H. and Yoshikawa, K.** (1996). Structure and expression of the mouse necdin gene. Identification of a postmitotic neuron-restrictive core promoter. *J Biol Chem* **271**, 918-924.
- Vela-Bueno, A., Kales, A., Soldatos, C. R., Dobladez-Blanco, B., Campos-Castello, J., Espino-Hurtado, P. and Olivan-Palacios, J.** (1984). Sleep in the Prader-Willi syndrome. Clinical and polygraphic findings. *Arch Neurol* **41**, 294-296.
- Venter, J. C. Adams, M. D. Myers, E. W. Li, P. W. Mural, R. J. Sutton, G. G. Smith, H. O. Yandell, M. Evans, C. A. Holt, R. A. et al.** (2001). The sequence of the human genome. *Science* **291**, 1304-1351.

- Vu, T. H. and Hoffman, A. R.** (1997). Imprinting of the Angelman syndrome gene, UBE3A, is restricted to brain. *Nat Genet* **17**, 12-13.
- Warnock, J. K. and Kestenbaum, T.** (1992). Pharmacologic treatment of severe skin-picking behaviors in Prader-Willi syndrome. Two case reports. *Arch Dermatol* **128**, 1623-1625.
- Warren, J. L. and Junt, E.** (1981). Cognitive processing in children with Prader-Willi syndrome. In *The Prader-Willi syndrome*, (ed. V. A. Holm, S. J. Sulzbacher and P. L. Pipes), pp. 161-177. Baltimore, MD: University Park Press.
- Wevrick, R. and Francke, U.** (1996). Diagnostic test for the Prader-Willi syndrome by SNRPN expression in blood. *Lancet* **348**, 1068-1069.
- Wevrick, R., Kerns, J. A. and Francke, U.** (1994). Identification of a novel paternally expressed gene in the Prader-Willi syndrome region. *Hum Mol Genet* **3**, 1877-1882.
- Wevrick, R., Kerns, J. A. and Francke, U.** (1996). The IPW gene is imprinted and is not expressed in the Prader-Willi syndrome. *Acta Genet Med Gemellol* **45**, 191-197.
- Wharton, R. H. and Bresnan, M. J.** (1989). Neonatal respiratory depression and delay in diagnosis in Prader-Willi syndrome. *Dev Med Child Neurol* **31**, 231-236.
- Wharton, R. H. and Loechner, K. J.** (1996). Genetic and clinical advances in Prader-Willi syndrome. *Curr Opin Pediatr* **8**, 618-624.
- White, R. A., Vorontosova, E., Chen, R., Lunte, S. M., Davies, M. I., Heppert, K. E., McNulty, S. G., Young, K. N., Butler, M. G., Brannan, C. I. et al.** (2002). A behavioral and correlated neurochemical mouse phenotype related to the absence of Snrpn, a locus associated with Prader-Willi Syndrome. *Am. J. Hum. Genet.* **71**, A1736.
- Whitman, B. Y. and Accardo, P.** (1987). Emotional symptoms in Prader-Willi syndrome adolescents. *Am J Med Genet* **28**, 897-905.
- Williams, C. A., Angelman, H., Clayton-Smith, J., Driscoll, D. J., Hendrickson, J. E., Knoll, J. H., Magenis, R. E., Schinzel, A., Wagstaff, J., Whidden, E. M. et al.** (1995). Angelman syndrome: consensus for diagnostic criteria. Angelman Syndrome Foundation. *Am J Med Genet* **56**, 237-238.

- Wirth, J., Back, E., Huttenhofer, A., Nothwang, H. G., Lich, C., Gross, S., Menzel, C., Schinzel, A., Kioschis, P., Tommerup, N. et al. (2001).** A translocation breakpoint cluster disrupts the newly defined 3' end of the SNURF-SNRPN transcription unit on chromosome 15. *Hum Mol Genet* **10**, 201-210.
- Wynshaw-Boris, A. (1996).** Model mice and human disease. *Nat Genet* **13**, 259-260.
- Xu, Y., Mural, R., Shah, M. and Uberbacher, E. (1994).** Recognizing exons in genomic sequence using GRAIL II. *Genet Eng (N Y)* **16**, 241-253.
- Yang, T., Adamson, T. E., Resnick, J. L., Leff, S., Wevrick, R., Francke, U., Jenkins, N. A., Copeland, N. G. and Brannan, C. I. (1998).** A mouse model for Prader-Willi syndrome imprinting-centre mutations. *Nat Genet* **19**, 25-31.
- Young, W. S., 3rd. (1992).** Regulation of gene expression in the hypothalamus: hybridization histochemical studies. *Ciba Found Symp* **168**, 127-138; discussion 138-143.
- Zellweger, H. (1981).** Diagnosis and Therapy in the First Phase of Prader-Willi Syndrome. In *The Prader-Willi Syndrome*, (ed. V. A. Holm, S. J. Sulzbacher and P. L. Pipes), pp. 55-68. Baltimore: University Park Press.

Curriculum Vitae

Contact Information Email: sylee@ualberta.ca
 Home phone: (780) 462-9136, Work phone (780) 492-5499

Education B.Sc. Honors Genetics 9/1993-5/1997
 University of Alberta, Alberta, Canada

 Ph.D. Medical Genetics 9/1997-present
 University of Alberta, Alberta, Canada
 Expected completion date: March 2003

Honors and Awards received

Dean's Silver Medal in Science, University of Alberta, 1997

Alberta Heritage Foundation for Medical Research (AHFMR) summer studentship, 1997

AHFMR studentship, January 1998-December 2002

Marie Louise Imrie Graduate Student Award, \$500 travel grant, 2001

Research Training

Undergraduate Cloning genes involved in Prader-Willi Syndrome using cDNA libraries.
 research project University of Alberta
 9/1996-12/1996 Supervisor: Dr. Rachel Wevrick

Undergraduate Cloning genes involved in muscle development in *Drosophila*
 research project *melanogaster*.
 1/1997-4/1997 University of Alberta
 Supervisor: Dr. John Bell

Summer student Identification of novel imprinted genes involved in Prader-Willi syndrome
 research project using a variety of molecular biology techniques.
 5/1997-8/1997 University of Alberta
 Supervisor: Dr. Rachel Wevrick

Graduate student Identification and expression patterns of Prader-Willi syndrome genes in
 9/1997-present mouse and humans, and the implications for mouse models and human
 phenotypes.
 University of Alberta
 Supervisor: Dr. Rachel Wevrick (780) 492-7908
 rachel.wevrick@ualberta.ca

Statement of Research Interests

My primary focus lies in using genetic approaches to understanding human neurological disease. I am interested in identifying and characterizing genes involved in neurological disorders as well as using mice to model these disorders. I have been studying the neurobehavioral imprinting disorder Prader-Willi syndrome (PWS) and the role of several candidate genes in the etiology of the syndrome. In addition to examining the expression of PWS genes in humans and mice, I have also studied a mouse deficient for the PWS candidate gene *Ndn*.

Publications

1. S. Lee and R. Wevrick (1997) "Glow in the Dark" crayons as inexpensive autoradiography markers. *Technical Tips Online* (<http://www.elsevier.com/locate/tto>) T01055
2. S. Lee and R. Wevrick (1999) Identification of novel imprinted transcripts in the Prader-Willi/Angelman syndrome deletion region: further evidence for regional imprinting control. *Am. J. Hum. Genet.*, **66**, 848-858.
3. S. Lee, S. Kozlov, L. Hernandez, S. J. Chamberlain, C.I. Brannan, C. L. Stewart and R. Wevrick. (2000) Expression and imprinting of MAGEL2 suggest a role in Prader-Willi syndrome and the homologous murine imprinting phenotype. *Hum. Mol. Genet.*, **9**, 1813-1819.
4. Ren*, J., Lee*, S., Gerard, M., Pagliardini, S., Stewart, C. L., Greer, J. J. and Wevrick, R. (2003). Absence of *Ndn*, encoding the Prader-Willi syndrome deleted gene *necdin*, results in congenital deficiency of central respiratory drive in neonatal mice. *J Neurosci.* **23**, 1569-1573. (* Authors contributed equally to the work).
5. Lee, S., Walker, C.L., and Wevrick, R. Prader-Willi syndrome transcripts are expressed in phenotypically significant regions of the developing mouse brain. Submitted.

Abstracts

1. S. Lee, and R. Wevrick. Characterization of novel genes in the Prader-Willi region. (1997). Faculty of Medicine and Oral Health Sciences Students' Research Day. Edmonton, AB. (Platform presentation by SL)
2. H.R. MacDonald, S. Lee, B.G. Elyas and R. Wevrick (1997). Gene identification in the PWS deletion region, which includes the imprinted *necdin* gene. International Chromosome 15 Workshop, Baltimore, MD. (Platform presentation by RW)
3. S. Lee, and R. Wevrick (1998) Characterization of novel genes in the Prader-Willi Syndrome region. CFBS 41st annual meeting/GSC annual meeting. Edmonton, AB.(Poster presentation by SL)

4. **S. Lee**, and R. Wevrick, (1999) A Novel Imprinted Transcript in the Prader-Willi Region. *Genetics 2000, Gene Discovery and Beyond*. Edmonton, AB. (Poster presentation by SL)
5. **S. Lee**, and R. Wevrick (1999) Construction of an imprinting status transcript map of 15q11-q13. *Am. J. Hum. Genet.* **65**, suppl. A2625. (Poster presentation by SL)
6. **S. Lee**, S. Kozlov, L. Hernandez, S.J. Chamberlain, C.I. Brannan, C.L. Stewart and R. Wevrick (2000) NDNL1, a necdin-like gene, is a candidate for Prader-Willi Syndrome and its homologous mouse imprinting phenotype. CGDN Annual Scientific Meeting 2000, Vancouver, B.C. (Poster presentation by RW)
7. R. Wevrick, J. Bischof, and **S. Lee** (2000) Organization of the imprinted domain on human chromosome 15q11-q13. Human Genome Meeting, 2000. Vancouver, BC. (Platform presentation by RW)
8. R. Wevrick, **S. Lee**, S. Kozlov, J.M. Bischof, S.L. Kuny, T.K. Chibuk, L. Hernandez, C.L. Stewart (2000). Characterization of the necdin gene family and its role in Prader-Willi Syndrome. *Am. J. Hum. Genet.* **67**, suppl. A1972. (Poster presentation by RW)
9. R. Wevrick, J. Bischof, S. Kuny, and **S. Lee** (2001) The necdin and MAGEL2 genes in Prader-Willi syndrome. CGDN Annual Scientific Meeting 2000, St. Saver des Monts, Quebec. (Poster presentation by RW)
10. **S. Lee**, J.M. Bischof, S. Kuny, and R. Wevrick (2001) *NDN* and *MAGEL2* as candidate genes for Prader-Willi Syndrome. 2001 International Prader-Willi Syndrome Conference, 2001. St. Paul, MN. (Poster presentation by SL)
11. **S. Lee**, S.L. Kuny, C. Walker, and R. Wevrick (2001) *NDN* and *MAGEL2* as candidate genes in Prader-Willi Syndrome. *Am. J. Hum. Genet.* **69**, suppl. A2289. (Poster presentation by SL)
12. R. Wevrick, C.L. Walker, S.L. Kuny, and **S. Lee**. (2002) Neurodevelopmental expression profiles of the murine homologs of the Prader-Willi syndrome genes: implications for murine models of PWS. Society for Neuroscience 32nd Annual Meeting. Orlando, FL. (Poster presentation by SL)
13. R. Wevrick, C.L. Walker and **S. Lee**. (2003) The genetic origin of obesity in Prader-Willi syndrome: neurodevelopmental expression profiles of the murine homologs of PWS genes. *Obesity: New Insights into Pathogenesis and Treatment*. Keystone, CO (Poster presentation by RW)

Conferences attended

Canadian Federation of Biological Sciences (CFBS) 41st annual meeting/GSC annual meeting. Edmonton, Alberta. June, 1998

Genetics 2000, Gene Discovery and Beyond. Edmonton, Alberta. April, 1999

49th annual meeting of the American Society of Human Genetics, San Francisco, CA., October, 1999

Medical Genetics in Alberta Research Day. Red Deer, Alberta, June 2000.

2001 International Prader-Willi Syndrome Conference. 4th triennial IPWSO Scientific Conference. 16th Annual PWSA (USA) Scientific Conference. St. Paul, MN. June, 2001

51st annual meeting of the American Society of Human Genetics, San Diego, CA. October, 2001

32nd annual meeting of the Society for Neuroscience, Orlando, FL. November, 2002